Joint Centre for Mesoscale Meteorology, Reading, UK

Wind profiler – Unified Model comparison statics

P. Panagi
E. M. Dicks

Internal Report No. 114
NWP Technical Report No. 309

March 2000

Met Office Joint Centre for Mesoscale Meteorology Department of Meteorology
University of Reading PO Box 243 Reading RG6 6BB United Kingdom
Tel: +44 (0)118 931 8425 Fax: +44 (0)118 931 8791
www.metoffice.com

Designed and produced by the Met Office © Crown copyright 2001 01/0240 The Met Office logo is a registered trademark.

WIND PROFILER - UNIFIED MODEL COMPARISON STATISTICS

Peter Panagi & Ed Dicks
JCMM
Dept. Meteorology
Univ. Reading
PO Box 243
Reading RG6 6BB
March 2000

ABSTRACT

We present here a description of the JCMM contribution to the wind profiler project, part of the COST78-CWINDE99 European profiler-model comparison project. We present the methods used to derive differences between the profilers and Unified Model and describe some of the basic unix and graphics procedures that have enabled us to derive statistics.

Introduction

This short report is concerned with the method used in deriving the statistics for comparing wind-profiler wind speeds and direction directly with operational Unified Model mesoscale output, as part of the COST76 - CWINDE99 project. For information on the profiler project look under

http://rs0300/~cwinde/cwinde99/cwinde99.html

This part of profiler project is a collaboration between the Met. Office and the University of Reading, looking into the benefits that wind profiler data can potentially bring to the operational Unified Model. In addition, a number of cases studies of specific research interest are to be undertaken; the results of these will be presented in other reports. The project is funded by the Met. Office.
Here, we present the initial computational requirements and set up of the project as well as the methods by which statistics are derived and the use of graphics to produce a daily hardcopy archive. Statistical results are presented, but their meteorological interpretation will be the subject of a later report, however preliminary results have been presented at the European Geophysical Society in 1998 (Panagi et al 1999). Specific system details are left to appendices.

Table 1 list those profilers which lie within the current UM mesoscale domain and for which statistics are derived. The MST profiler sites at Aberystwyth, Camborne, Dunkeswell and Pendine are all situated in the UK, while Cabauw is in the Netherlands and La Ferte Vidame in France. In addition, we supply model statistics for the location of the 3GHz Doppler radar at Chilbolton in the UK. The profilers at Aberystwyth, Camborne, Dunkeswell, Pendine and Cabauw work in two modes, high and low, each with a different vertical resolution and base scan height.

Some of the information in Table 1 has changed over the course of the project, as the profilers have been adjusted for better performance, but is up to date at the time of writing (March 2000).

PROFILER	LAT	LON	BASE	MAX	DZ	DT
ABERYSTWYTH	52.42N	4.00W	1700m	16700m	150.0m	12'
CAMBORNE	50.13N	5.10W	305m	8202m	202.5m	30'
CAMBORNE	50.13N	5.10W	189m	2155m	57.8m	30'
DUNKESWELL	50.87N	3.23W	549m	8329m	202.4m	30'
DUNKESWELL	50.87N	3.23W	376m	2284m	57.8m	30'
PENDINE	51.75N	4.52W	325m	8014m	404.7m	30'
PENDINE	51.75N	4.52W	115m	2038m	101.2m	30'
CABAUW	51.95N	4.88E	622m	5276m	202.4m	60'
CABAUW	51.95N	4.88E	137m	1930m	57.8m	60'
LA FERTE VIDAME	48.61N	0.87E	1848m	16848m	500.0m	60'

Table 1: The profiler sites for which statistics are currently available. The BASE and MAX parameters refer to the heights over which the profiler may be active, although frequently there are missing data because the reflected signal is too weak. The DZ parameter is the sampling height (metres) and the DT column gives the time between successive obervations in minutes.

Profiler BUFR data to hourly-averaged data

For a direct comparison with the Unified Model, the profiler data need to be somehow averaged so that the time resolution matches that of the UM data which are available hourly (initially, 24 hours of profiler BUFR encoded data are converted to a single pp-file format for subsequent processing; the procedure is outlined in Appendix B).

The hourly averaging procedure is as follows:

Take a normalised, hourly average (d_0), centred on each hour, of the profiler data (d_j), according to

$$< d_0 > = \left(\sum_j w_j d_j \right) \Big/ \sum_k w_k \qquad \text{(eq. 1)}$$

(it is implicitly assumed that all parameters and variables are also a function of height.) The weights w_j are calculated by applying a triangular filter centred on the hour (t_0), namely

$$w_i = 1 - 2\|t_0 - t_j\|, \quad t_0 - 1/2 < t_j < t_0 + 1/2$$
$$w_i = 0, \qquad \textit{elsewhere}$$

with t_j measured in fractional hours, so that profiler data nearer the hour get a greater weighting accordingly, and profiler data greater than 30 minutes away from the hour make no contribution to the hourly mean. There is no vertical averaging

Figures 1 and 2 are the 12 minute and hourly-averaged Aberystwyth data (obtained from the 12 minute data) for July 31st 1999. Inevitably, a certain amount of fine structure seen at high temporal resolution is lost during the averaging process. These and subsequent figures have been plotted using JPLOT running under IDL (Panagi & Dicks, 1997 – this document can be viewed at http://www.meto.gov.uk/mm0100/~appp/uwern/jplot)

surface pressure (p*), orographic height (φ*), temperature (T), u-wind, v-wind, ω and specific humidity (q)

all on model (numerical η) levels, w.r.t. the horizontal grid

From this basic set of model parameters, we can derive various diagnostics from which the winds will be used for a direct comparison with the profiler data. We use the MDIAG suite of programs at JCMM (Panagi & Dicks, 1997, http://www.meto.gov.uk/mm0100/~appp/uwern/mdiag) to compute the diagnostics.

The procedure is as follows:

1. Re-map UM data on model levels onto a uniform 50mb grid between 1000mb and 50mb.
2. Convert ω (Pa/s) to vertical velocity w (m/s) assuming the hydrostatic relation $w = -\omega / \rho g$.
3. Convert u and v on the horizontal grid to westerly and southerly and compute the magnitude and direction from the components.
4. Extract a 24-hour time-height cross-section of the winds at each of the profiler sites (in fact the nearest UM grid point is used).
5. Re-map the time-height cross-sections from pressure (mb) to height (m) using the same vertical resolution as the profiler.

The final product is a 24-hour time-height cross-section of the winds u, v, w, horizontal speed and direction at hourly intervals at each of the profiler sites, starting at 00Z and finishing at 24Z on each day (more details can be found in Appendix A).

Table 2 below lists altitude information for both the actual profiler and nearest UM Mesoscale model altitude.

Station	Lat	Lon	Ht	Nearest MES		MES Ht
Aberystwyth	**52.42**	**-4.00**	**50**	**52.44**	**-3.96**	**178**
Camborne	**50.13**	**-5.10**	**88**	**50.11**	**-5.09**	**0**
Cabauw	**51.95**	**4.88**	**0**	**52.00**	**4.82**	**3**
Dunkeswell	**50.87**	**-3.23**	**253**	**50.91**	**-3.21**	**195**
Pendine	**51.75**	**-4.52**	**7**	**51.77**	**-4.47**	**41**
La Ferte Vidame	**48.61**	**0.87**	**245**	**48.66**	**0.81**	**217**

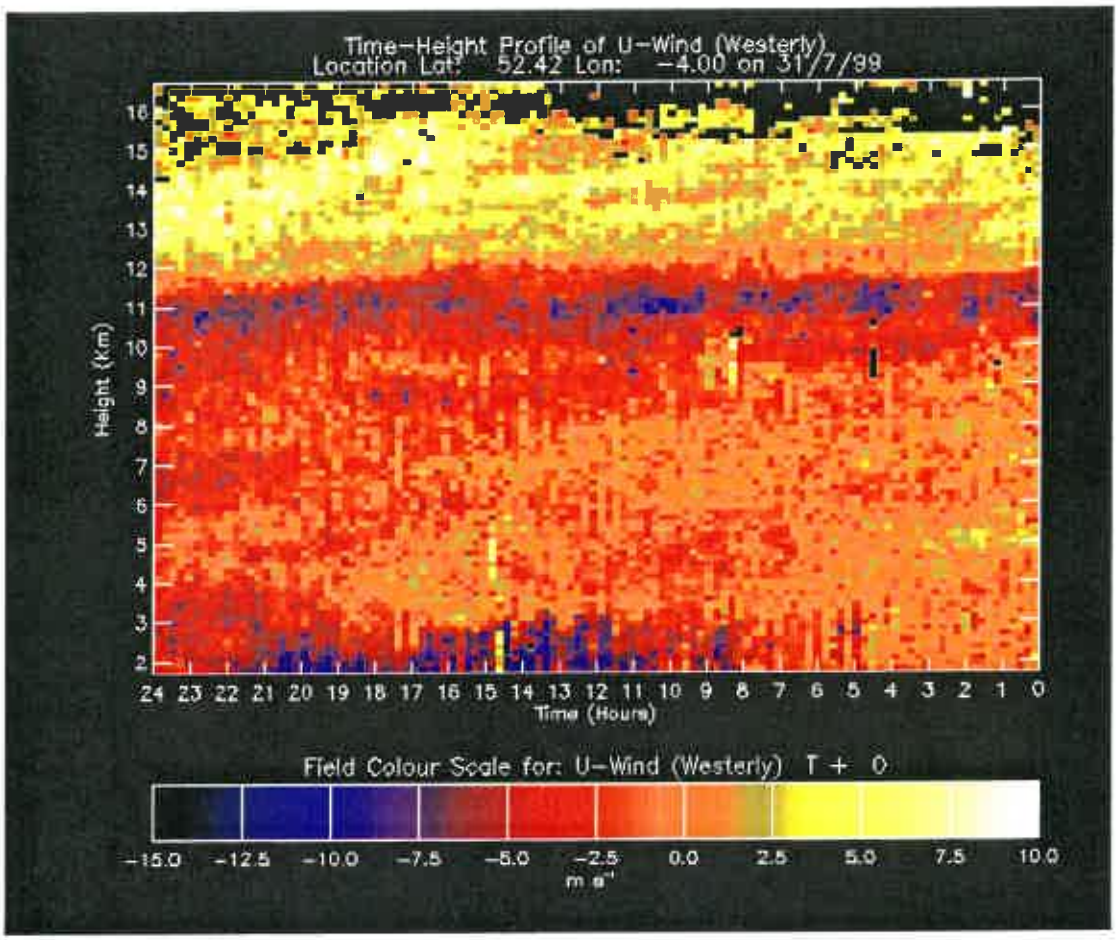

Fig.1: 12-minute resolution Aberystwyth MST profiler horizontal u-wind data for 31st July 1999. Black areas at high altitudes indicate missing data.

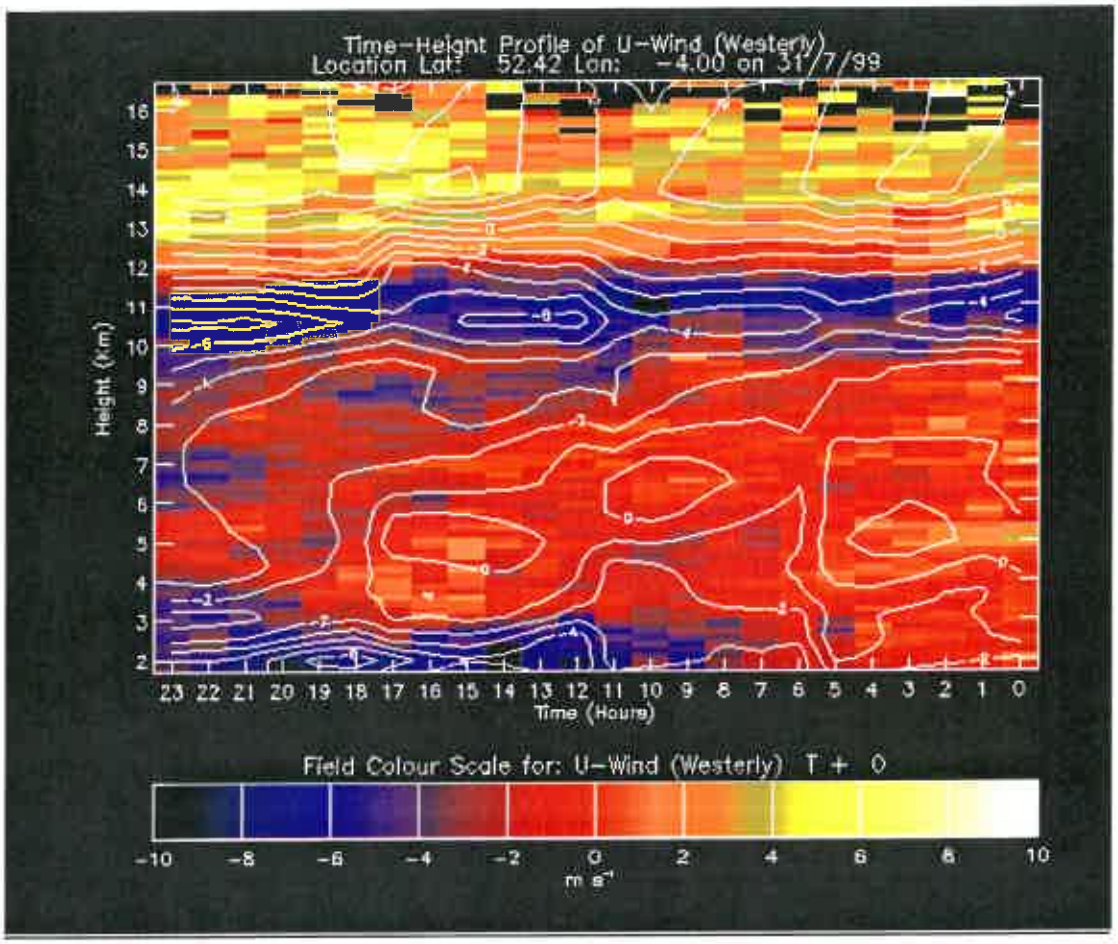

Fig. 2 Hourly-averaged Aberystwyth MST profiler u-wind data for 31st July 1999, obtained from the 12-minute data calculated according to (eq. 1). Overplotted are contours of the Unified Model u-wind extracted at the nearest point to the profiler (following section).

Unified Model Mesoscale data

The Unified Model Mesoscale area, since June 1998, covers a 146x182 horizontal and 38-level vertical domain, on a rotated latitude/longitude grid. The approximate horizontal grid resolution is 0.11x0.11 degrees, or about 12.8km. Figure 3 below shows the u-wind at 850mb over the UK mesoscale domain at 12Z on July 31st 1999.

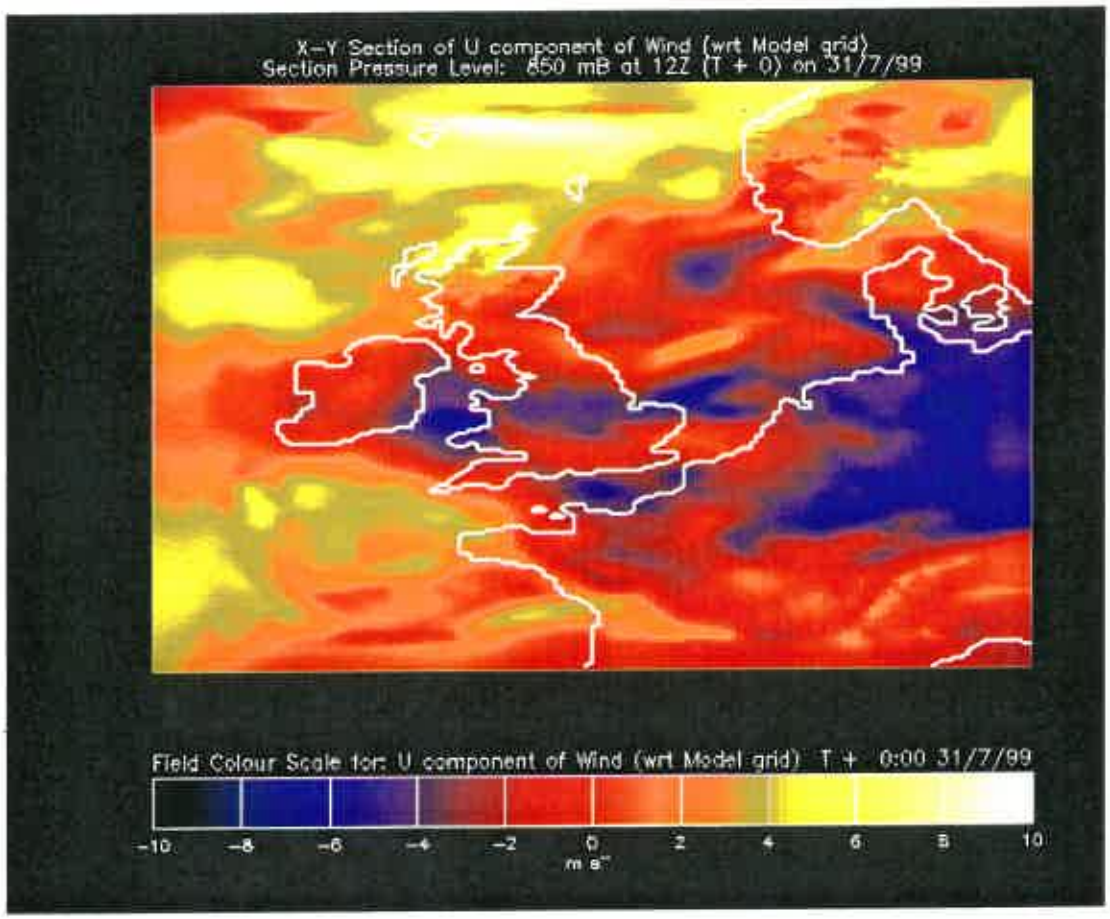

Figure 3: The UK mesoscale domain. Plotted is the u-wind at 850mb at 12Z on 31st July 1999.

The UM UK mesoscale domain data are available daily as four forecasts generated at 00Z, 06Z, 12Z and18Z. Each forecast provides analyses and hourly forecasts for T+0, T+1,....T+5 (in fact, the forecasts go out to T+36, but forecasts beyond T+5 are of no relevance to this project at present).
Each forecast provides the following fields

Computed Statistics

We compute daily statistics, for each of the sites, for each forecast T+0, T+1, ... T+5; this is as a sum of the first 5 hours of the 4 forecasts starting at 00Z, 06Z, 12Z and 18Z. In particular, we compute a mean of the magnitude of the difference between profiler and UM over some period P, namely

$$MEAN = \frac{1}{N}\sum_{P}(profiler - UM)$$

as a function of height, and an average of the RMS deviation between profiler and UM over a period P, namely

$$RMS = \sqrt{\frac{\sum_{P}(profiler - UM)^2}{N}}$$

also as a function of height. Here, N represents the number of observations that make a contribution, since there may be missing data at certain times and heights due to insufficient signal from the profiler.

Monthly-averaged results

The following show monthly means and the monthly RMS deviation of u-wind, v-wind, wind speed and direction for the months March 1999 to March 2000, for the profilers Aberystwyth (ABWWP), Cabauw (CABWP), Camborne (CAMWP), Dunkeswell (DUNWP), La Ferte Vidame (LFVWP) and Pendine (PENWP). The plots are for deviations between profiler and model analyses (T+0).

The labelling and format of the plots is as follows:
(a) – (d) show the mean difference averaged over the month as a function of height.
(e) – (h) show the RMS deviation averaged over the month as a function of height.
The titles indicate which field is being plotted, the abcissa units are the year and month over which the average is made (YYMM) and the ordinate the height.

The plots have been grouped by profiler, so that there is continuous record of each profiler over the period for which we have been able to derive statistics.

The final sets of plots, Figures 75-79, show the mean monthly RMS deviation (ABWWP-UM) of each of the 6 forecasts T+0, T+1 ..... T+5 of the wind speed, direction, vertical velocity, u-wind and v-wind, for the month of July 1999.

DAILY ARCHIVES

In addition to the daily profiler statistics, we produce hardcopy archives of various diagnostics, derived from the UM data, with a view to producing 2 or 3 case studies that will show the potential impact that profiler observations may have on the UM forecast. Also, it may be possible to categorise any significant differences between profiler and UM into a small number of distinct weather events/types. In addition, the daily hardcopy archive will include precipitation maps from the UK network radar, to supplement understanding. The case studies will be presented elsewhere.

APPENDIX A

UNIX scripts, FORTRAN programs and directory structure

The 6-hourly UM forecasts from T+0 to T+5 are copied across to

/data/rs0200/oppp/${DATE}.${FC}Z.pp

some 1-2 hours after their availability on COSMOS. The extraction of the required fields from the rolling UM fieldsfile archive, and the subsequent transfer to the HP workstation RS0200 is regulated by 4 "cron" scripts, residing as

/home/rs0200/oppp/Scripts/get.${FC}Z.scr

Thus for each day we obtain 4 mesoscale forecast files, from T+0 to T+5, of the fields $p*, T, u, v, q, \omega, cldlwc, cldice, orography$, all on model η-levels. Each file is approximated 165Mb in size.
The model-level files are then run through the program MDIAG (Panagi & Dicks, 1997) to re-map data onto constant pressure surfaces, and then generate the following diagnostics on 50hPa pressure surface between 1000hPa and 50hPa

$u-wind \quad u$

$v-wind \quad v$

$wind \ \ speed \quad V=\sqrt{u^2+v^2}$

$wind \ \ direction$

$$absolute \ \ vorticity \quad \xi=\frac{1}{a\cos\varphi}\left(\frac{\partial v}{\partial\lambda}-\frac{\partial(u\cos\varphi)}{\partial\varphi}\right)+f$$

$$vertical \ \ velocity \quad w=-\frac{\omega}{\rho g}$$

$potential\,temperature \quad \theta$

$\partial\vartheta/\partial p$

$wet-bulb\ potential\,temperature \quad \vartheta_w$

$$dry \ \ PV \quad Q=-g\left(-\frac{1}{a\cos\varphi}\frac{\partial v}{\partial p}\frac{\partial\theta}{\partial\lambda}+\frac{1}{a}\frac{\partial u}{\partial p}\frac{\partial\theta}{\partial\varphi}+\frac{\partial\theta}{\partial p}\xi\right)$$

$$dry \ \ static \ \ stability \ N^2=-\frac{\rho g^2}{\theta}\left(\frac{\partial\theta}{\partial p}\right)$$

$moist \ \ static \ \ stability$

$geopotential \ \ height$

$relative \ \ humidity \ \ w.r.t. \ \ ice$

$cloud \ \ liquid \ \ water$

$cloud \ \ ice$

The resulting files named according to the convention

/data/rs0200/oppp/${DATA}.${FC}Z.pp.mdiag

After the 18Z forecast has been copied and the diagnostics computed, the TIME-HEIGHT cross-sections at the profiler sites are extracted by re-mapping the pressure-level fields onto a height field (metres) that matches the vertical sampling of the individual profiler. At this stage, the model-level data are archived onto DLT for potential use as case studies.

The next stage is to hourly-average the profiler data and compute differences with the UM data. The time-height data and difference data are ftp'd across from rs0200 to mm0600 where subsequent IDL procedures plot the daily archive of required fields.

All commands and programs are executed using the CRON scripts

/home/rs0200/oppp/Scripts/get.${FC}Z.cron

APPENDIX B

Conversion of Profiler BUFR data to PP format.

A generic conversion program has been written to convert BUFR encoded data from the profiler sites to PP format data (time versus height), and can potentially be used for any profiler site.

The first thing to note is that, for plotting purposes, the PP format data arrays must be regular in both time and height. This means that for each individual site it must be decided a-priori as to the number of required data dimensions in the time and height senses. These values are set in the conversion program (a set for each profiler site) so the process knows exactly how much data to expect and hence can act accordingly if any data items and/or data files are missing. These dimensions are set by assigning a nominal time interval (dt) to the profiler site (this is usually trivial as the dt is usually constant, and in fact only varies slightly for site ABWWP). The range in time is always from 0Z to 0Z on the following day, hence with the nominal dt we can work out how many time points (Nt) are required. The height dimension is decided upon by taking the lowest available height up to some pre-decided maximum height (dz is always constant), hence giving the number of height points Nh. All fields written to the PP format files are then of dimension Nt by Nh.

If any data items or data files are missing then the conversion program assigns an appropriate missing data indicator to the relevant entries of the data arrays. Also, if the data quality flags are set in the BUFR files to indicate poor quality data then these data items are not used, and instead the missing data indicator is used. Also, the profiler site ABWWP sometimes delivers data at an increased time increment to the usual, (for example 15 minutes compared to the usual nominal 12.75 minutes). When this happens the resultant PP data set cannot be used as the assignment of data becomes irregular; if this is detected a warning message is written to the log file.

The conversion of the BUFR data to PP format has been automated in a "cron" job. This spawns 3 "at" jobs, 2 of which perform the data conversions and the other the generation of an

automatic log file (1 for each day and containing all sites) which summarises the amount of missing data.

At present, the profiler sites are processed in 2 batches, hence the 2 "at" jobs. The first processes sites ABWWP, CAMWP, CB2WP, DUNWP, DN2WP, PENWP, and PN2WP, whilst the second job processes sites CABWP, CB2WP and LFVWP. The second job is run 24 hours later than the first job as some of the required data has not arrived in time for all the sites to be processed together.

The data processing takes place on the HP machine rs0200 at the Beaufort Park site, all code and scripts reside in directory

/data/rs0200/cwinde/bin

The cron script is: master_ppf

This calls the script makeppf for each site, for example to process data for 26/01/99 and site ABWWP the calling sequence would be:

ksh makeppf ABWWP 1999 01 26

The makeppf script then calls a Fortran executable with a separate executable existing for each site, which are compiled from the source code bufr2pp.f, using the script compile_b2p. The conversion program requires an initial data file containing the number and names of the input BUFR files, this is created by the script makeppf. The log file generation script is called makeppf_log.

ACKNOWLEDGEMENTS: Thanks to Myles Turp at Beaufort Park for making available the BUFR-encoded daily profiler data, and to Keith Browning for reviewing this report prior to publication.

REFERENCES

Panagi P.M., Dicks E.M., **1997,**
"Met. Office Unified Model data, diagnostics, graphics programs and other observational data available from JCMM through the aegis of the Universities Weather Research Network UWERN", **JCMM Internal report, 69**

Panagi P.M., Dicks E.M., Hamer G.L., Nash J., **1999,**
"Preliminary results of the routine comparison of wind profiler data with the UK Met. Office Mesoscale model vertical wind profiles", proc. 1998 EGS, The Hague, *accepted*

Fig. 4a (ABWWP–UM) u–wind

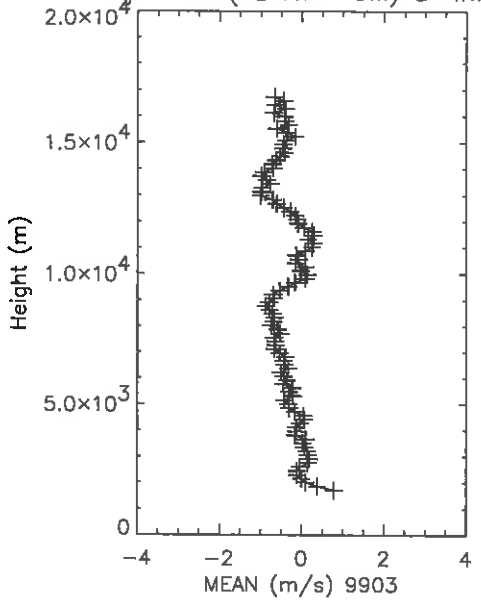

Fig. 4b (ABWWP–UM) v–wind

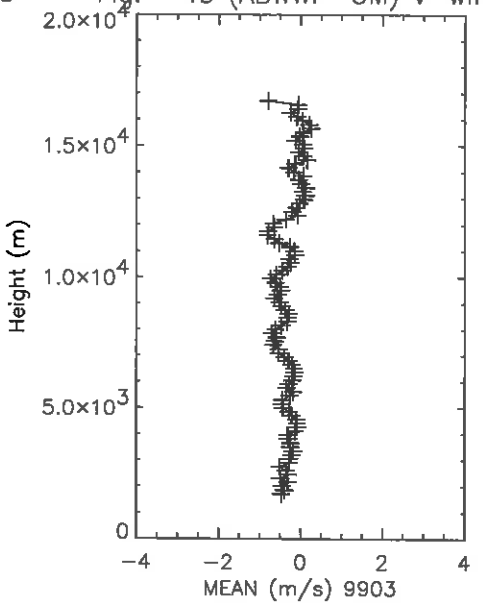

Fig. 4c (ABWWP–UM) speed

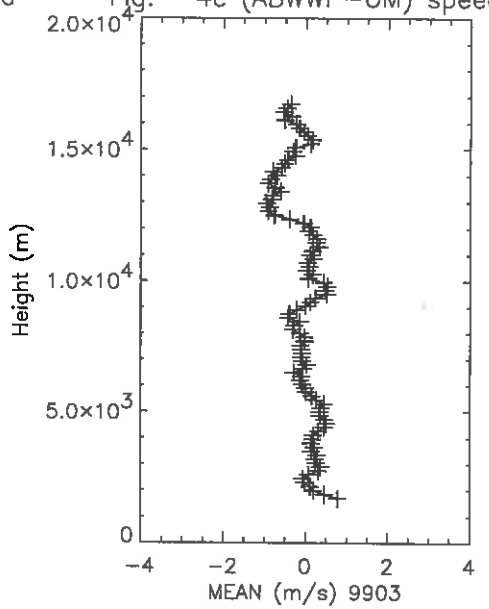

Fig. 4d (ABWWP–UM) dirn.

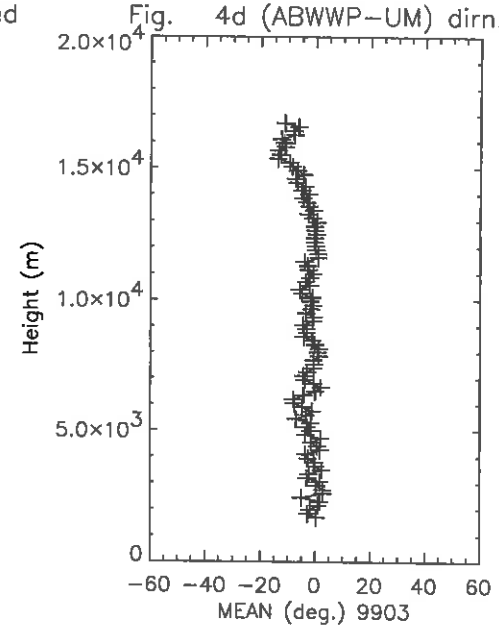

Fig. 4e (ABWWP–UM) u–wind

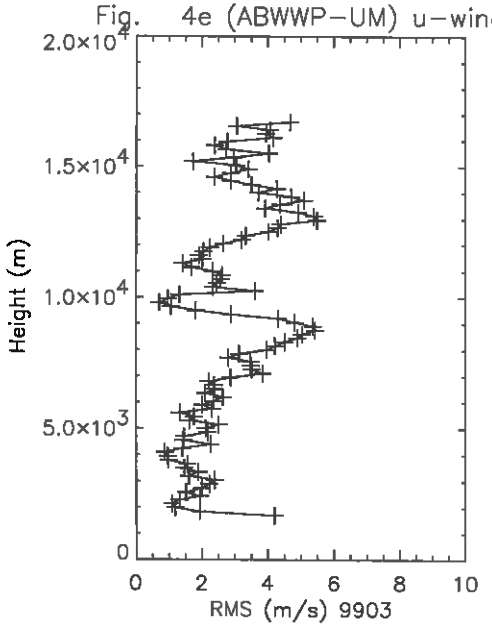

Fig. 4f (ABWWP–UM) v–wind

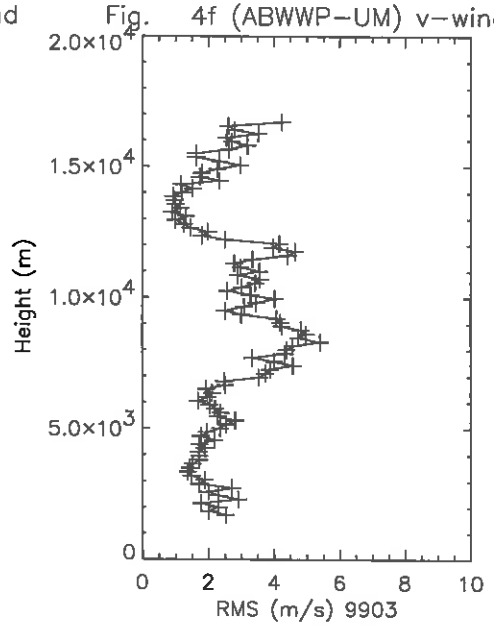

Fig. 4g (ABWWP–UM) speed

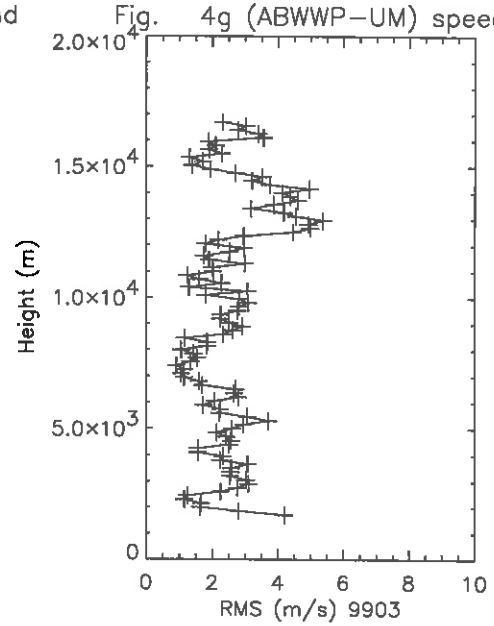

Fig. 4h (ABWWP–UM) dirn.

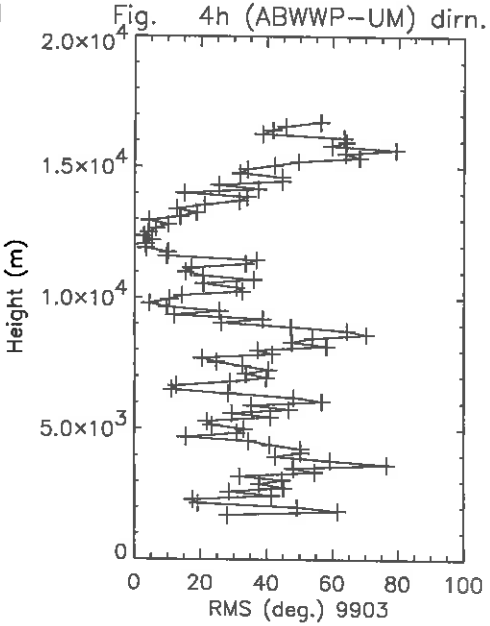

Fig. 5a (ABWWP–UM) u–wind

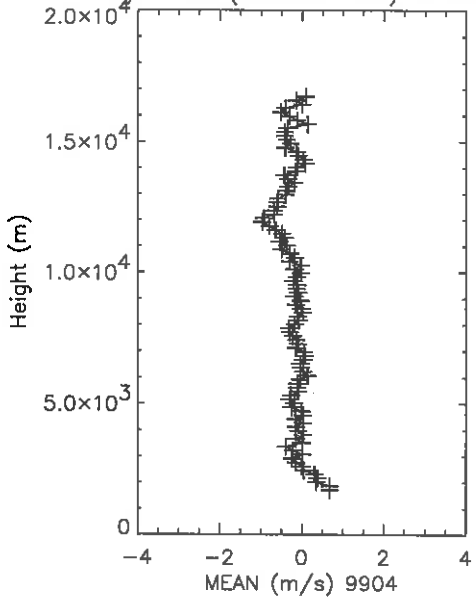

Fig. 5b (ABWWP–UM) v–wind

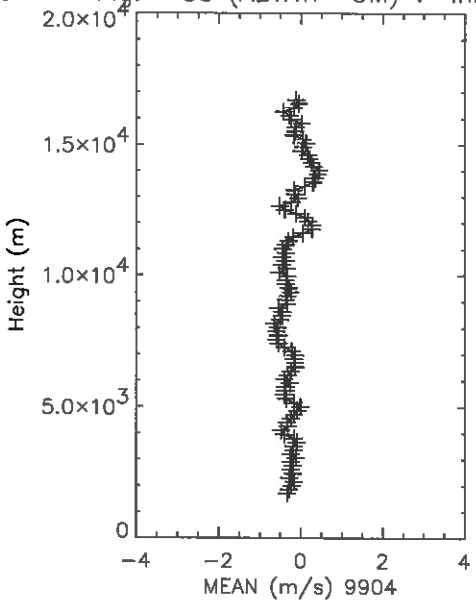

Fig. 5c (ABWWP–UM) speed

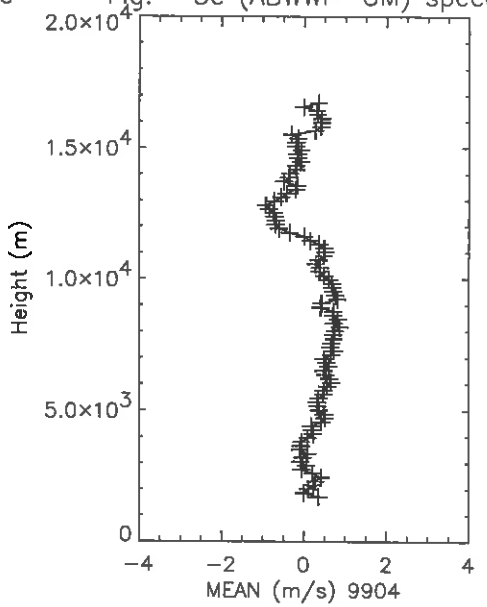

Fig. 5d (ABWWP–UM) dirn.

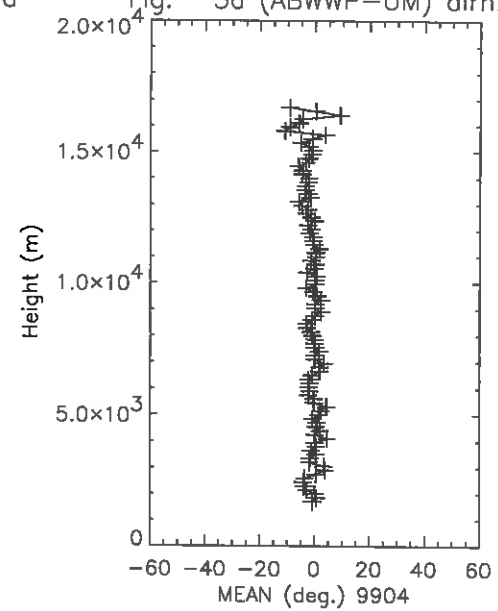

Fig. 5e (ABWWP–UM) u–wind

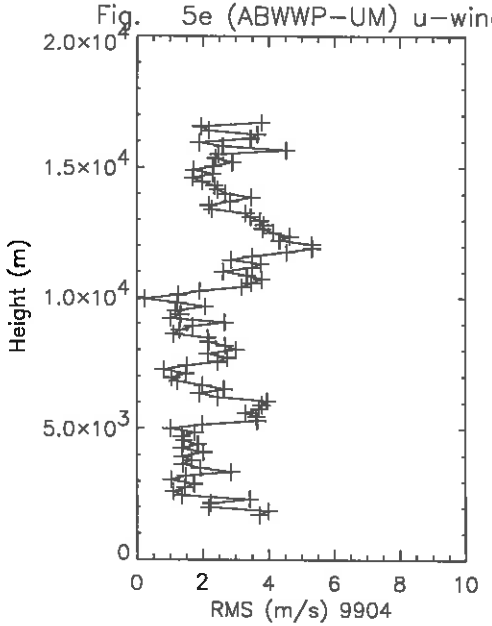

Fig. 5f (ABWWP–UM) v–wind

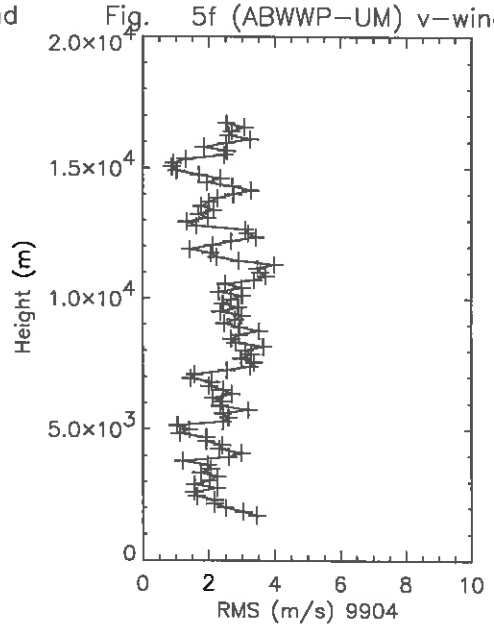

Fig. 5g (ABWWP–UM) speed

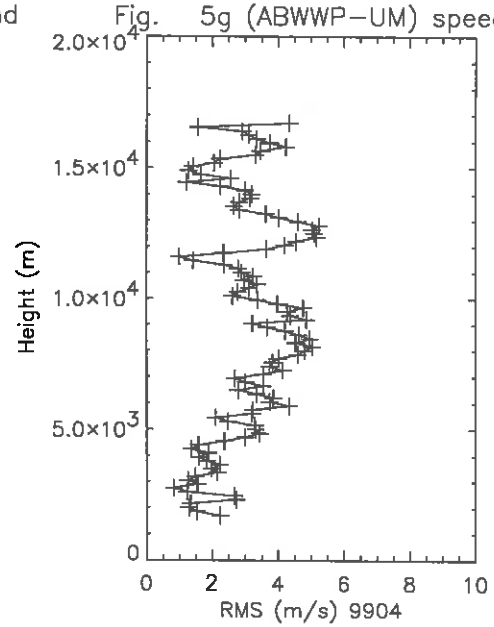

Fig. 5h (ABWWP–UM) dirn.

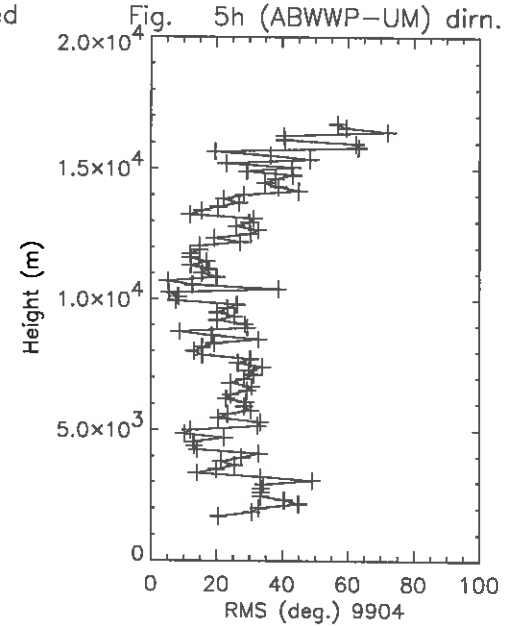

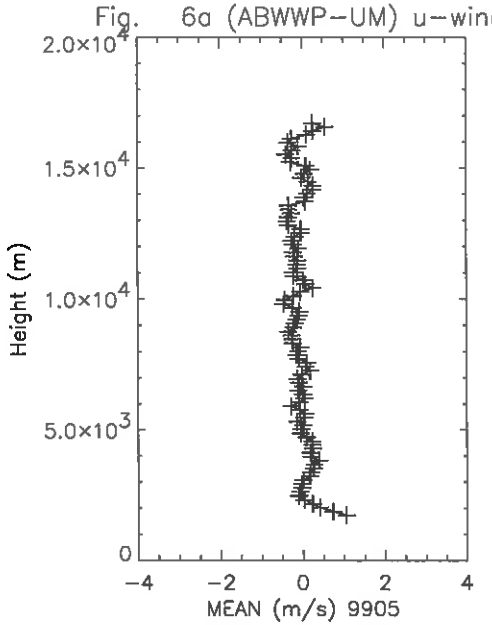
Fig. 6a (ABWWP–UM) u–wind
Height (m)
2.0×10^4
1.5×10^4
1.0×10^4
5.0×10^3
0
−4 −2 0 2 4
MEAN (m/s) 9905

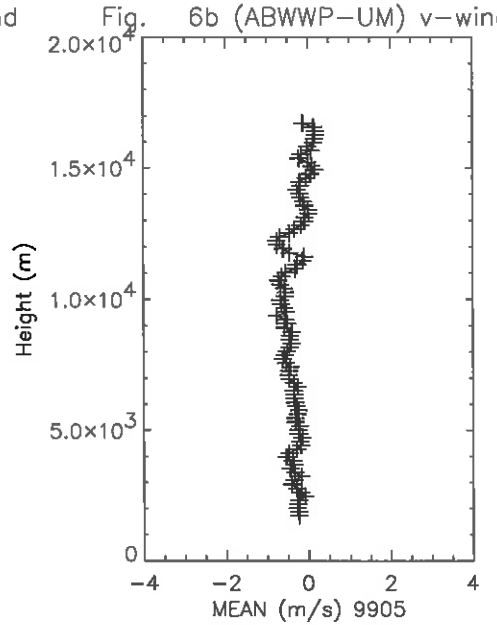
Fig. 6b (ABWWP–UM) v–wind
Height (m)
2.0×10^4
1.5×10^4
1.0×10^4
5.0×10^3
0
−4 −2 0 2 4
MEAN (m/s) 9905

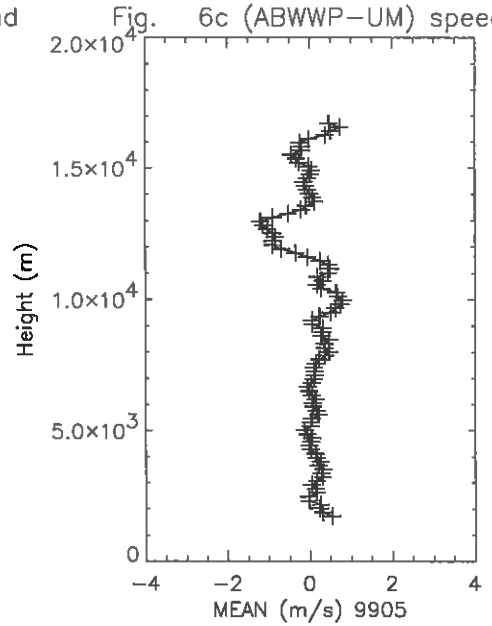
Fig. 6c (ABWWP–UM) speed
Height (m)
2.0×10^4
1.5×10^4
1.0×10^4
5.0×10^3
0
−4 −2 0 2 4
MEAN (m/s) 9905

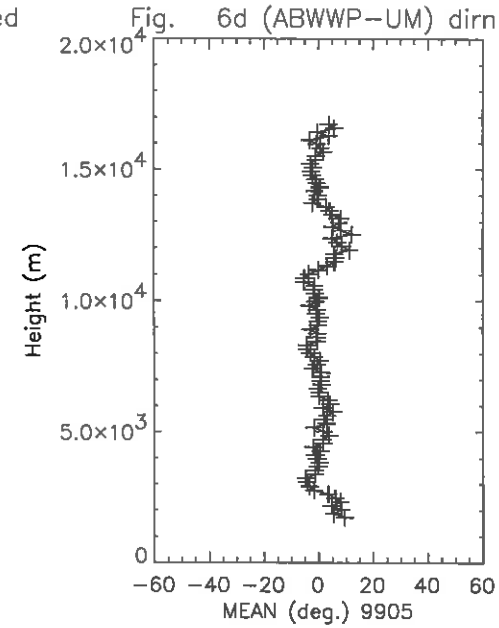
Fig. 6d (ABWWP–UM) dirn.
Height (m)
2.0×10^4
1.5×10^4
1.0×10^4
5.0×10^3
0
−60 −40 −20 0 20 40 60
MEAN (deg.) 9905

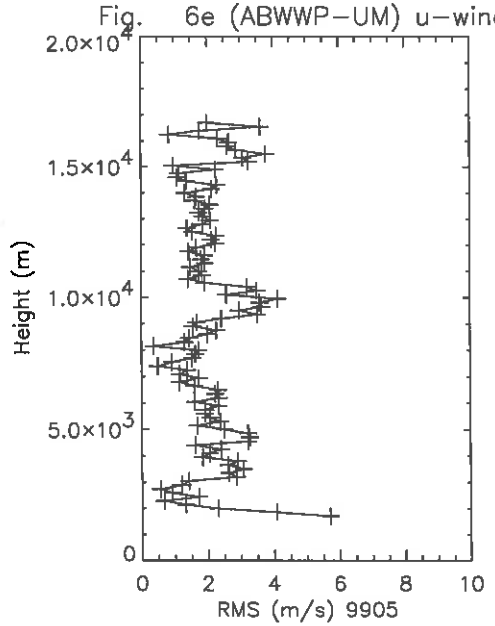
Fig. 6e (ABWWP–UM) u–wind
Height (m)
2.0×10^4
1.5×10^4
1.0×10^4
5.0×10^3
0
0 2 4 6 8 10
RMS (m/s) 9905

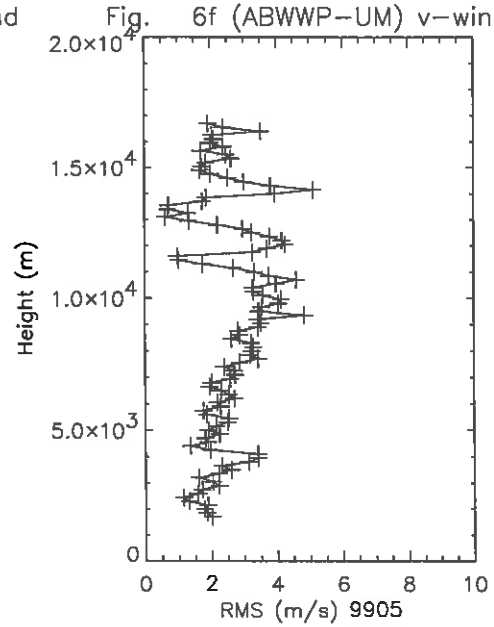
Fig. 6f (ABWWP–UM) v–wind
Height (m)
2.0×10^4
1.5×10^4
1.0×10^4
5.0×10^3
0
0 2 4 6 8 10
RMS (m/s) 9905

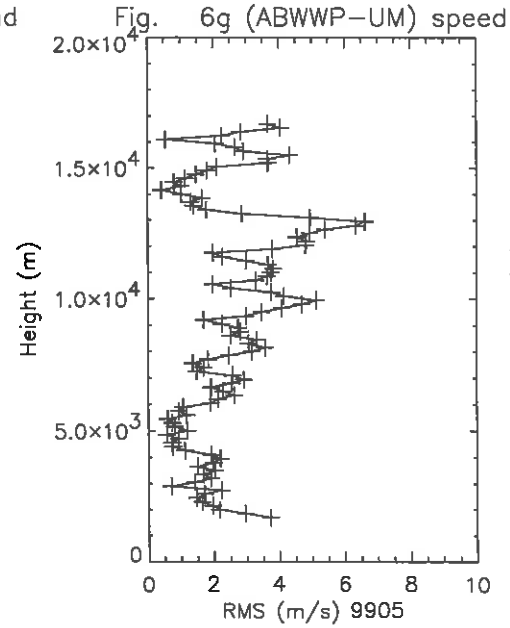
Fig. 6g (ABWWP–UM) speed
Height (m)
2.0×10^4
1.5×10^4
1.0×10^4
5.0×10^3
0
0 2 4 6 8 10
RMS (m/s) 9905

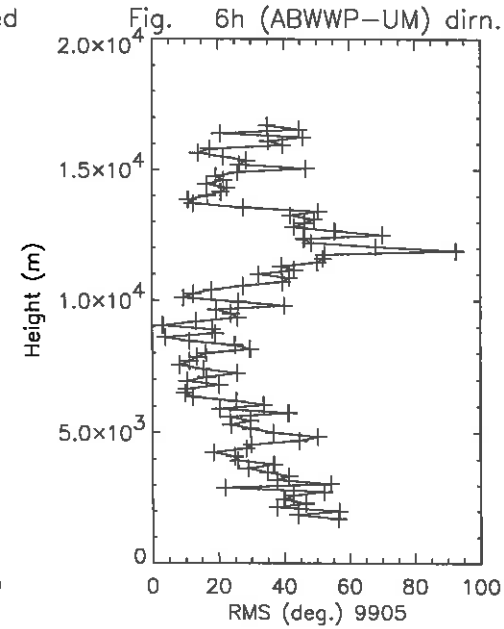
Fig. 6h (ABWWP–UM) dirn.
Height (m)
2.0×10^4
1.5×10^4
1.0×10^4
5.0×10^3
0
0 20 40 60 80 100
RMS (deg.) 9905

Fig. 7a (ABWWP–UM) u–wind

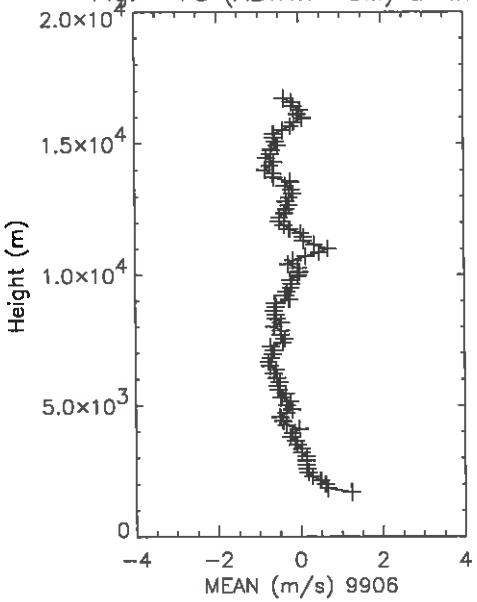

Fig. 7b (ABWWP–UM) v–wind

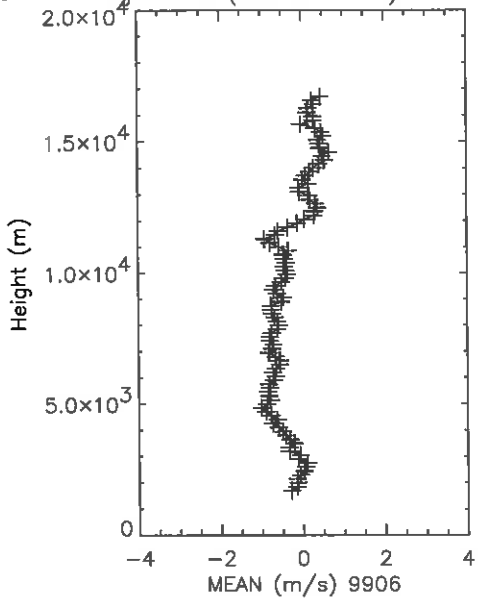

Fig. 7c (ABWWP–UM) speed

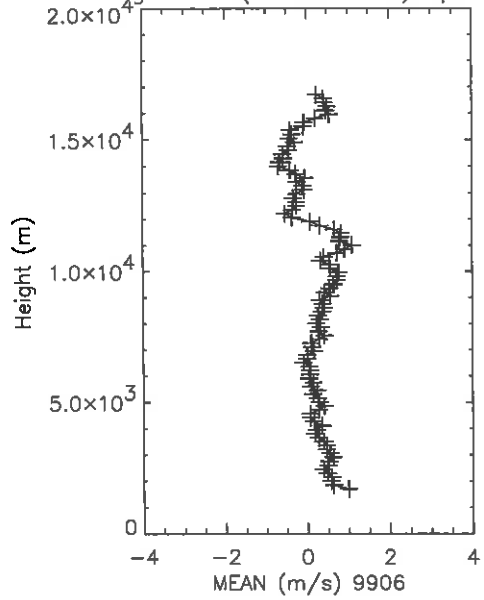

Fig. 7d (ABWWP–UM) dirn.

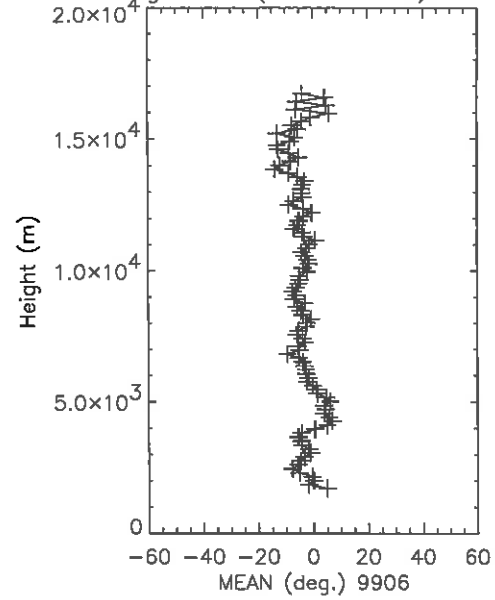

Fig. 7e (ABWWP–UM) u–wind

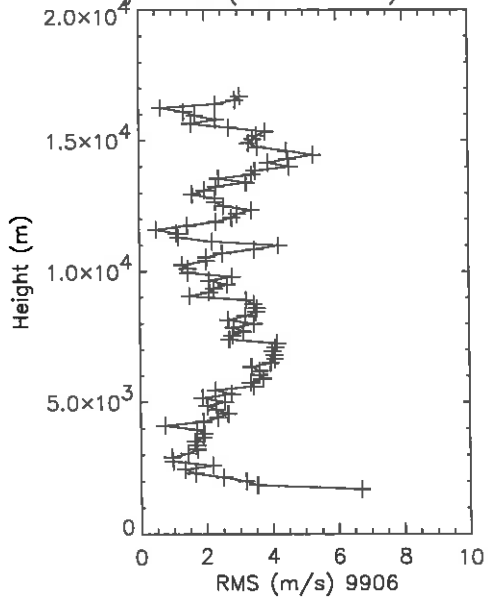

Fig. 7f (ABWWP–UM) v–wind

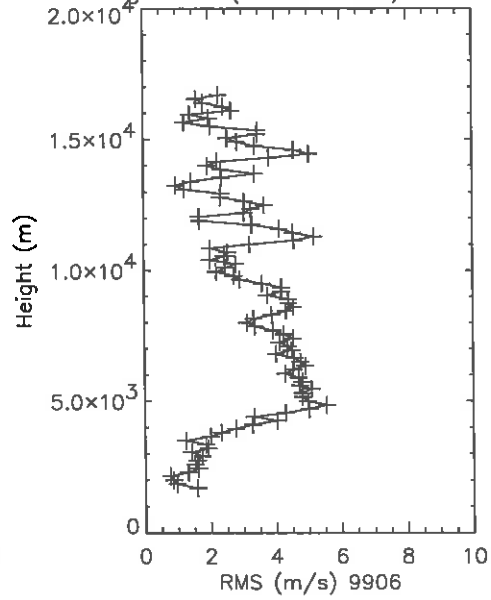

Fig. 7g (ABWWP–UM) speed

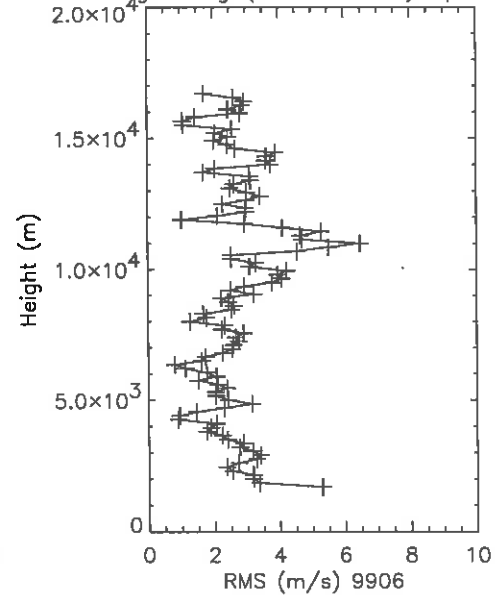

Fig. 7h (ABWWP–UM) dirn.

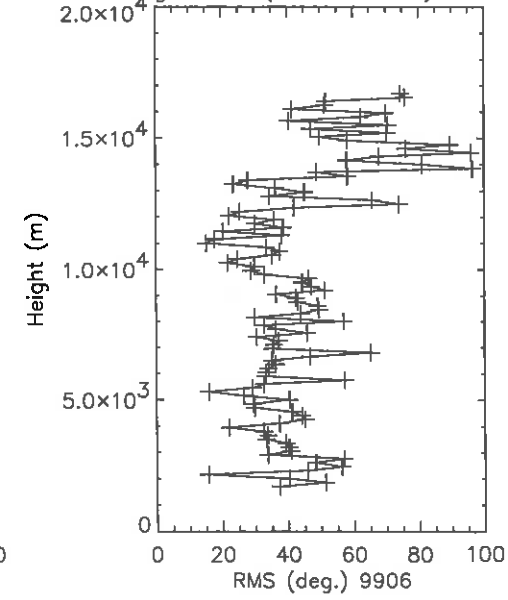

Fig. 8a (ABWWP−UM) u−wind

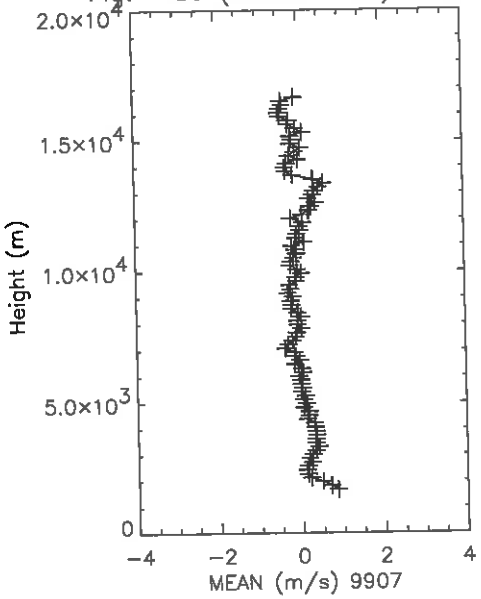

Fig. 8b (ABWWP−UM) v−wind

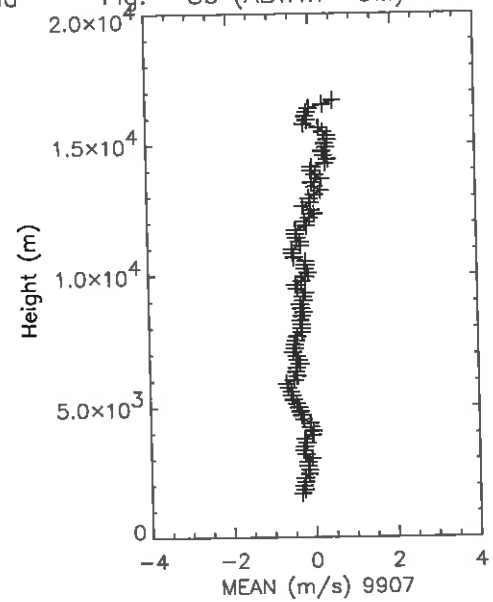

Fig. 8c (ABWWP−UM) speed

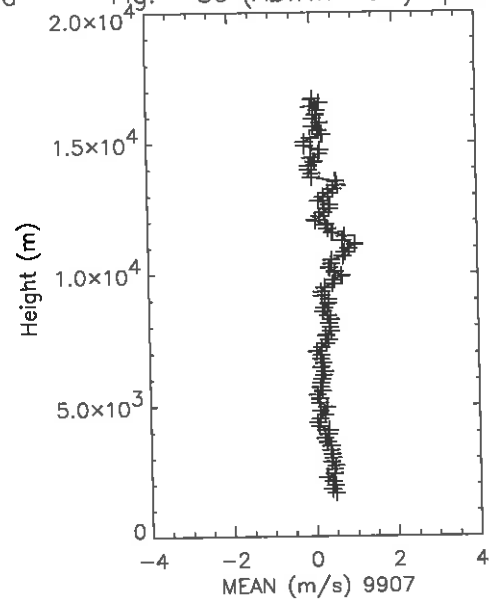

Fig. 8d (ABWWP−UM) dirn.

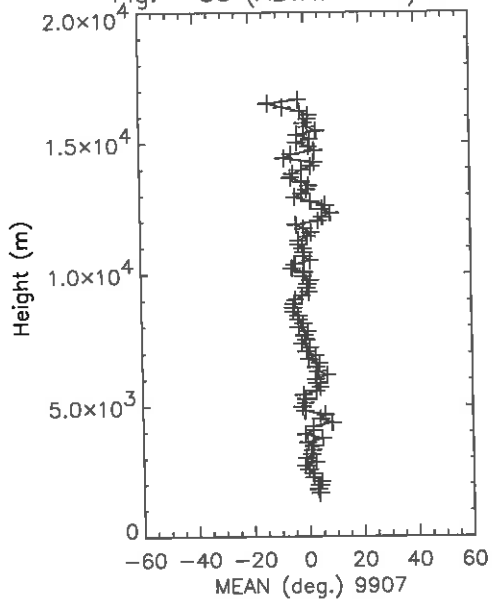

Fig. 8e (ABWWP−UM) u−wind

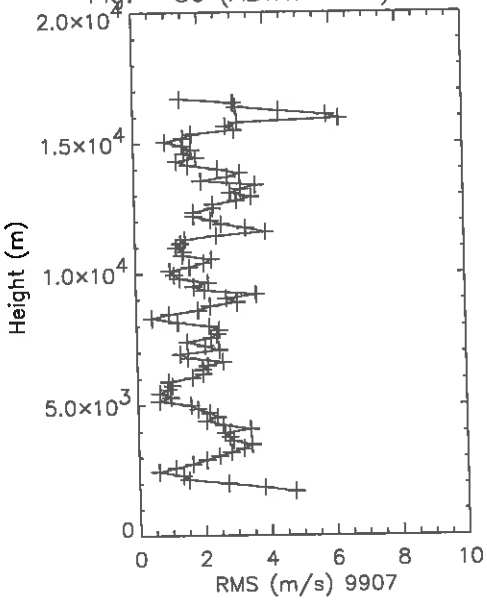

Fig. 8f (ABWWP−UM) v−wind

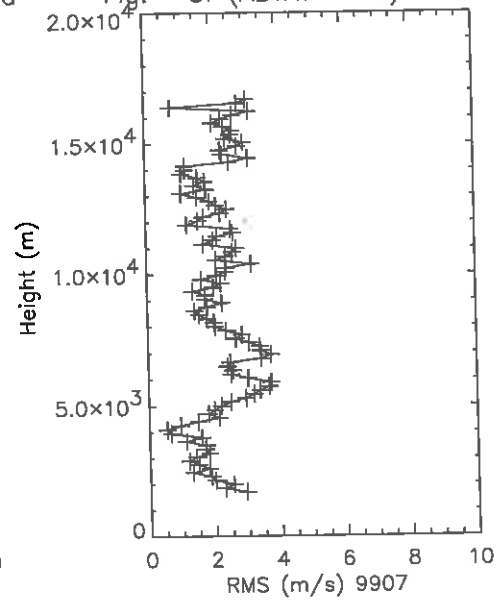

Fig. 8g (ABWWP−UM) speed

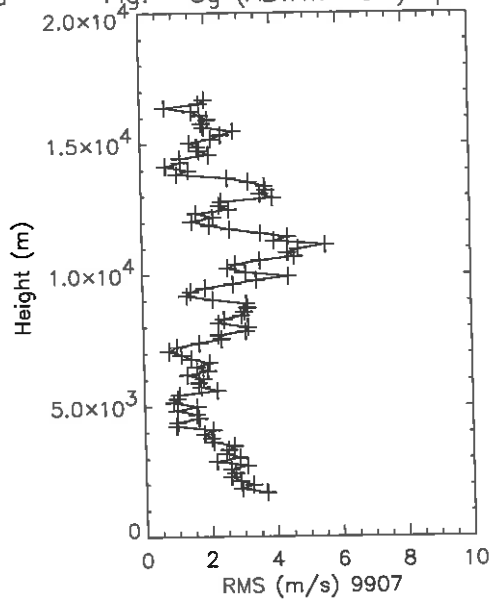

Fig. 8h (ABWWP−UM) dirn.

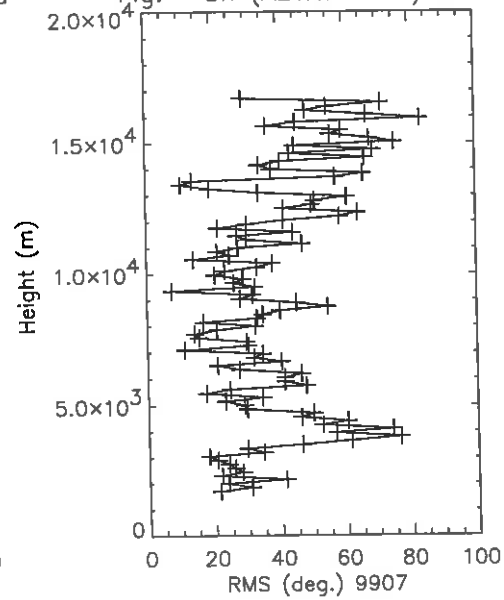

Fig. 9a (ABWWP−UM) u−wind

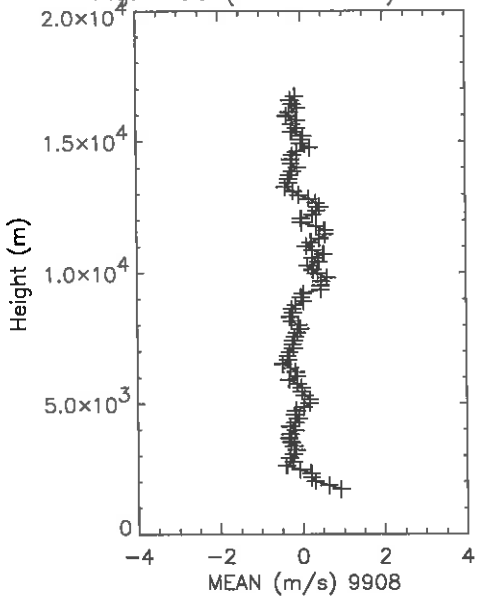

Fig. 9b (ABWWP−UM) v−wind

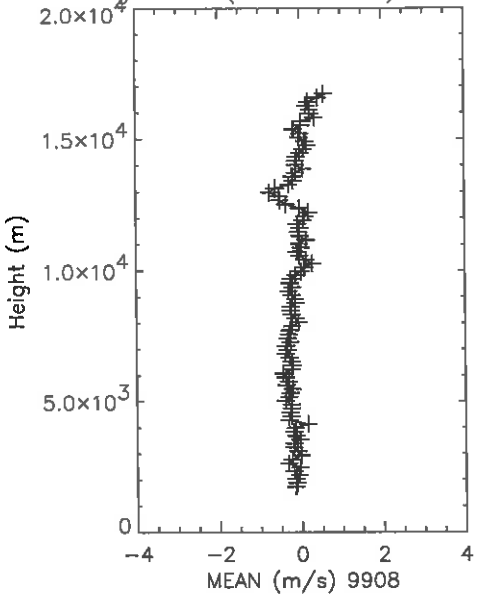

Fig. 9c (ABWWP−UM) speed

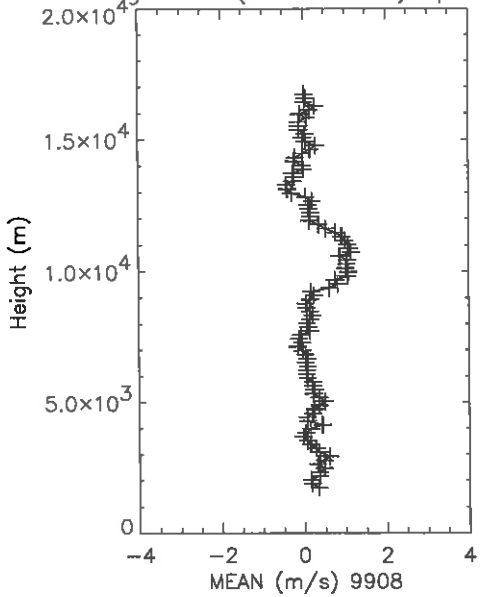

Fig. 9d (ABWWP−UM) dirn.

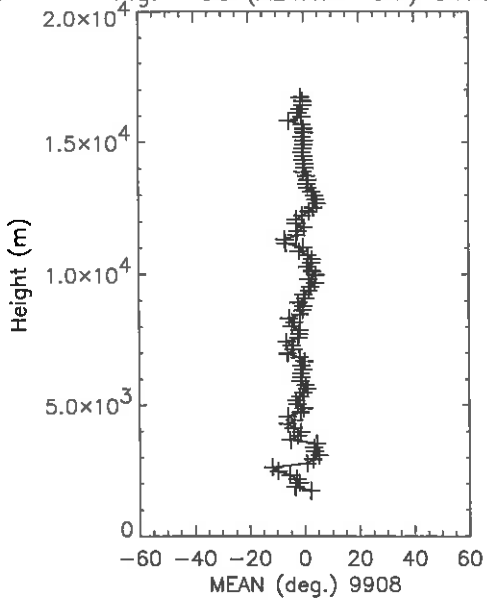

Fig. 9e (ABWWP−UM) u−wind

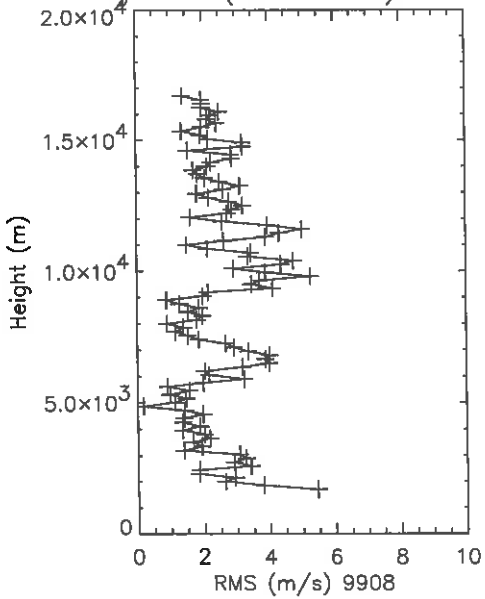

Fig. 9f (ABWWP−UM) v−wind

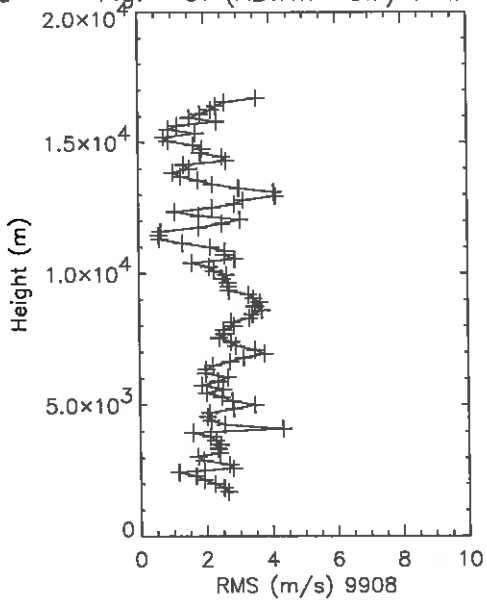

Fig. 9g (ABWWP−UM) speed

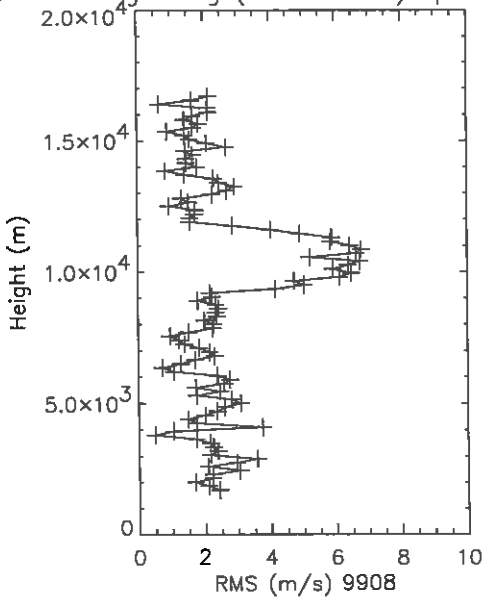

Fig. 9h (ABWWP−UM) dirn.

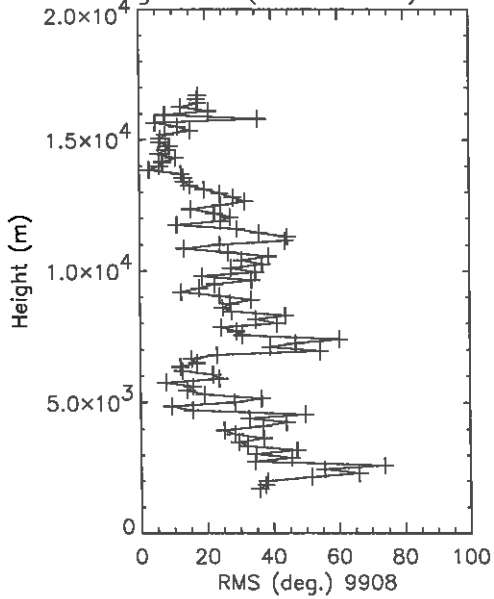

Fig. 10a (ABWWP–UM) u–wind

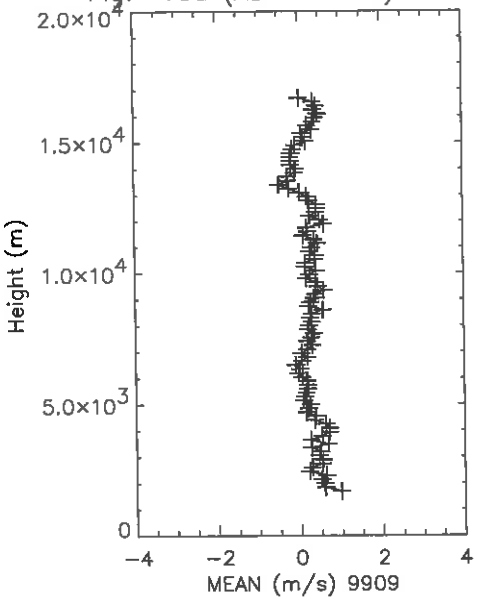

Fig. 10b (ABWWP–UM) v–wind

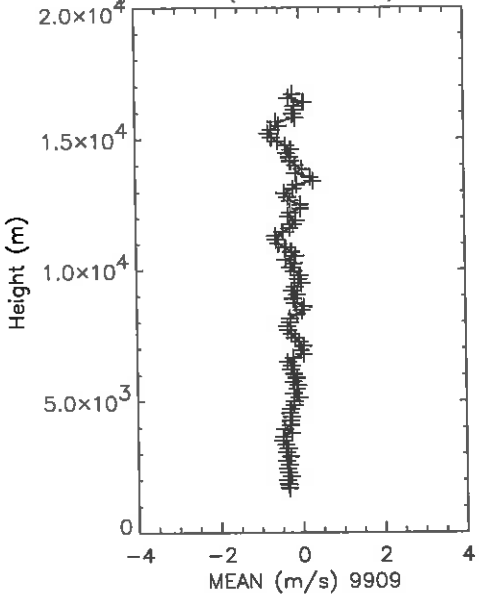

Fig. 10c (ABWWP–UM) speed

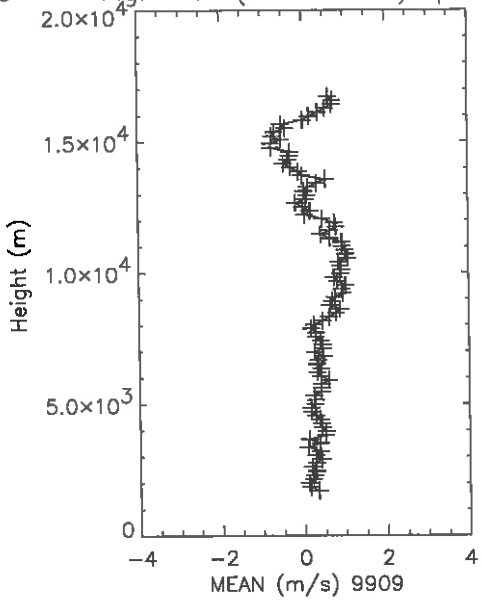

Fig. 10d (ABWWP–UM) dirn.

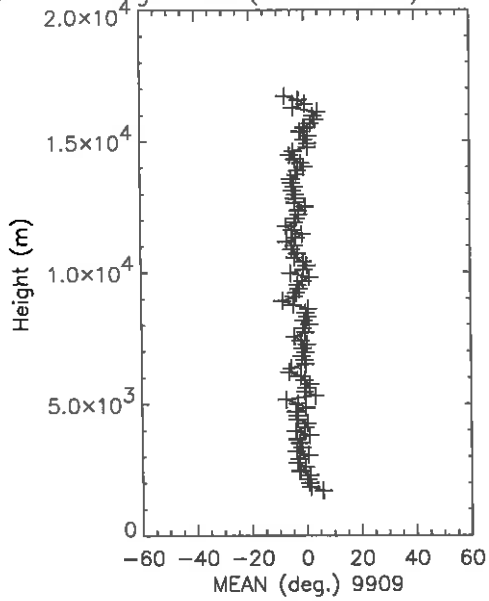

Fig. 10e (ABWWP–UM) u–wind

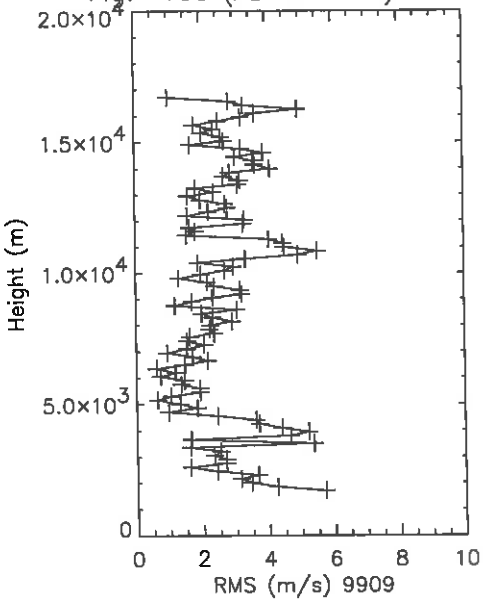

Fig. 10f (ABWWP–UM) v–wind

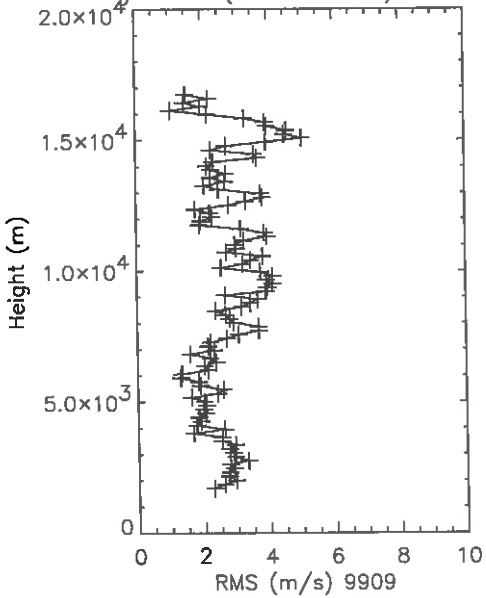

Fig. 10g (ABWWP–UM) speed

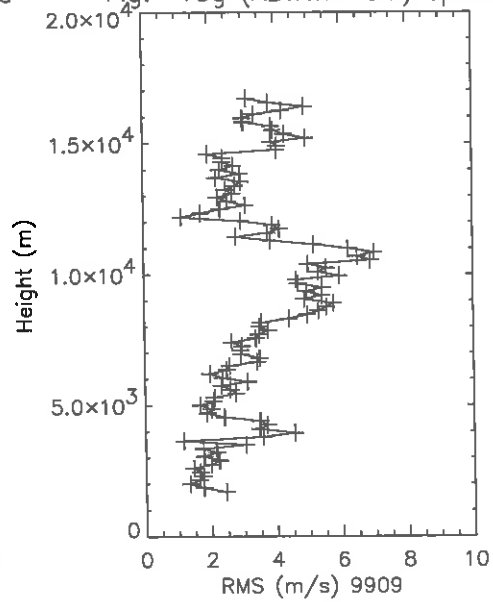

Fig. 10h (ABWWP–UM) dirn.

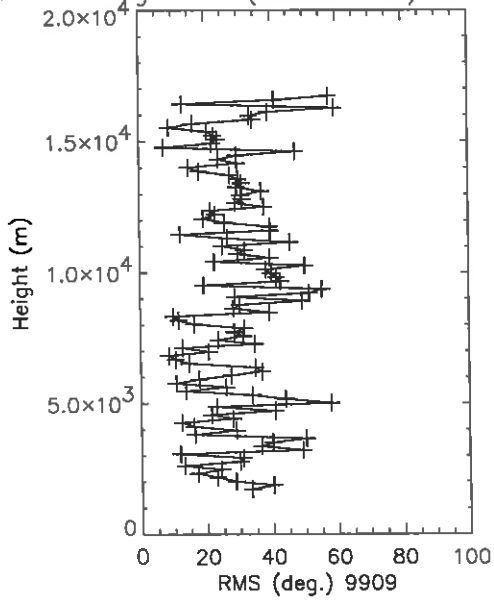

Fig. 11a (ABWWP–UM) u–wind

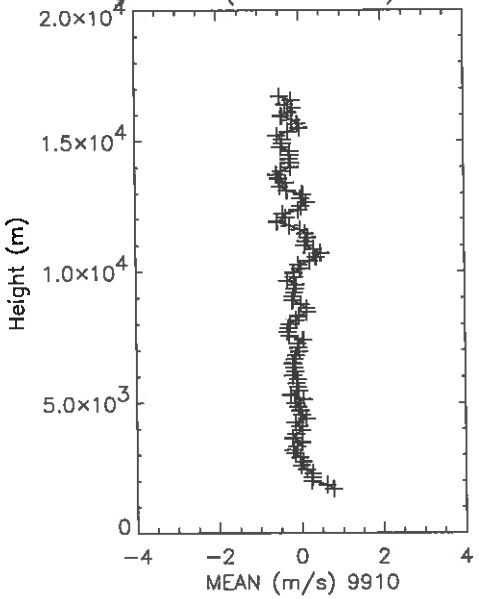

Fig. 11b (ABWWP–UM) v–wind

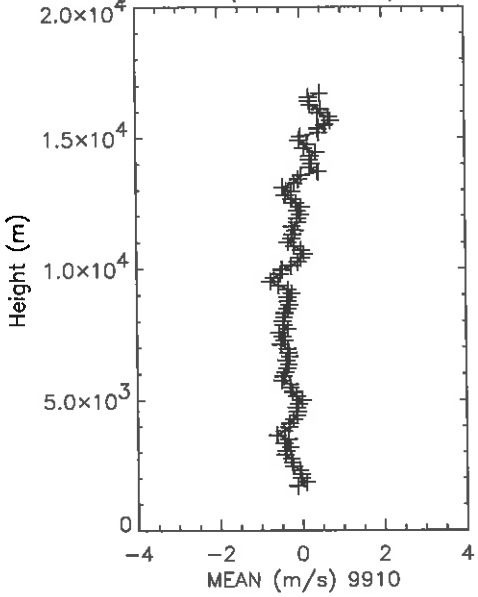

Fig. 11c (ABWWP–UM) speed

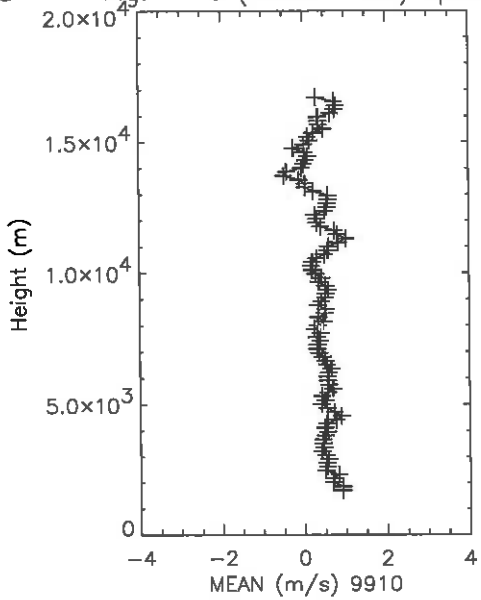

Fig. 11d (ABWWP–UM) dirn.

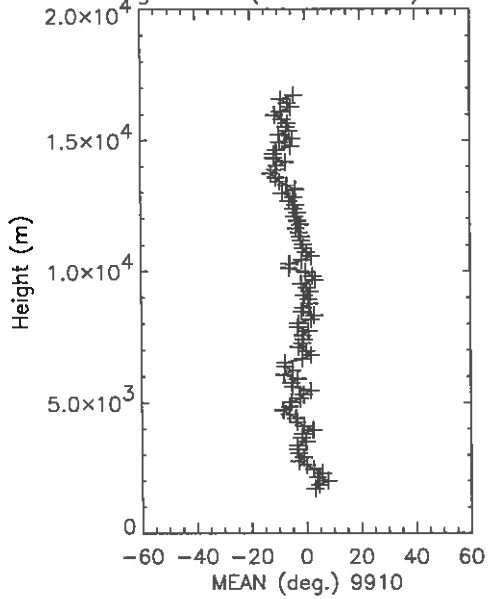

Fig. 11e (ABWWP–UM) u–wind

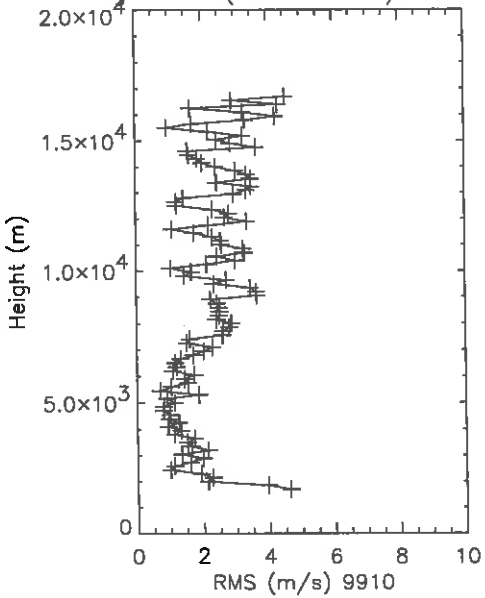

Fig. 11f (ABWWP–UM) v–wind

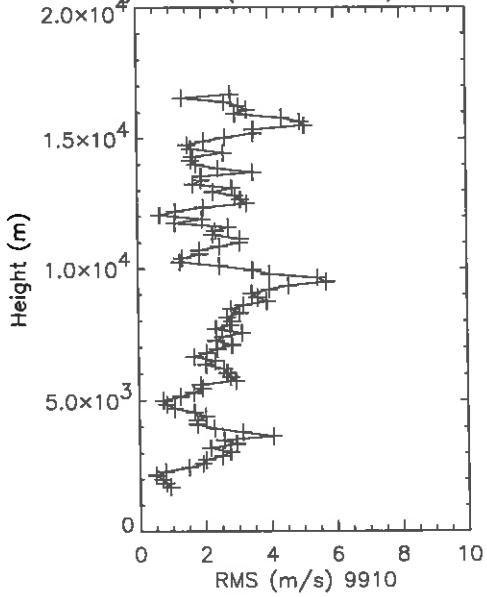

Fig. 11g (ABWWP–UM) speed

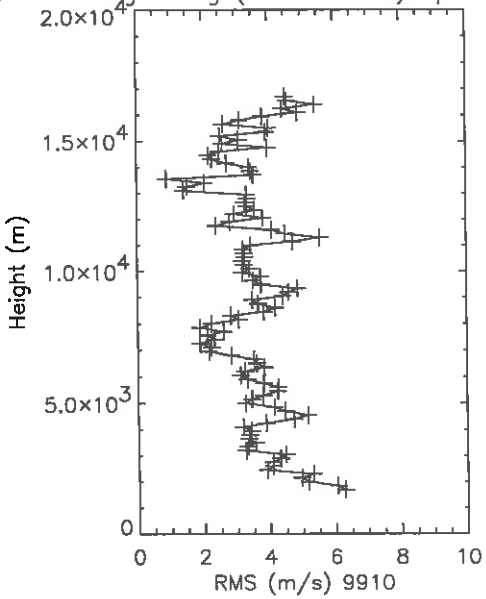

Fig. 11h (ABWWP–UM) dirn.

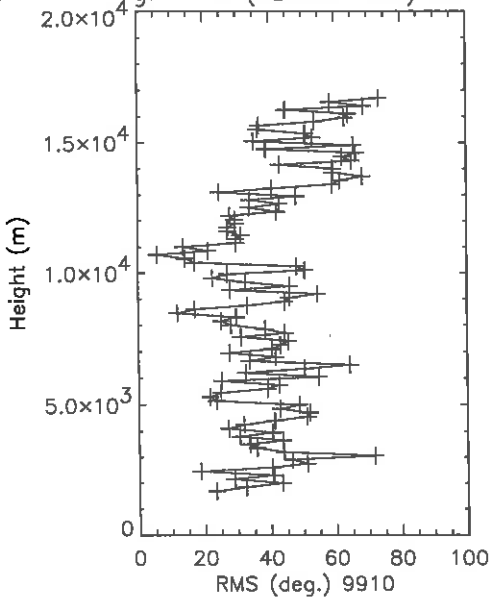

Fig. 12a (ABWWP–UM) u–wind

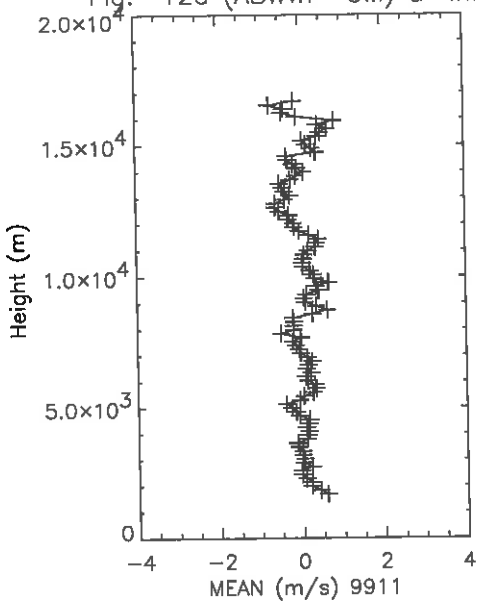

Fig. 12b (ABWWP–UM) v–wind

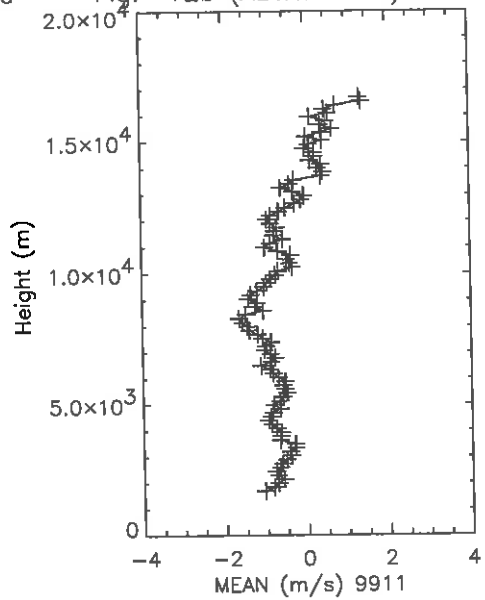

Fig. 12c (ABWWP–UM) speed

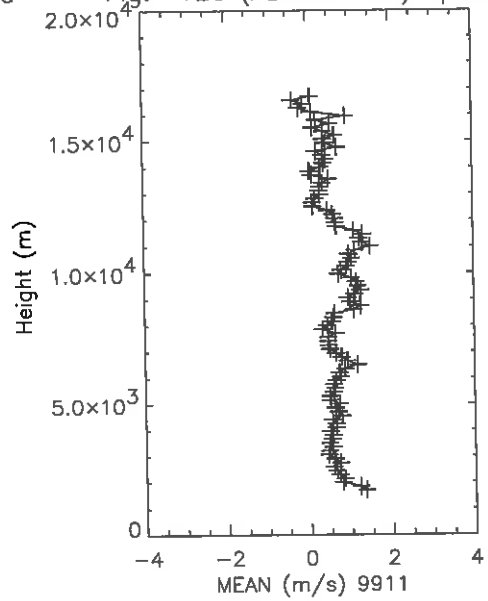

Fig. 12d (ABWWP–UM) dirn.

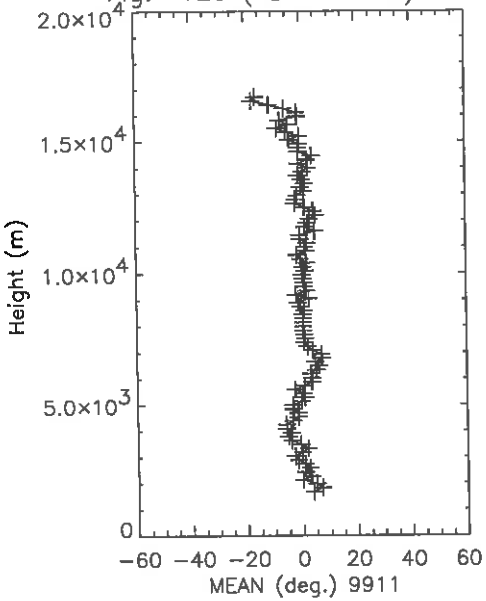

Fig. 12e (ABWWP–UM) u–wind

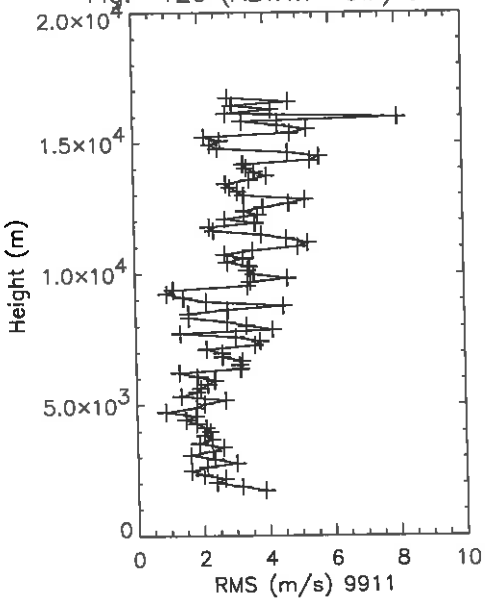

Fig. 12f (ABWWP–UM) v–wind

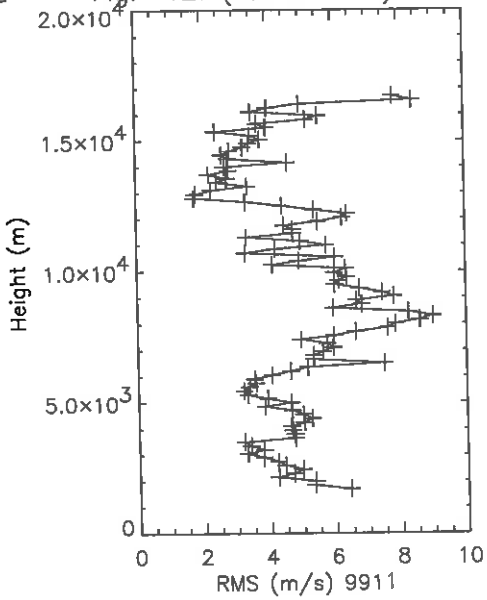

Fig. 12g (ABWWP–UM) speed

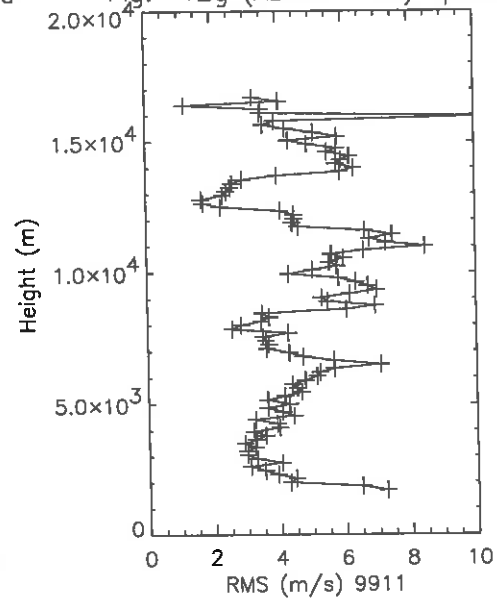

Fig. 12h (ABWWP–UM) dirn.

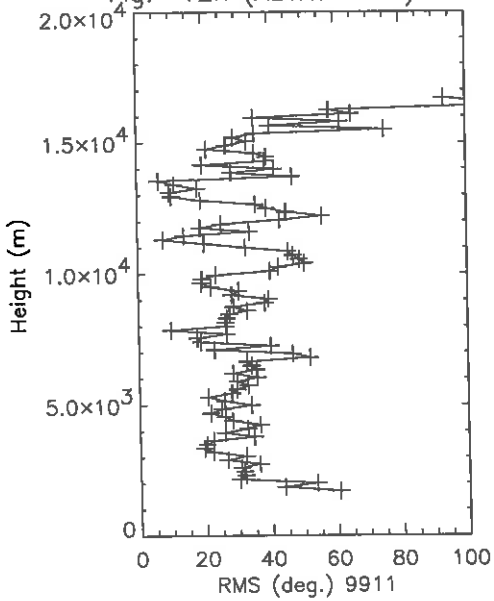

Fig. 13a (ABWWP–UM) u–wind

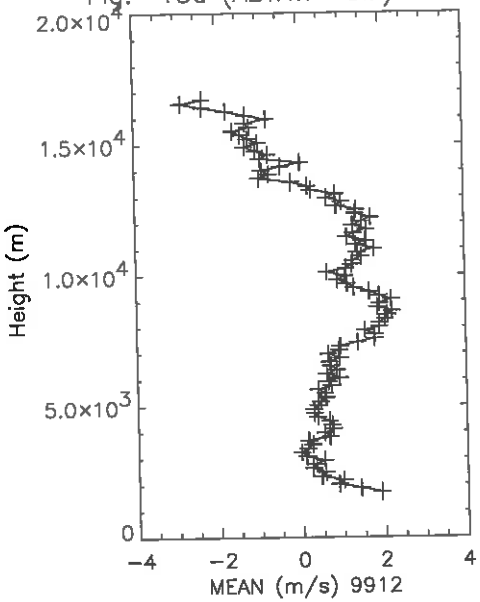

Fig. 13b (ABWWP–UM) v–wind

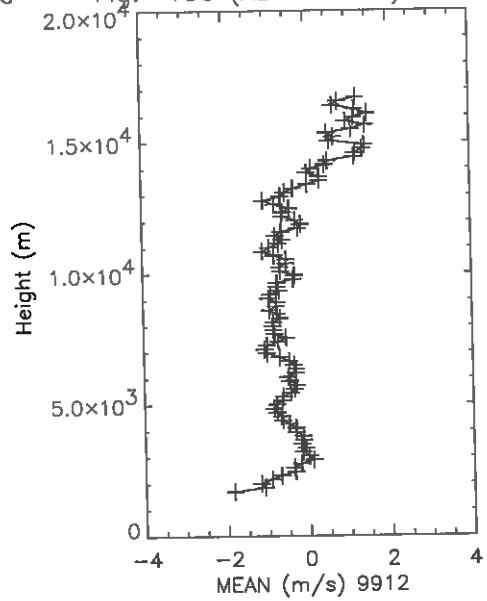

Fig. 13c (ABWWP–UM) speed

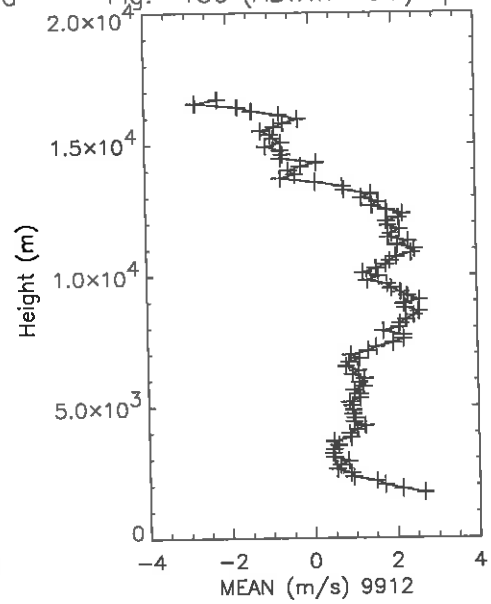

Fig. 13d (ABWWP–UM) dirn.

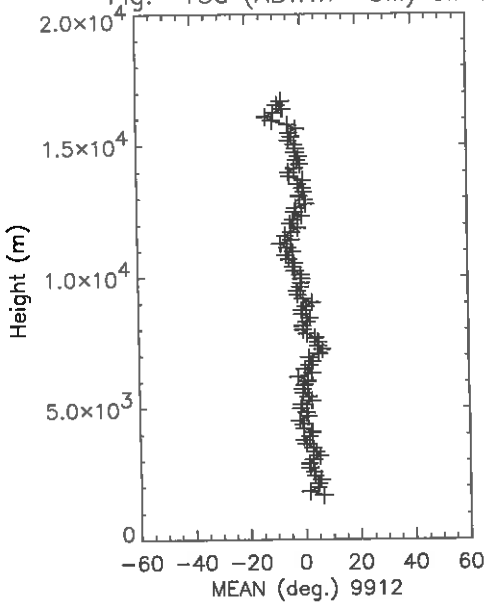

Fig. 13e (ABWWP–UM) u–wind

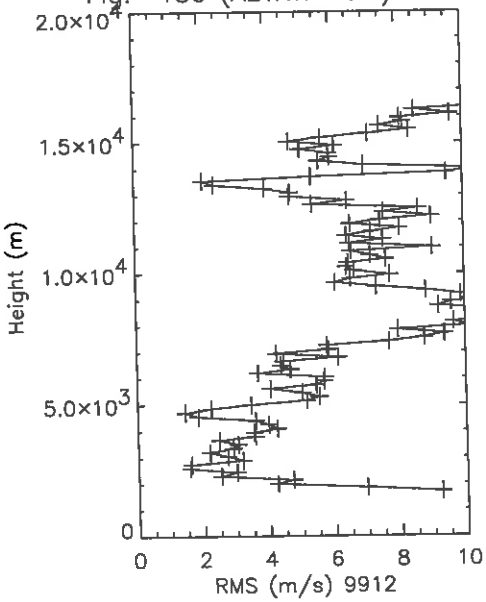

Fig. 13f (ABWWP–UM) v–wind

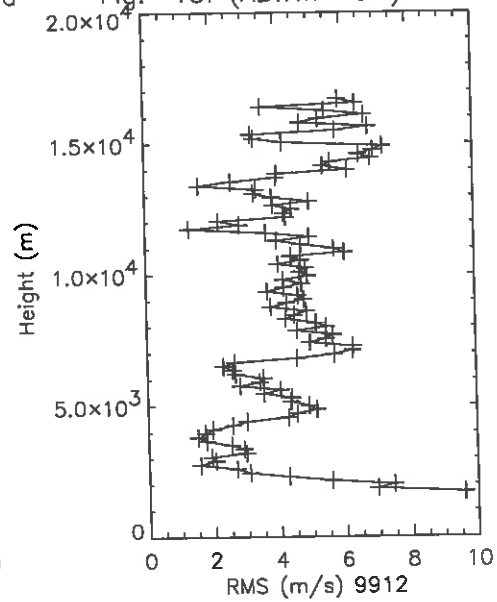

Fig. 13g (ABWWP–UM) speed

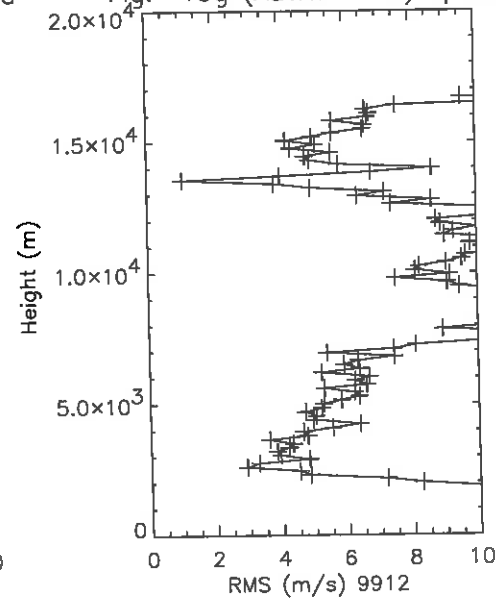

Fig. 13h (ABWWP–UM) dirn.

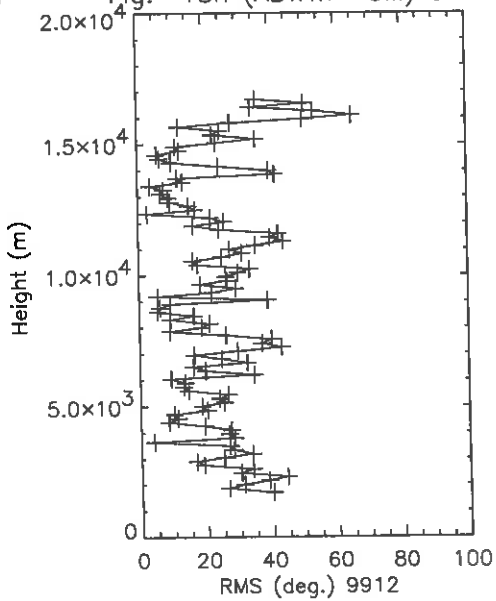

Fig. 14a (ABWWP–UM) u–wind

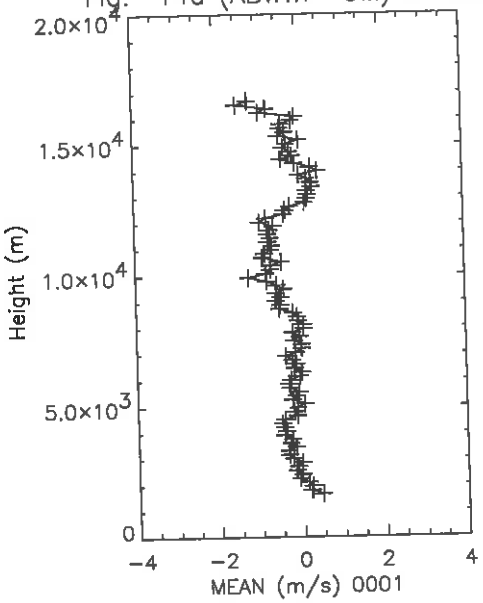

Fig. 14b (ABWWP–UM) v–wind

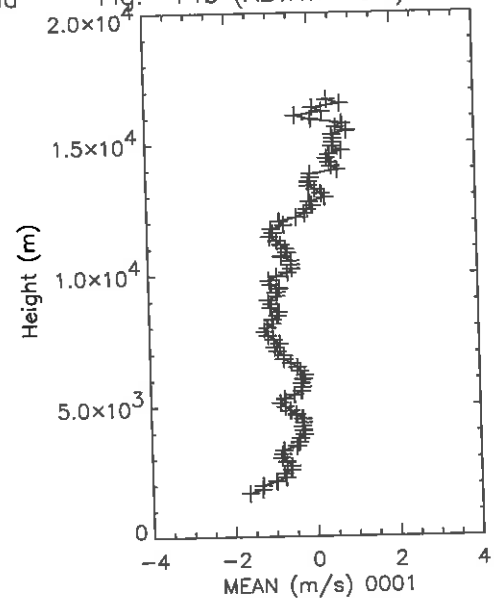

Fig. 14c (ABWWP–UM) speed

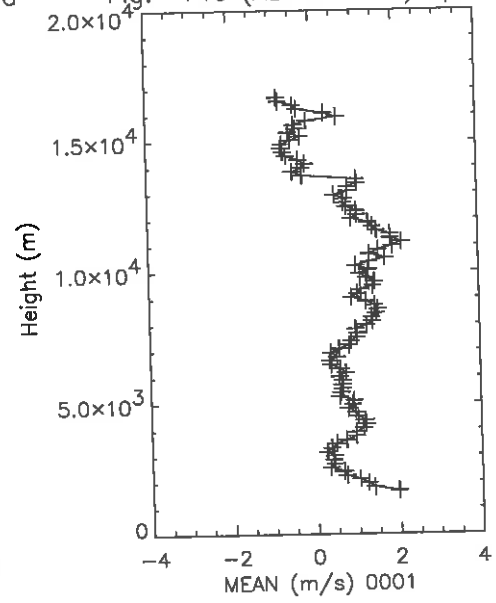

Fig. 14d (ABWWP–UM) dirn.

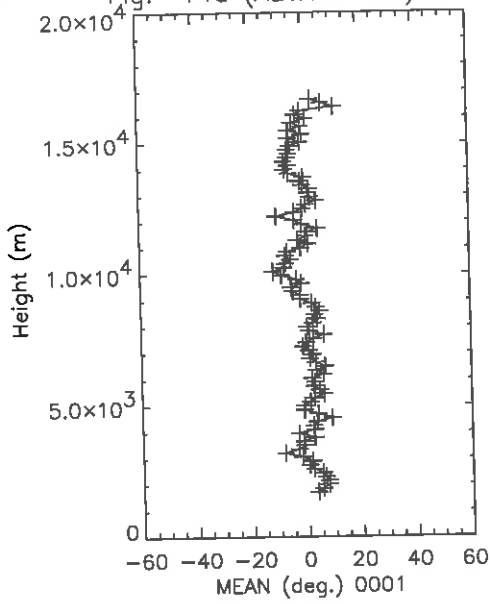

Fig. 14e (ABWWP–UM) u–wind

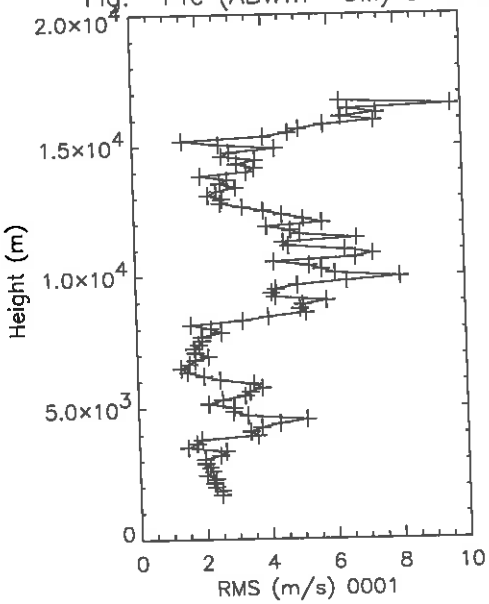

Fig. 14f (ABWWP–UM) v–wind

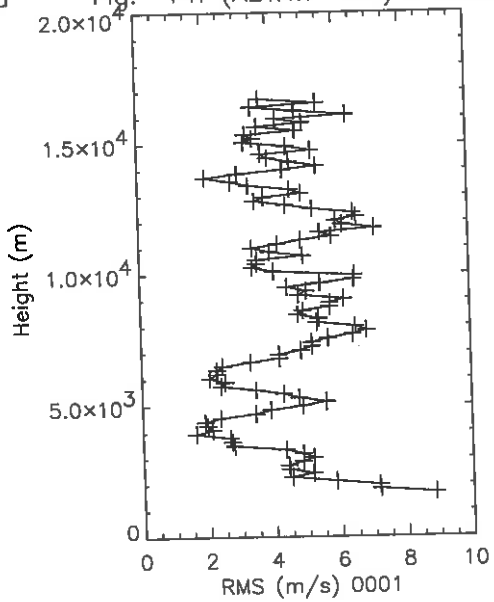

Fig. 14g (ABWWP–UM) speed

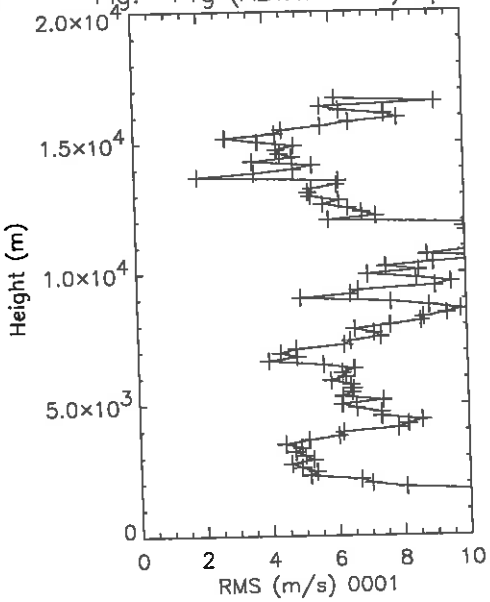

Fig. 14h (ABWWP–UM) dirn.

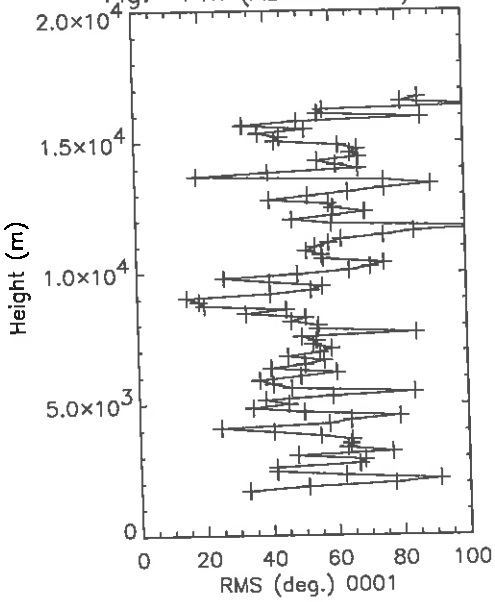

Fig. 15a (ABWWP–UM) u–wind

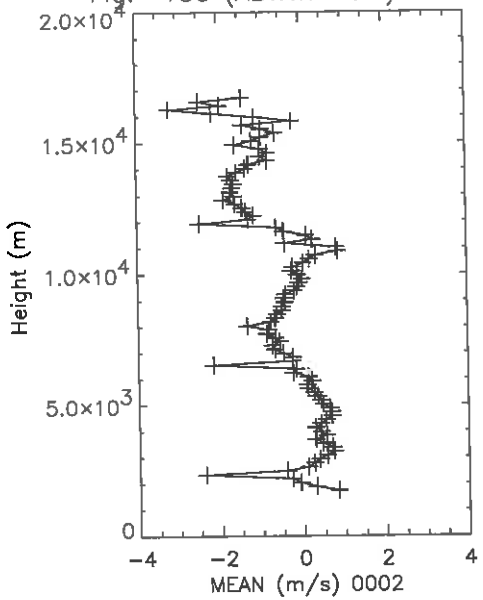

Fig. 15b (ABWWP–UM) v–wind

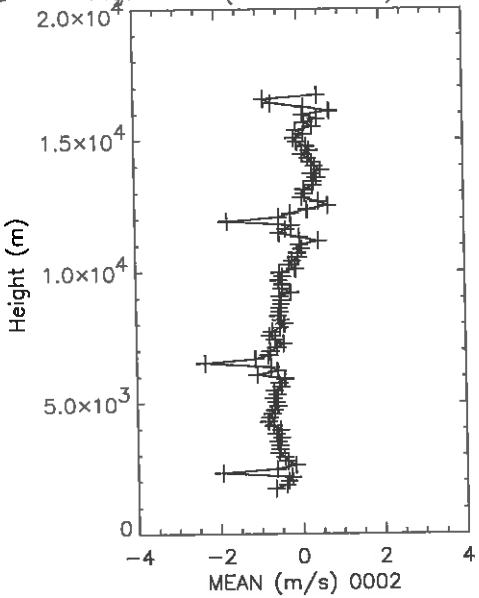

Fig. 15c (ABWWP–UM) speed

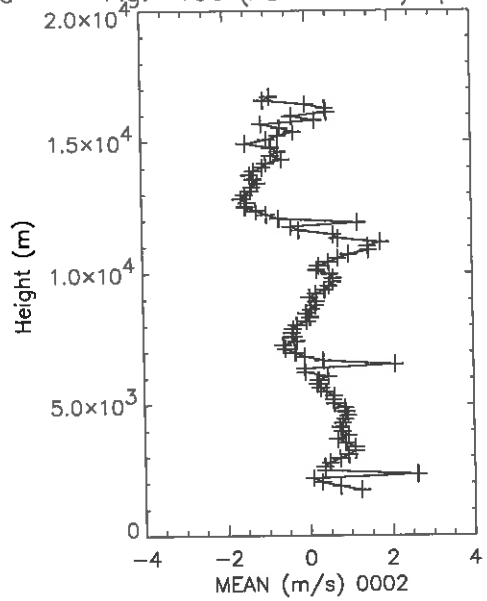

Fig. 15d (ABWWP–UM) dirn.

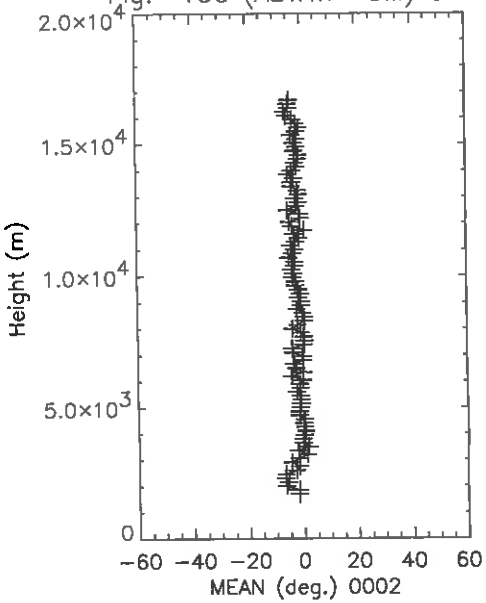

Fig. 15e (ABWWP–UM) u–wind

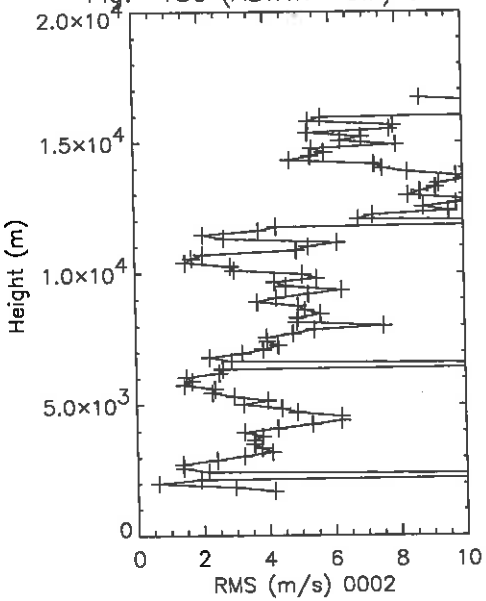

Fig. 15f (ABWWP–UM) v–wind

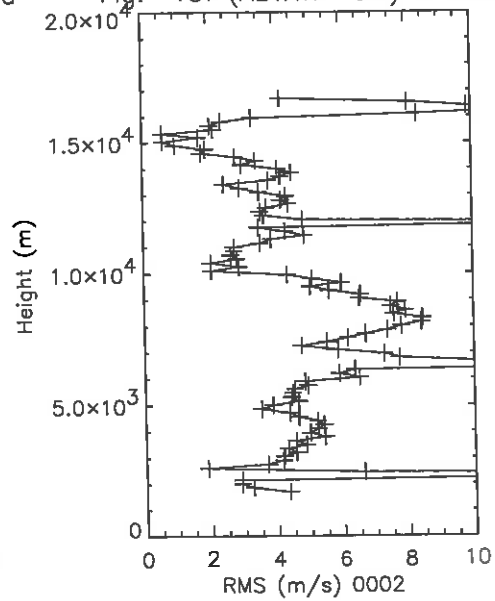

Fig. 15g (ABWWP–UM) speed

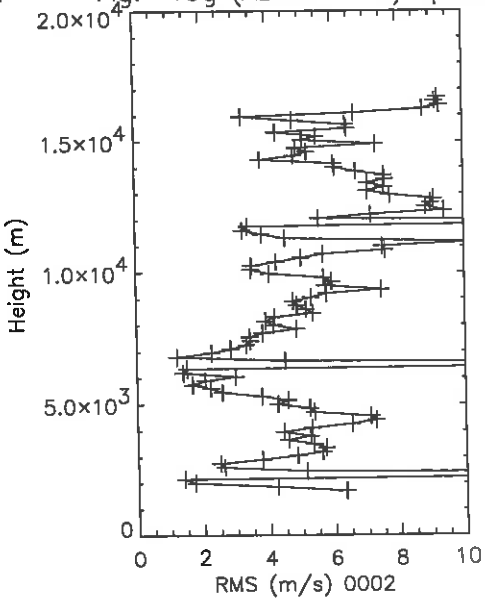

Fig. 15h (ABWWP–UM) dirn.

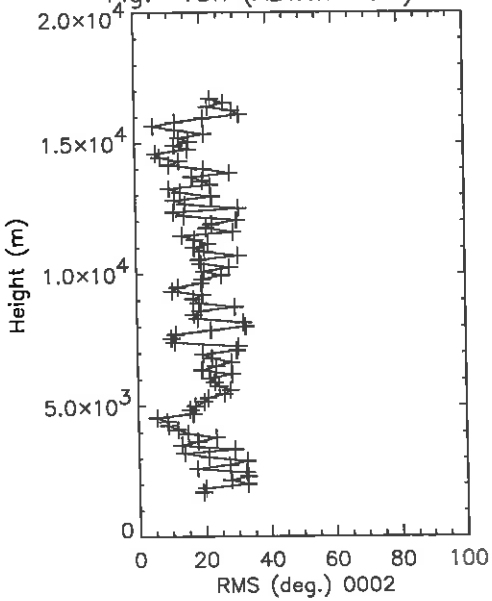

Fig. 16a (ABWWP–UM) u–wind

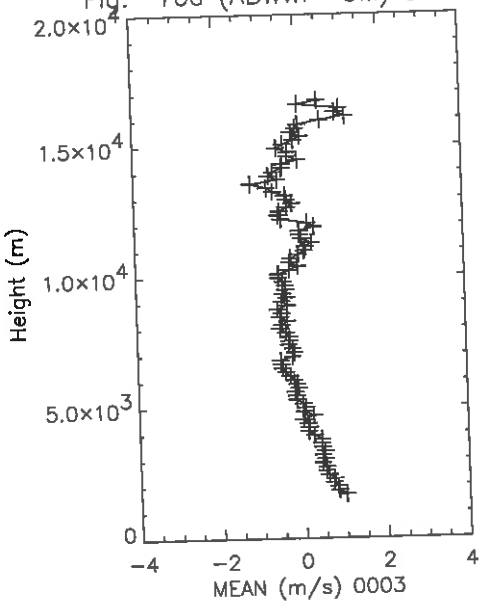

Fig. 16b (ABWWP–UM) v–wind

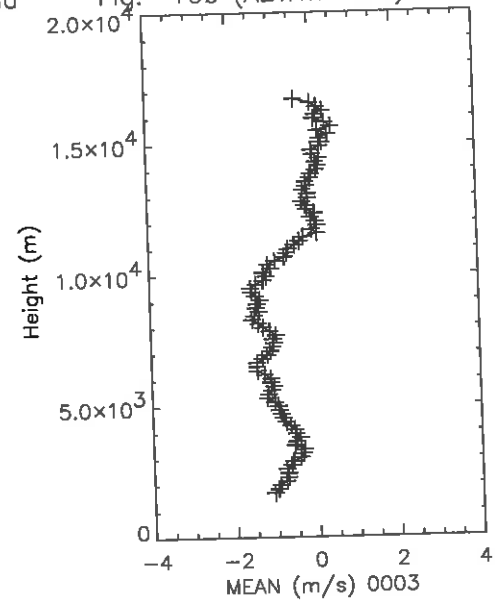

Fig. 16c (ABWWP–UM) speed

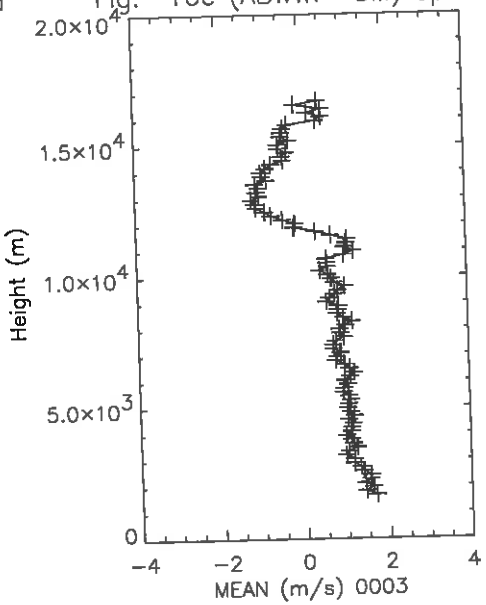

Fig. 16d (ABWWP–UM) dirn.

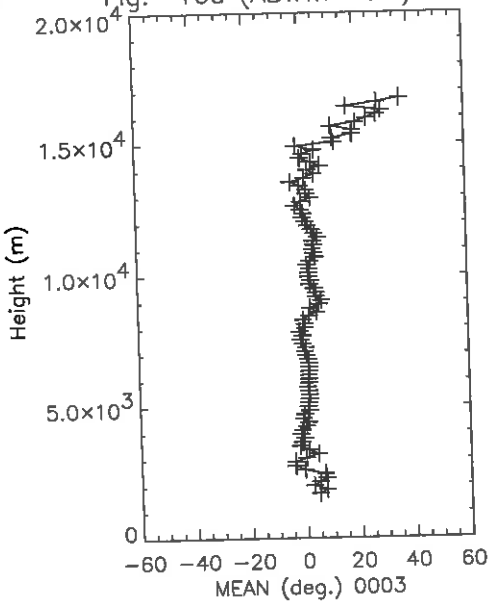

Fig. 16e (ABWWP–UM) u–wind

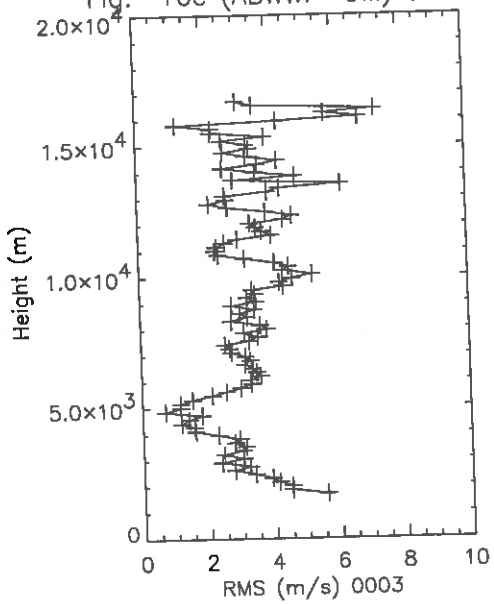

Fig. 16f (ABWWP–UM) v–wind

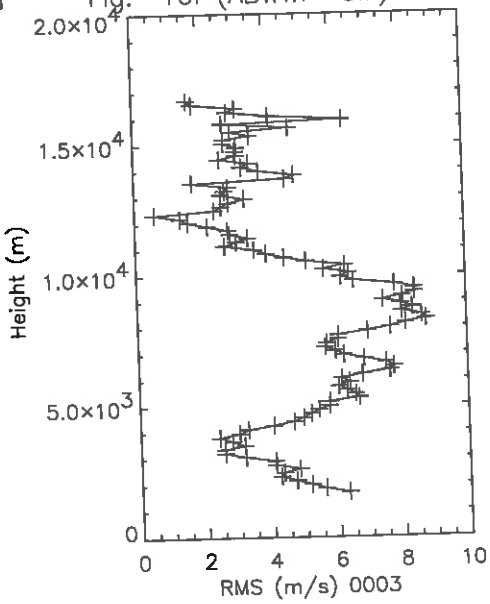

Fig. 16g (ABWWP–UM) speed

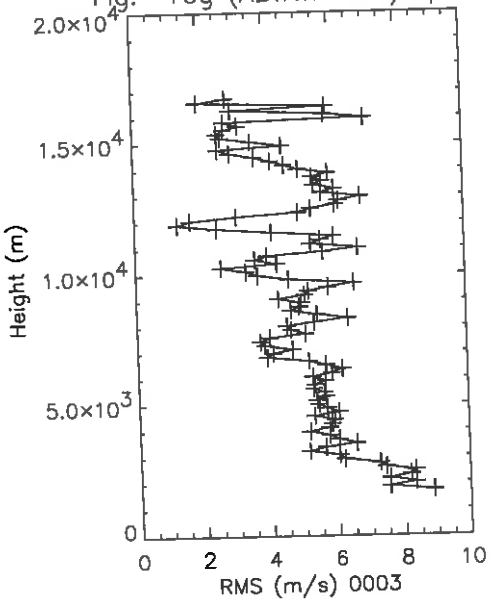

Fig. 16h (ABWWP–UM) dirn.

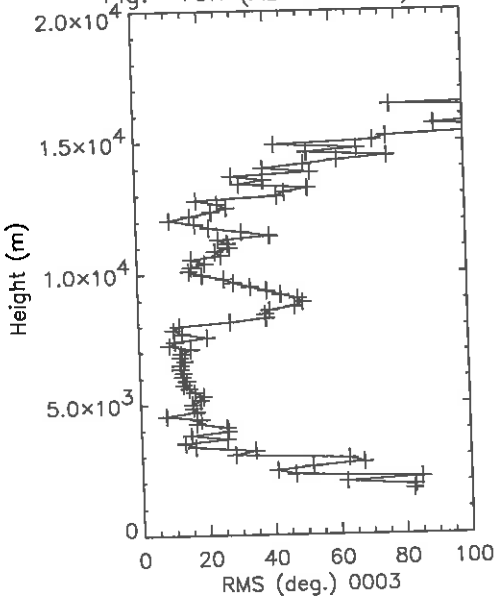

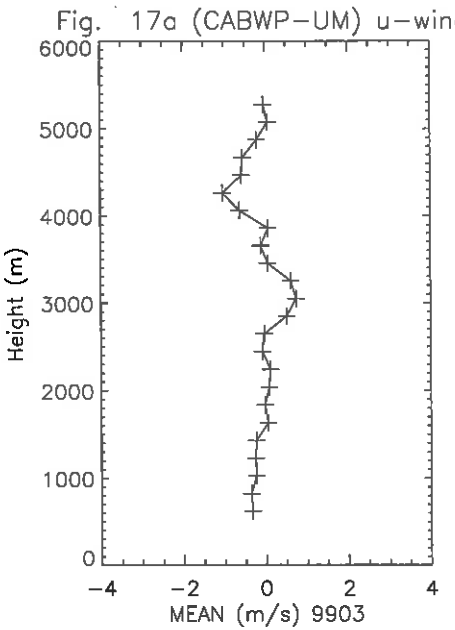
Fig. 17a (CABWP–UM) u–wind
Height (m)
MEAN (m/s) 9903

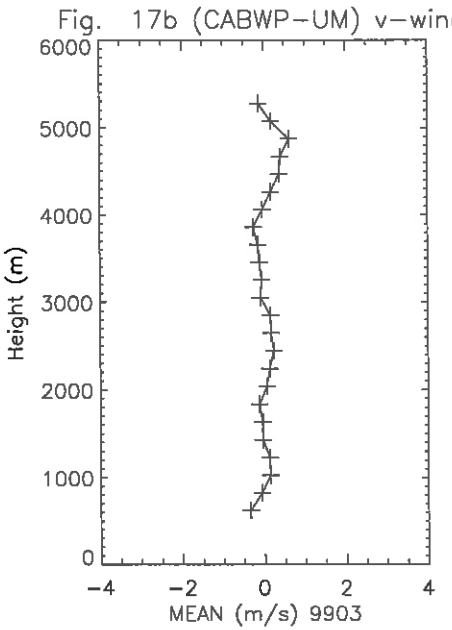
Fig. 17b (CABWP–UM) v–wind
Height (m)
MEAN (m/s) 9903

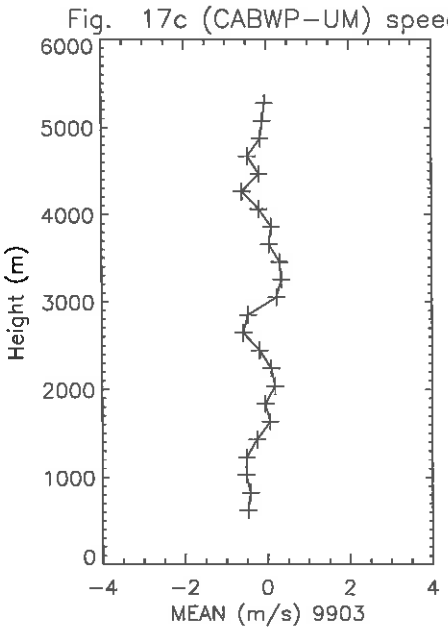
Fig. 17c (CABWP–UM) speed
Height (m)
MEAN (m/s) 9903

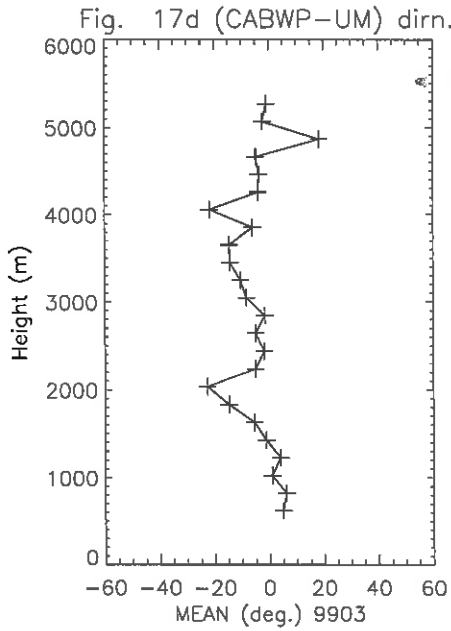
Fig. 17d (CABWP–UM) dirn.
Height (m)
MEAN (deg.) 9903

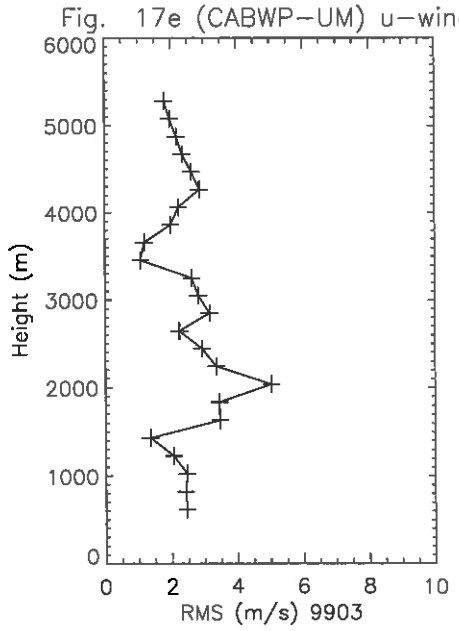
Fig. 17e (CABWP–UM) u–wind
Height (m)
RMS (m/s) 9903

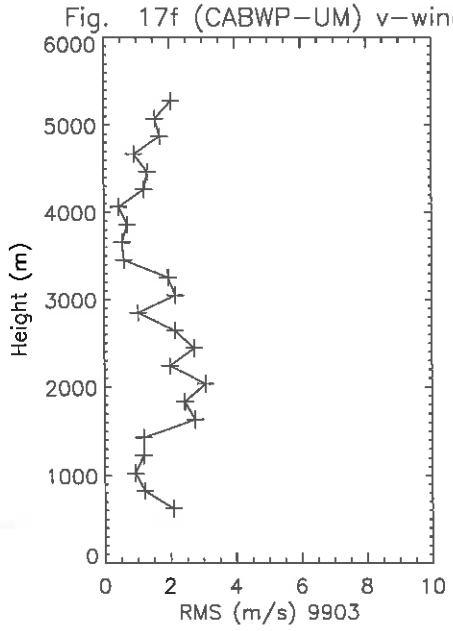
Fig. 17f (CABWP–UM) v–wind
Height (m)
RMS (m/s) 9903

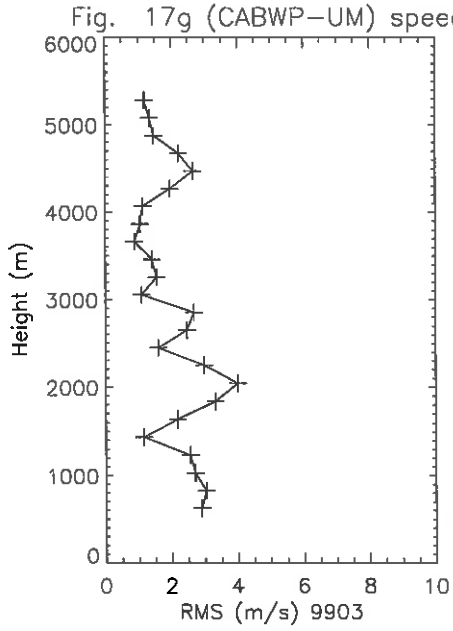
Fig. 17g (CABWP–UM) speed
Height (m)
RMS (m/s) 9903

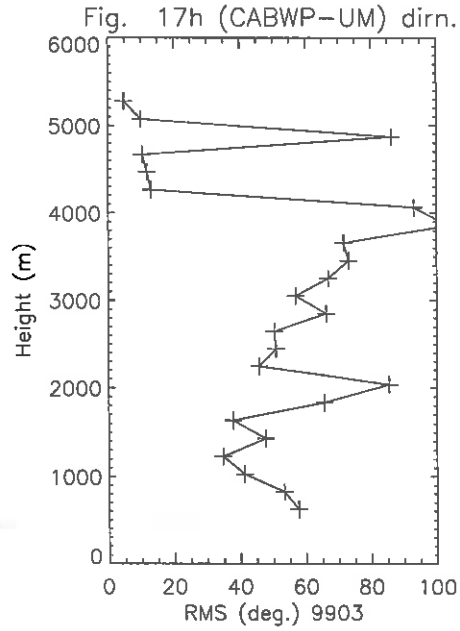
Fig. 17h (CABWP–UM) dirn.
Height (m)
RMS (deg.) 9903

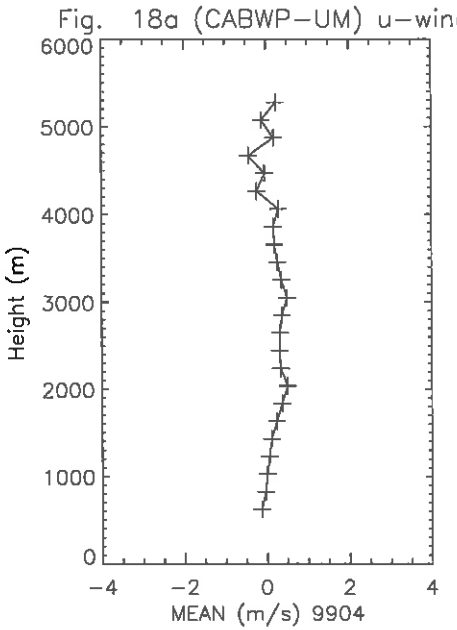
Fig. 18a (CABWP–UM) u–wind
Height (m)
MEAN (m/s) 9904

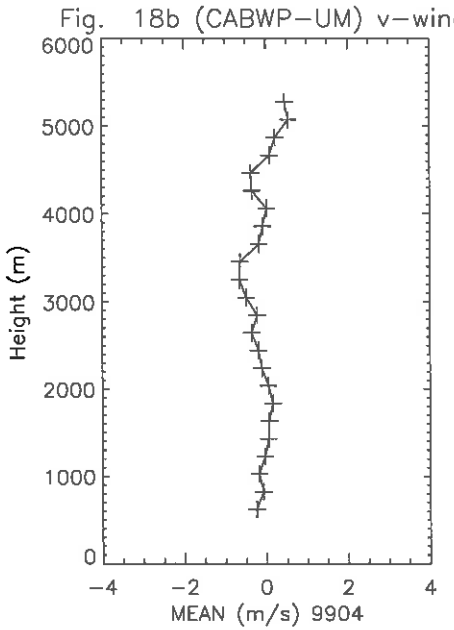
Fig. 18b (CABWP–UM) v–wind
Height (m)
MEAN (m/s) 9904

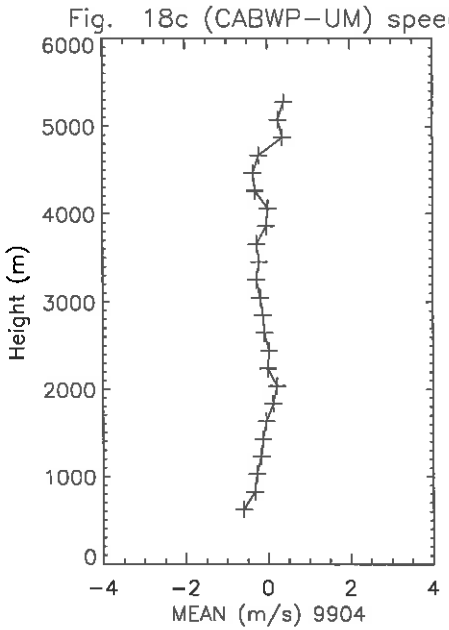
Fig. 18c (CABWP–UM) speed
Height (m)
MEAN (m/s) 9904

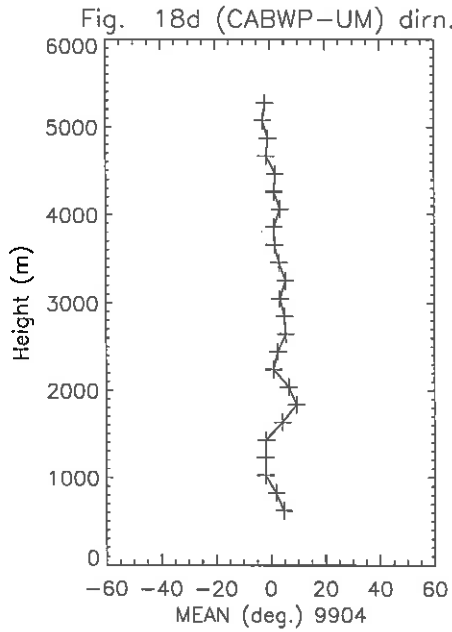
Fig. 18d (CABWP–UM) dirn.
Height (m)
MEAN (deg.) 9904

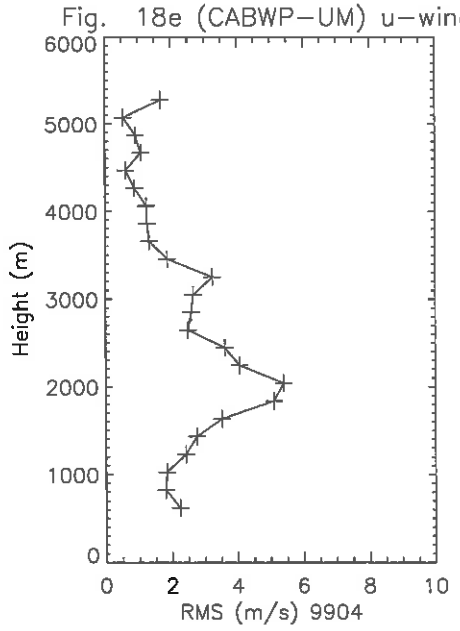
Fig. 18e (CABWP–UM) u–wind
Height (m)
RMS (m/s) 9904

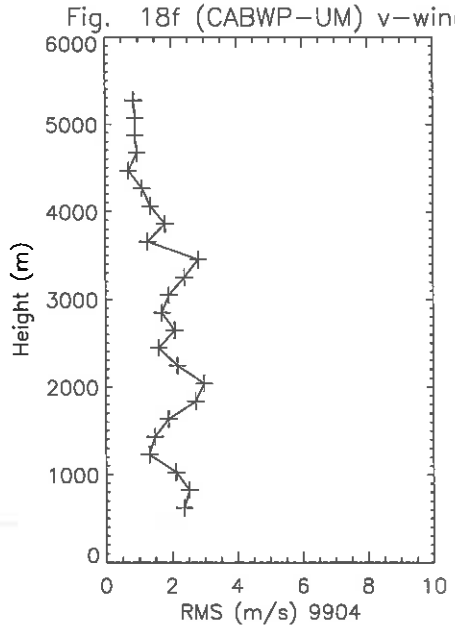
Fig. 18f (CABWP–UM) v–wind
Height (m)
RMS (m/s) 9904

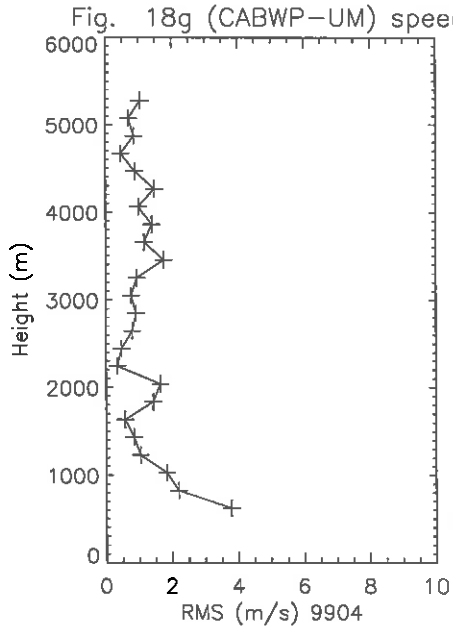
Fig. 18g (CABWP–UM) speed
Height (m)
RMS (m/s) 9904

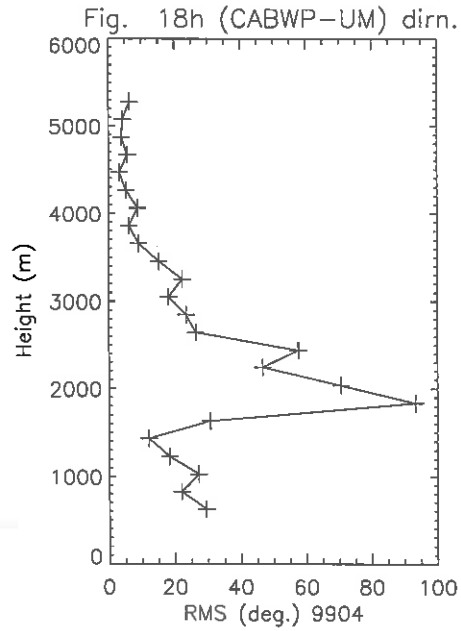
Fig. 18h (CABWP–UM) dirn.
Height (m)
RMS (deg.) 9904

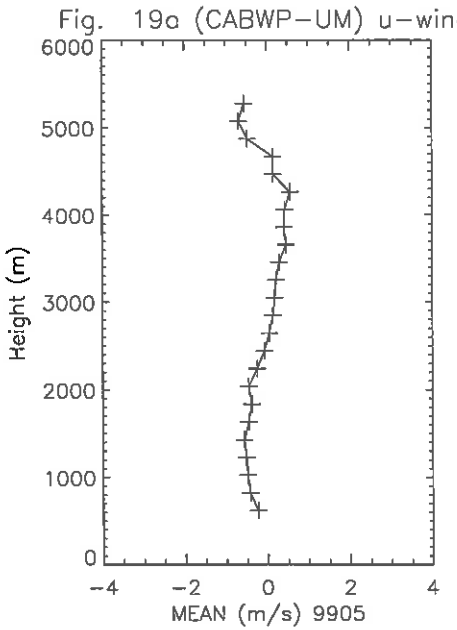
Fig. 19a (CABWP–UM) u–wind
Height (m)
MEAN (m/s) 9905

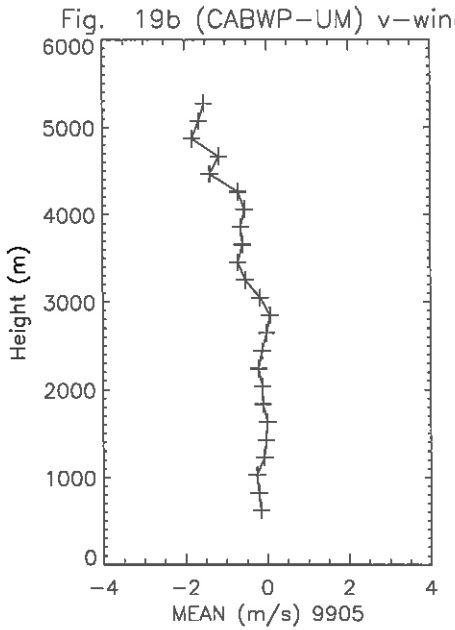
Fig. 19b (CABWP–UM) v–wind
Height (m)
MEAN (m/s) 9905

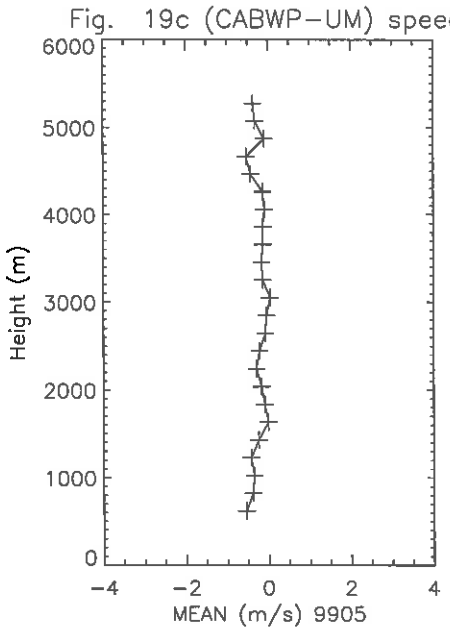
Fig. 19c (CABWP–UM) speed
Height (m)
MEAN (m/s) 9905

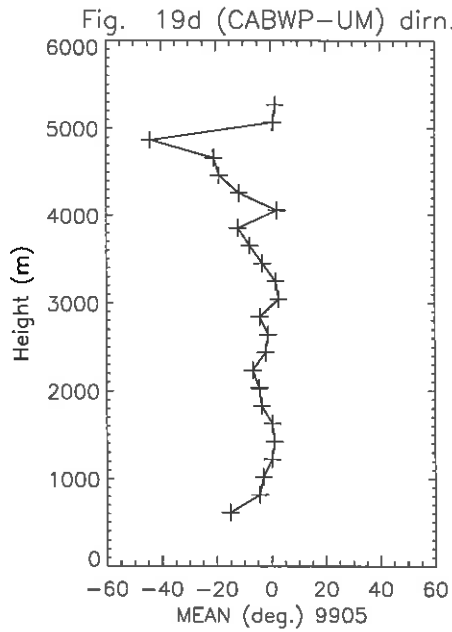
Fig. 19d (CABWP–UM) dirn.
Height (m)
MEAN (deg.) 9905

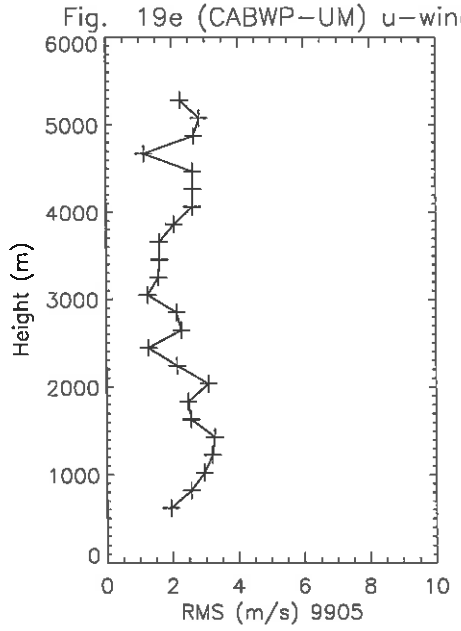
Fig. 19e (CABWP–UM) u–wind
Height (m)
RMS (m/s) 9905

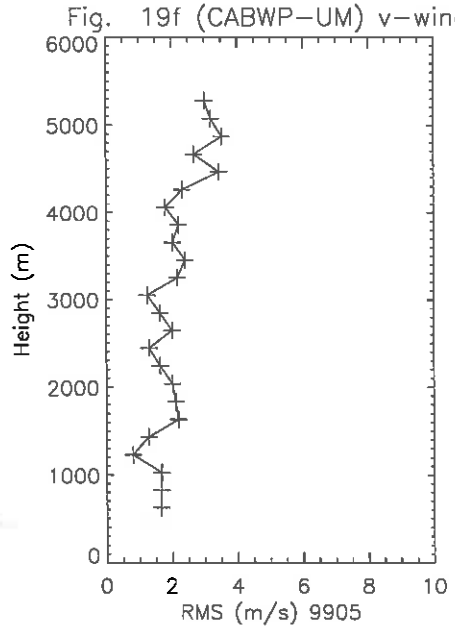
Fig. 19f (CABWP–UM) v–wind
Height (m)
RMS (m/s) 9905

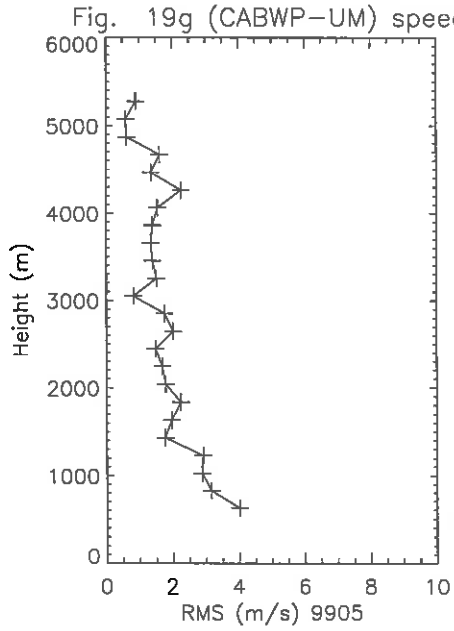
Fig. 19g (CABWP–UM) speed
Height (m)
RMS (m/s) 9905

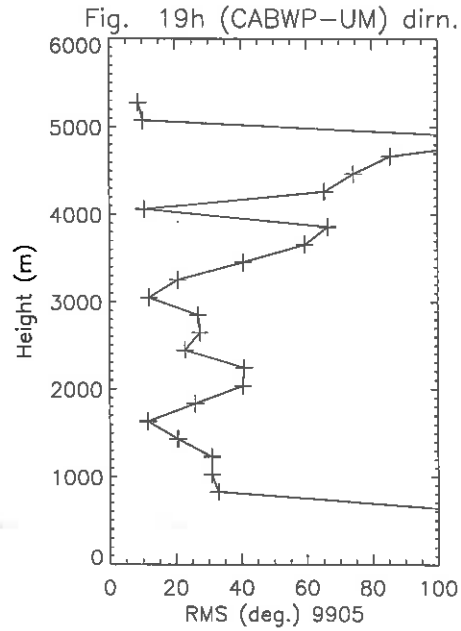
Fig. 19h (CABWP–UM) dirn.
Height (m)
RMS (deg.) 9905

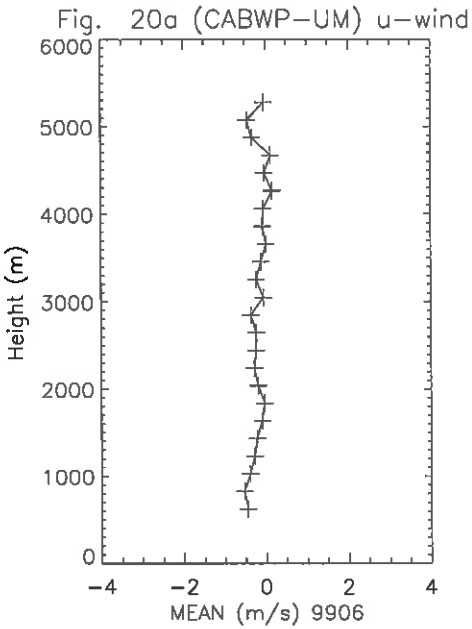
Fig. 20a (CABWP–UM) u–wind
Height (m)
MEAN (m/s) 9906

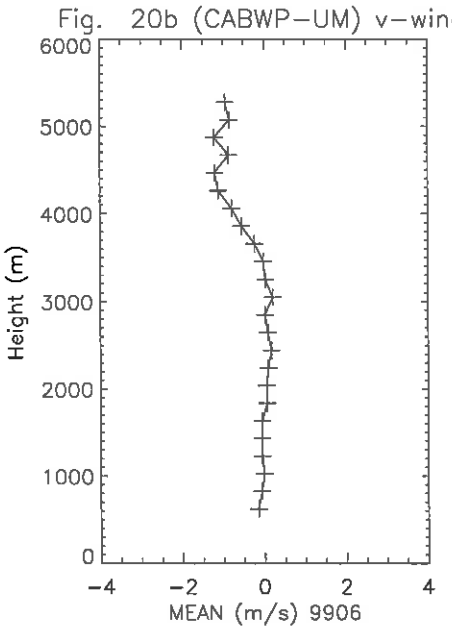
Fig. 20b (CABWP–UM) v–wind
Height (m)
MEAN (m/s) 9906

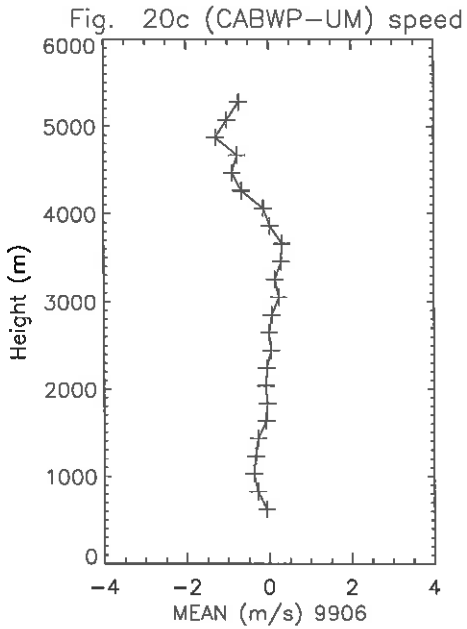
Fig. 20c (CABWP–UM) speed
Height (m)
MEAN (m/s) 9906

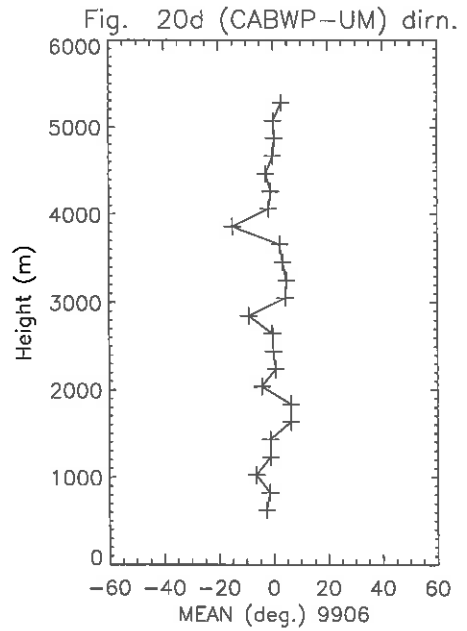
Fig. 20d (CABWP–UM) dirn.
Height (m)
MEAN (deg.) 9906

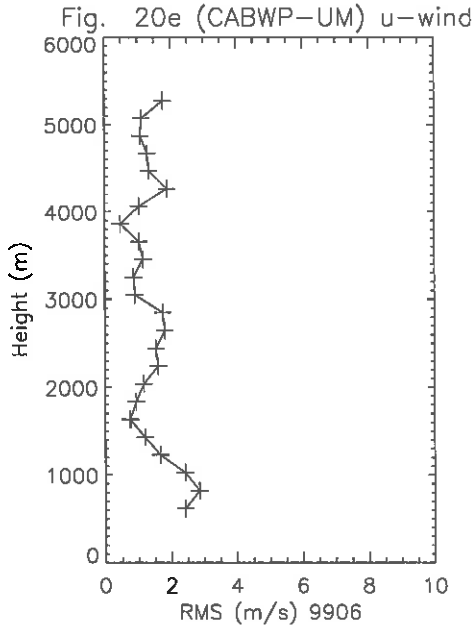
Fig. 20e (CABWP–UM) u–wind
Height (m)
RMS (m/s) 9906

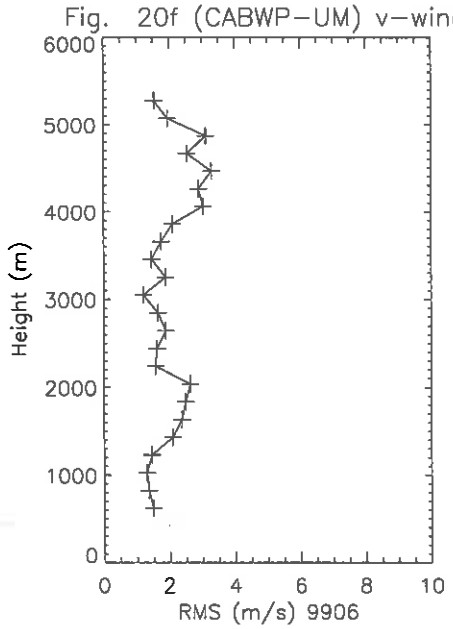
Fig. 20f (CABWP–UM) v–wind
Height (m)
RMS (m/s) 9906

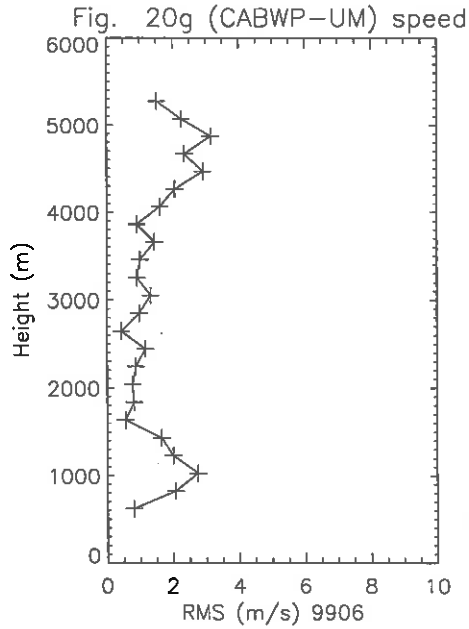
Fig. 20g (CABWP–UM) speed
Height (m)
RMS (m/s) 9906

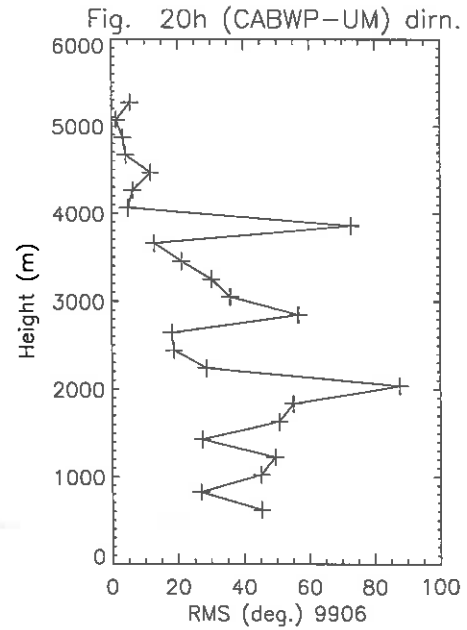
Fig. 20h (CABWP–UM) dirn.
Height (m)
RMS (deg.) 9906

Fig. 21a (CABWP–UM) u–wind

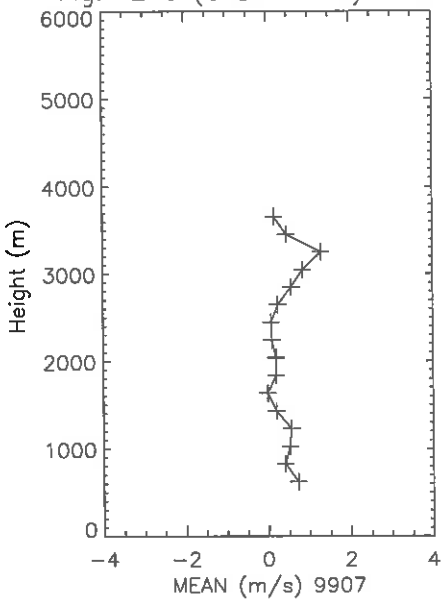

Fig. 21b (CABWP–UM) v–wind

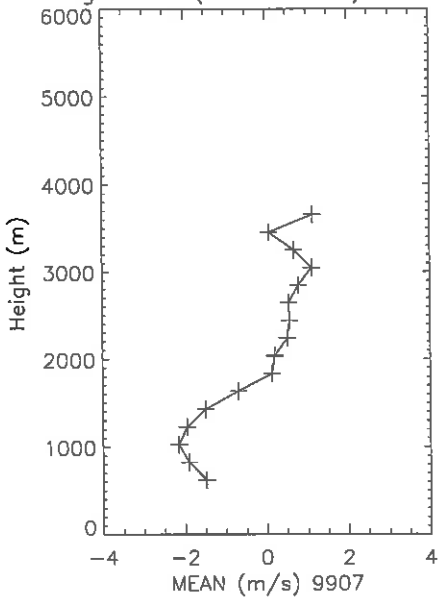

Fig. 21c (CABWP–UM) speed

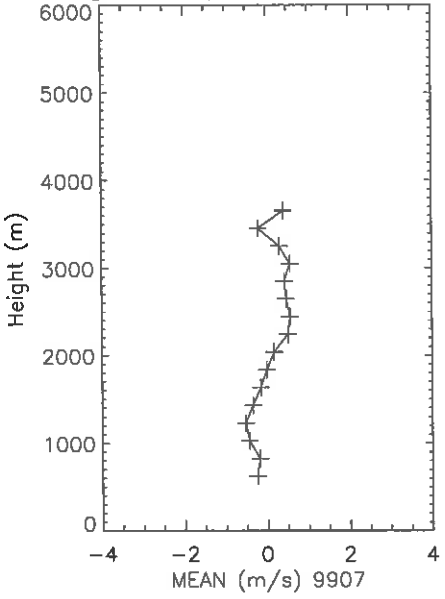

Fig. 21d (CABWP–UM) dirn.

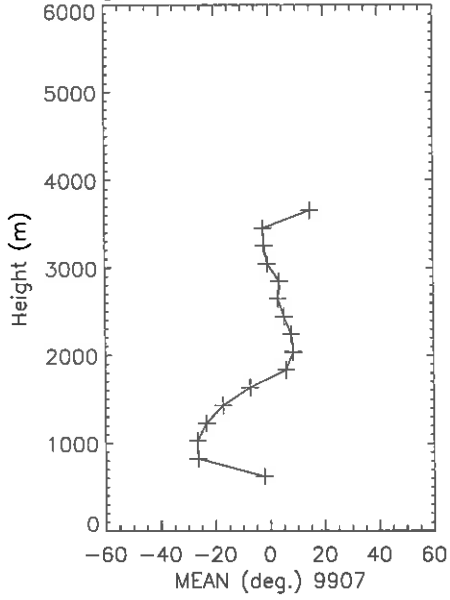

Fig. 21e (CABWP–UM) u–wind

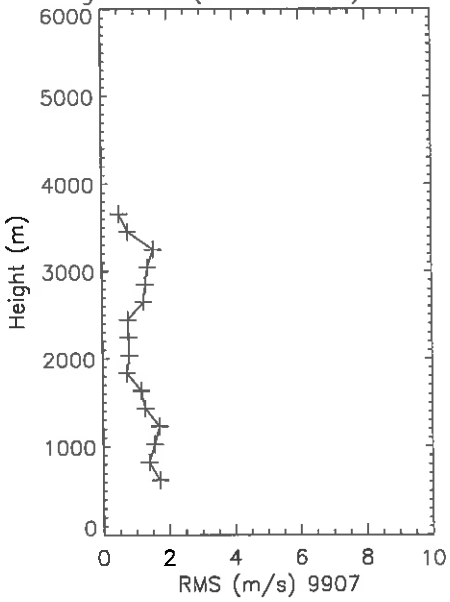

Fig. 21f (CABWP–UM) v–wind

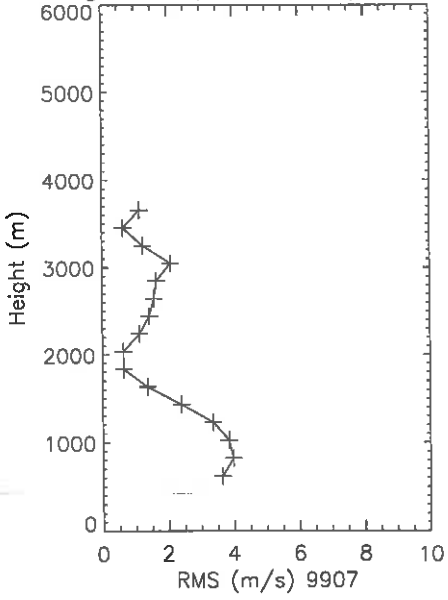

Fig. 21g (CABWP–UM) speed

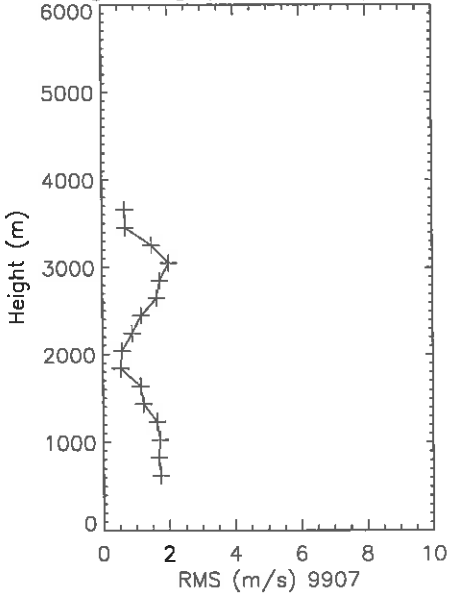

Fig. 21h (CABWP–UM) dirn.

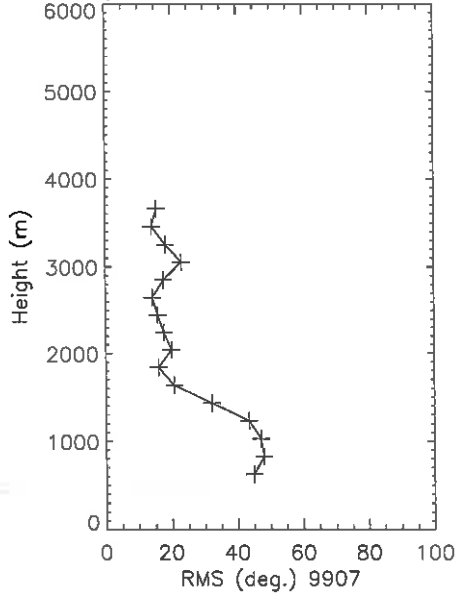

Fig. 22a (CABWP–UM) u–wind

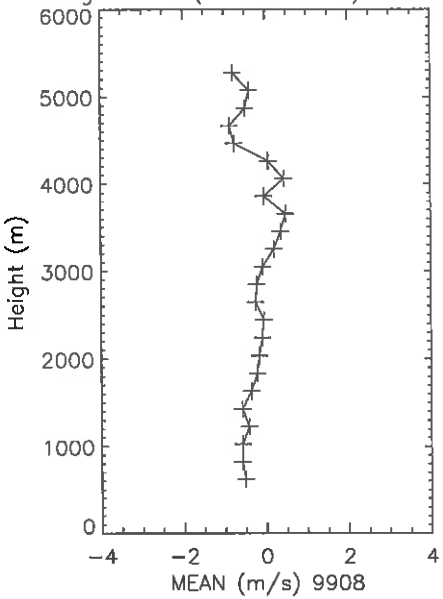

Fig. 22b (CABWP–UM) v–wind

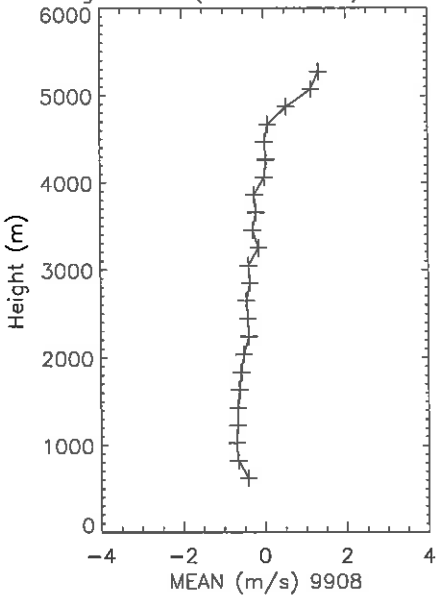

Fig. 22c (CABWP–UM) speed

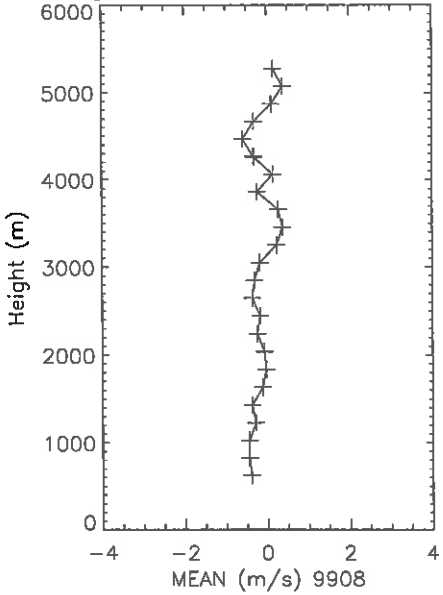

Fig. 22d (CABWP–UM) dirn.

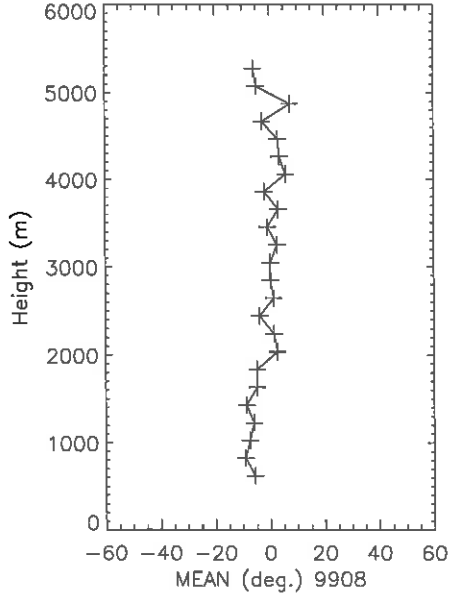

Fig. 22e (CABWP–UM) u–wind

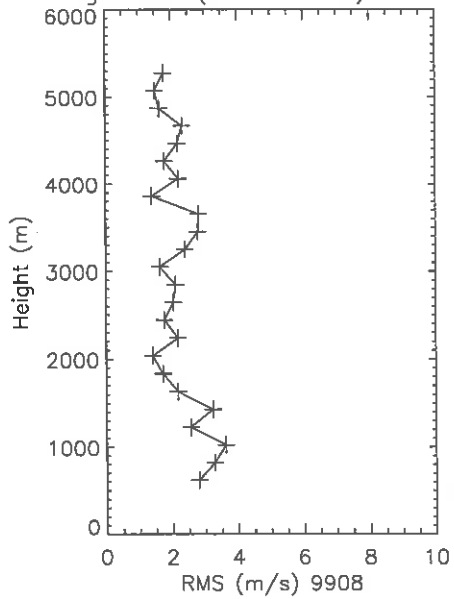

Fig. 22f (CABWP–UM) v–wind

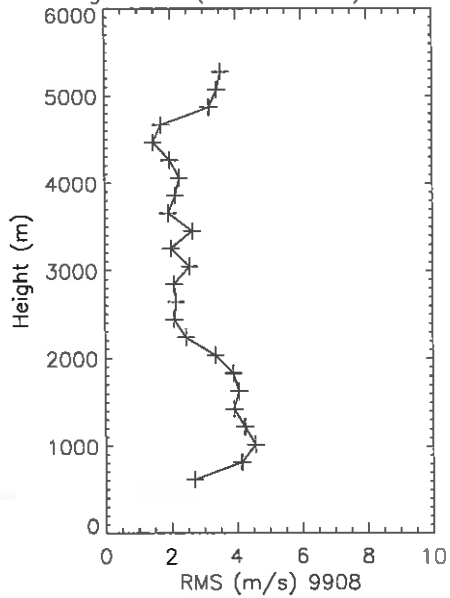

Fig. 22g (CABWP–UM) speed

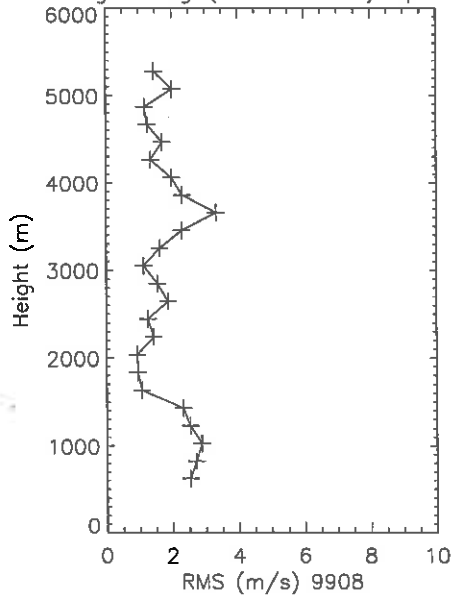

Fig. 22h (CABWP–UM) dirn.

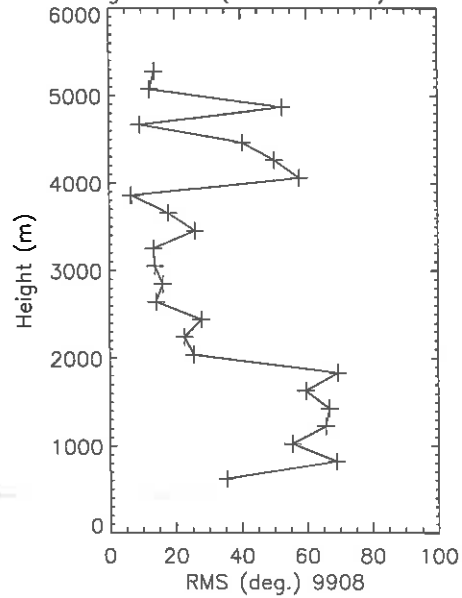

Fig. 23a (CABWP–UM) u–wind

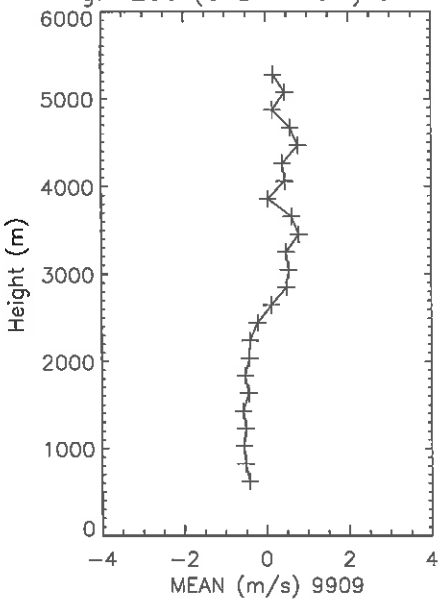

Fig. 23b (CABWP–UM) v–wind

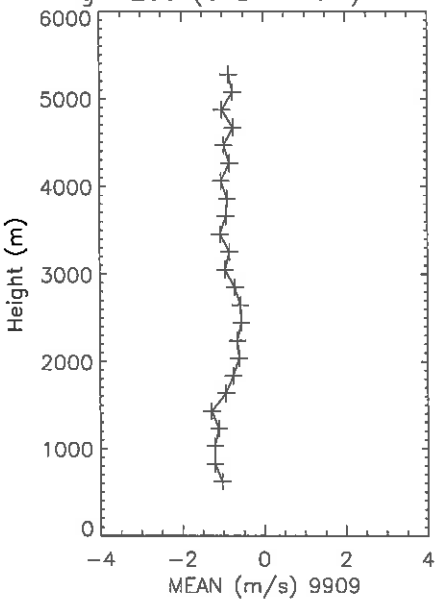

Fig. 23c (CABWP–UM) speed

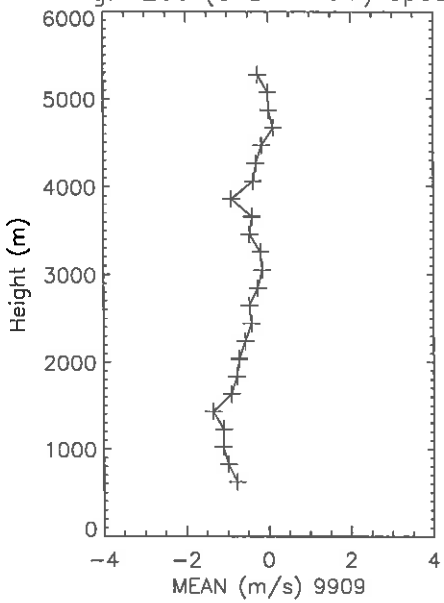

Fig. 23d (CABWP–UM) dirn.

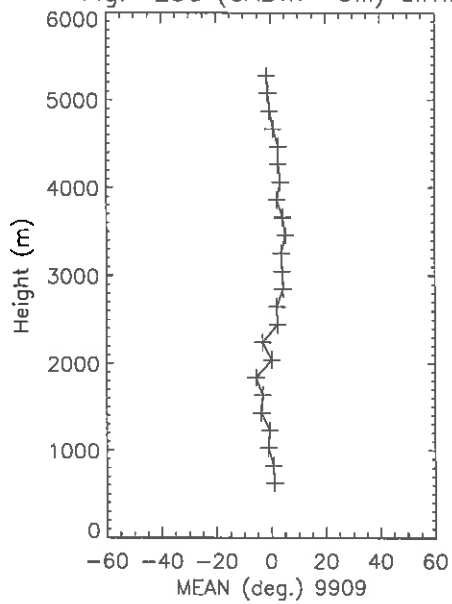

Fig. 23e (CABWP–UM) u–wind

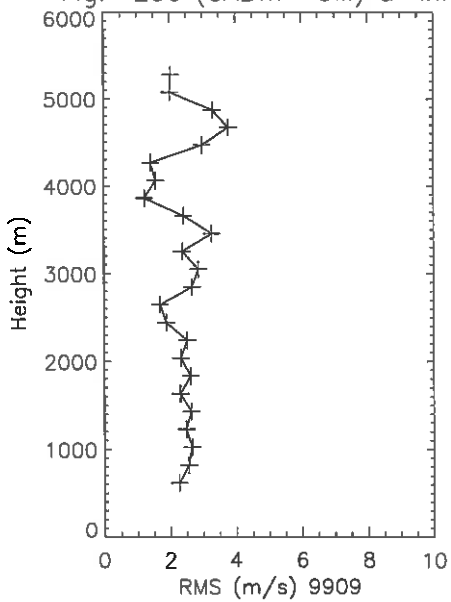

Fig. 23f (CABWP–UM) v–wind

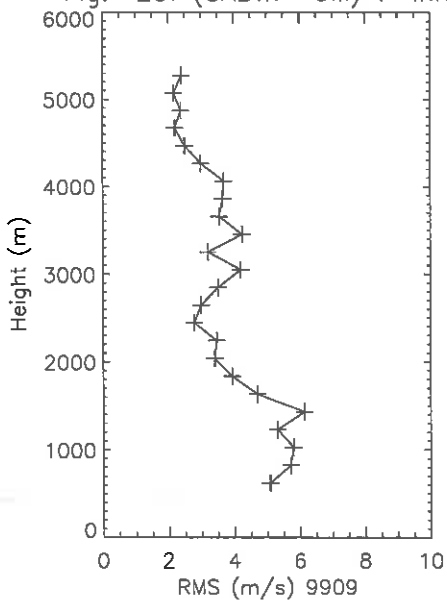

Fig. 23g (CABWP–UM) speed

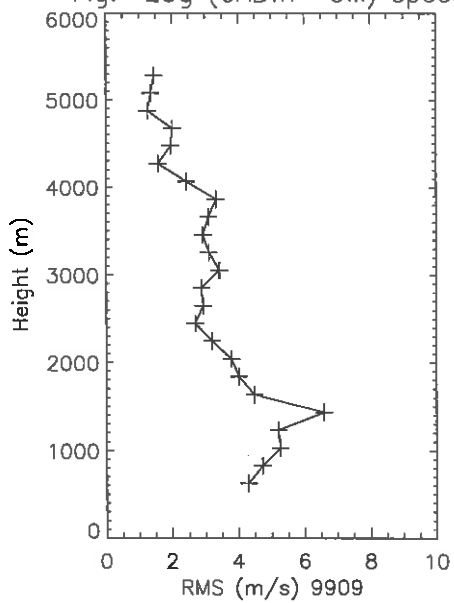

Fig. 23h (CABWP–UM) dirn.

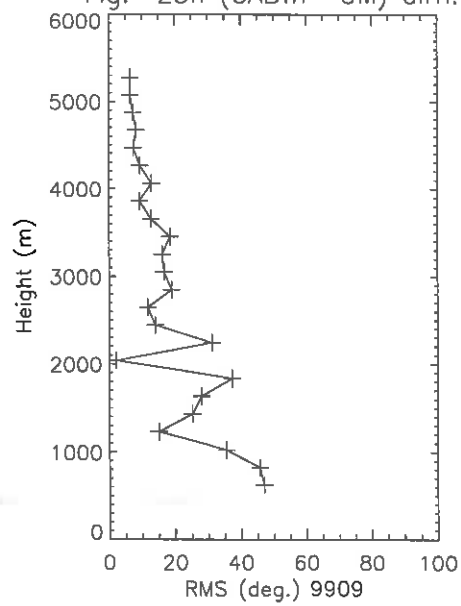

Fig. 24a (CABWP–UM) u–wind

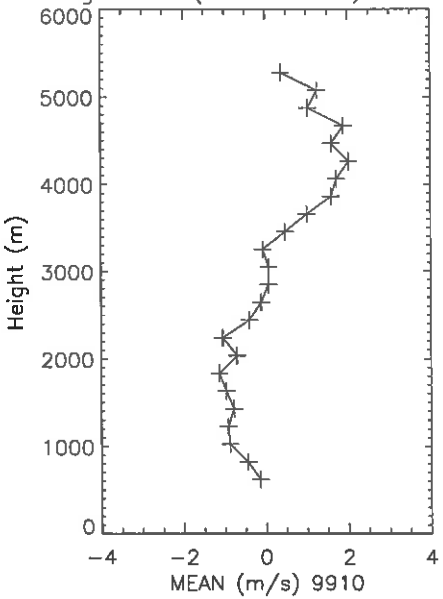

Fig. 24b (CABWP–UM) v–wind

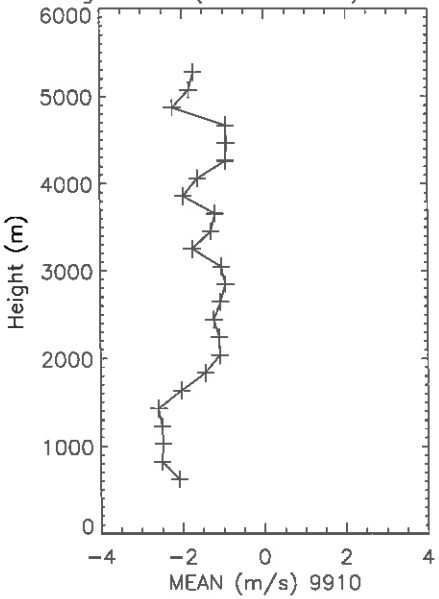

Fig. 24c (CABWP–UM) speed

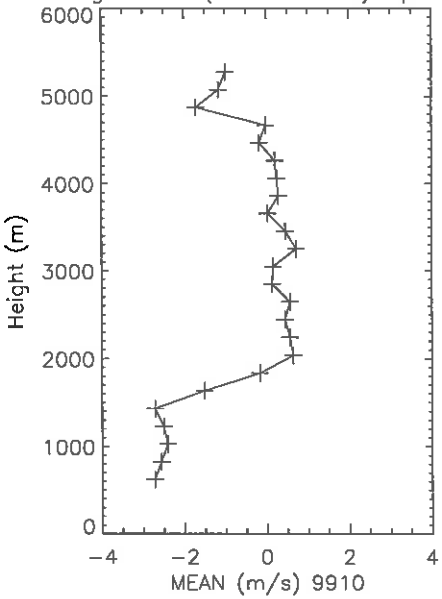

Fig. 24d (CABWP–UM) dirn.

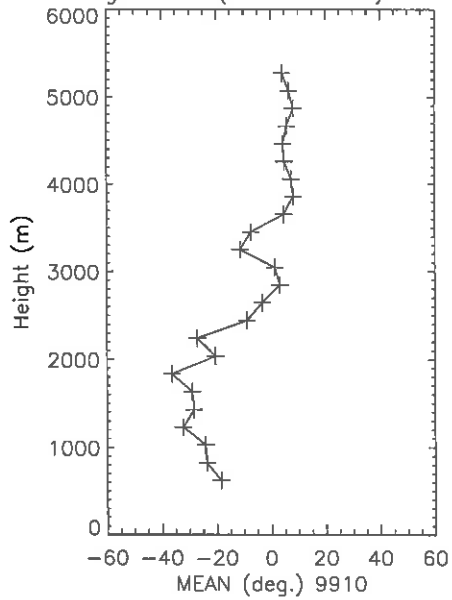

Fig. 24e (CABWP–UM) u–wind

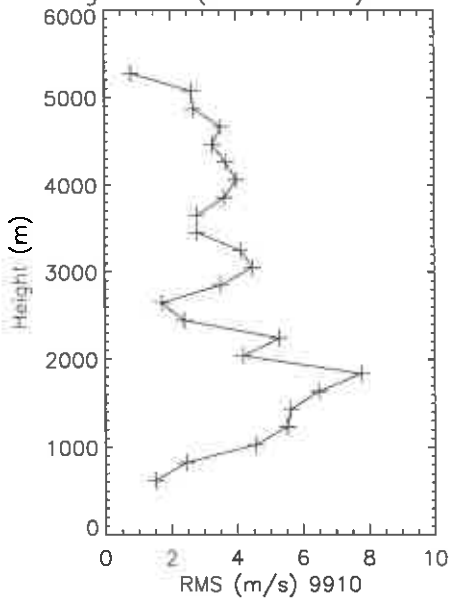

Fig. 24f (CABWP–UM) v–wind

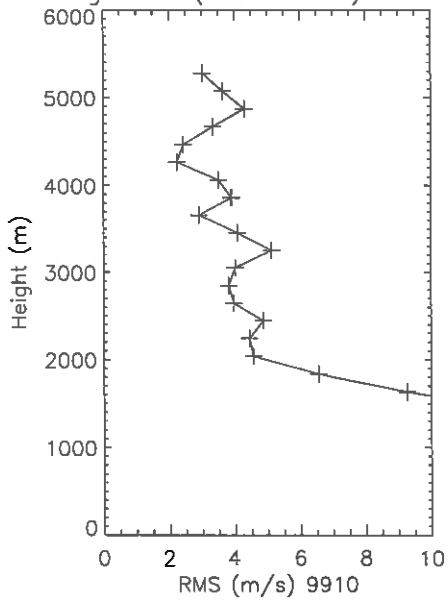

Fig. 24g (CABWP–UM) speed

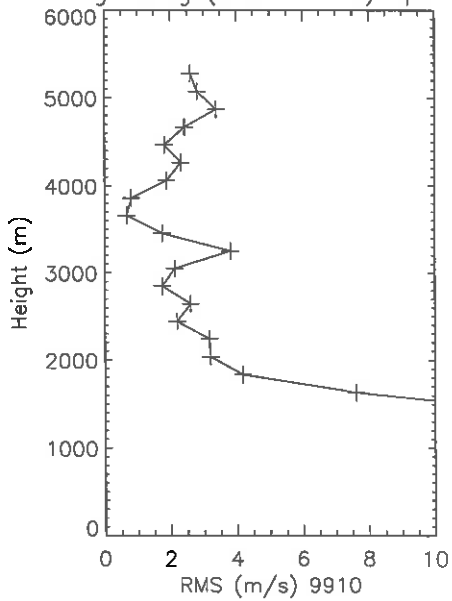

Fig. 24h (CABWP–UM) dirn.

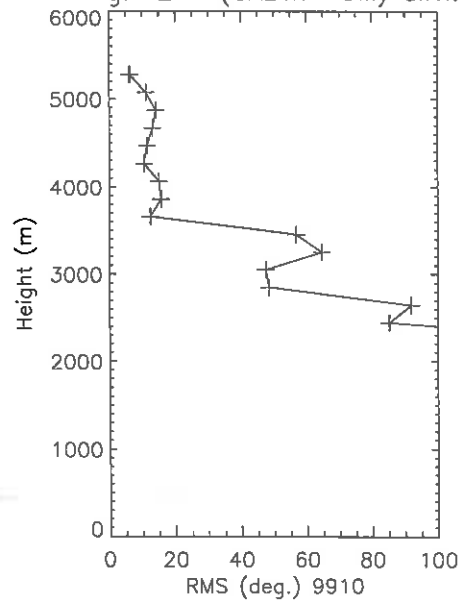

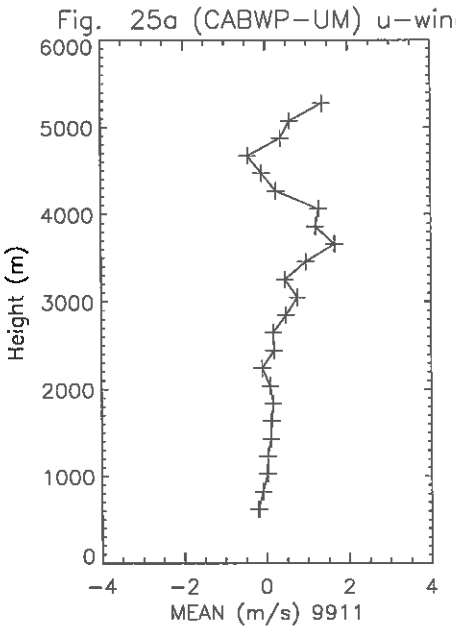
Fig. 25a (CABWP-UM) u-wind
Height (m)
MEAN (m/s) 9911

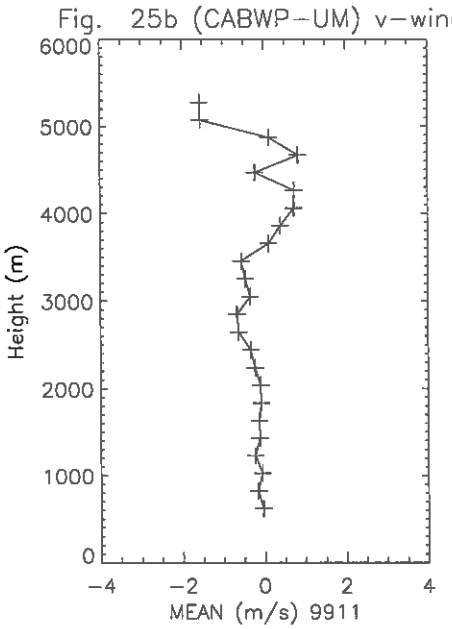
Fig. 25b (CABWP-UM) v-wind
Height (m)
MEAN (m/s) 9911

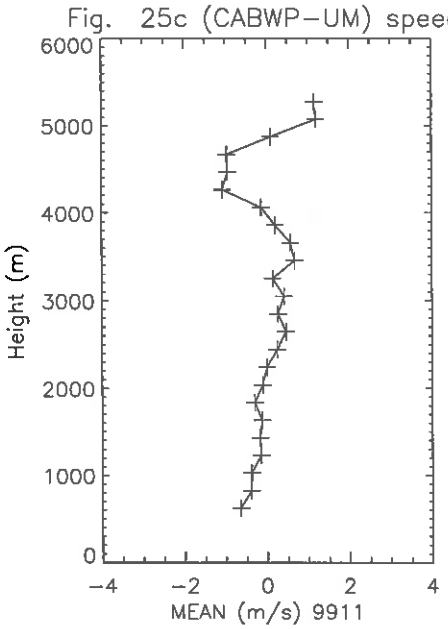
Fig. 25c (CABWP-UM) speed
Height (m)
MEAN (m/s) 9911

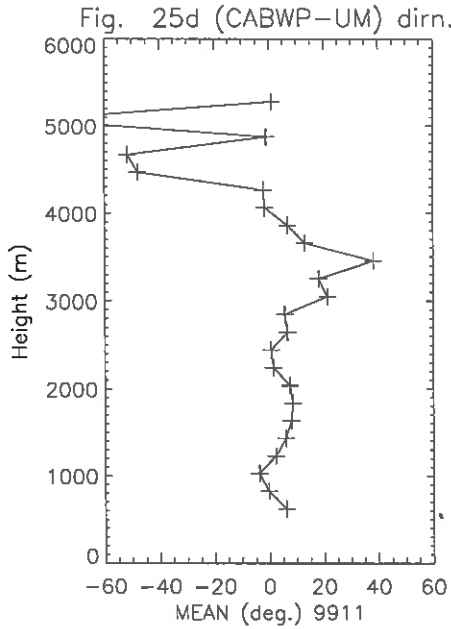
Fig. 25d (CABWP-UM) dirn.
Height (m)
MEAN (deg.) 9911

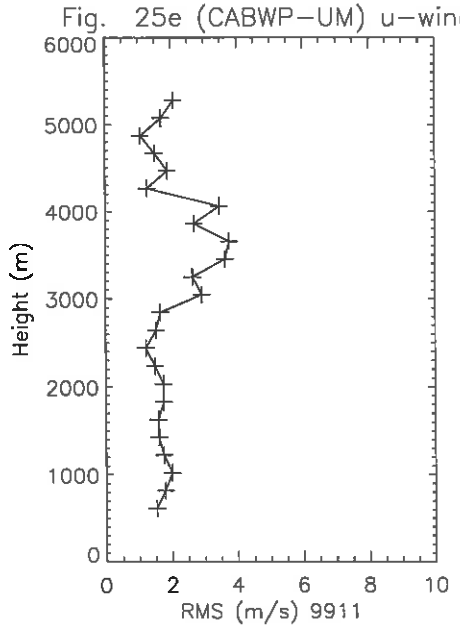
Fig. 25e (CABWP-UM) u-wind
Height (m)
RMS (m/s) 9911

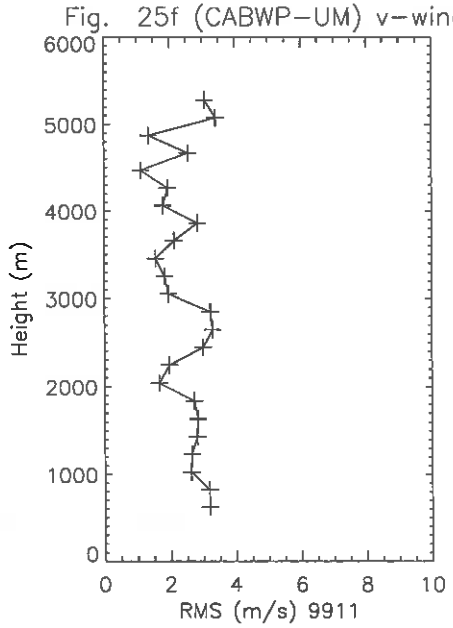
Fig. 25f (CABWP-UM) v-wind
Height (m)
RMS (m/s) 9911

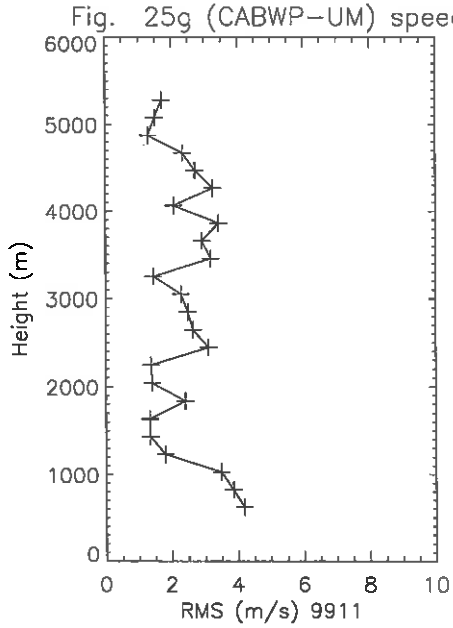
Fig. 25g (CABWP-UM) speed
Height (m)
RMS (m/s) 9911

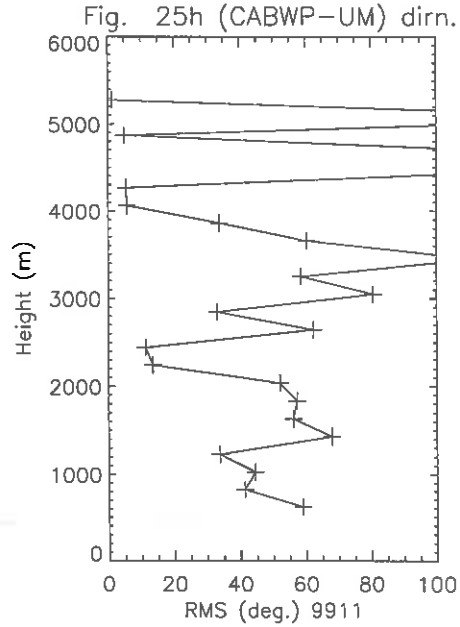
Fig. 25h (CABWP-UM) dirn.
Height (m)
RMS (deg.) 9911

Fig. 26a (CABWP–UM) u–wind

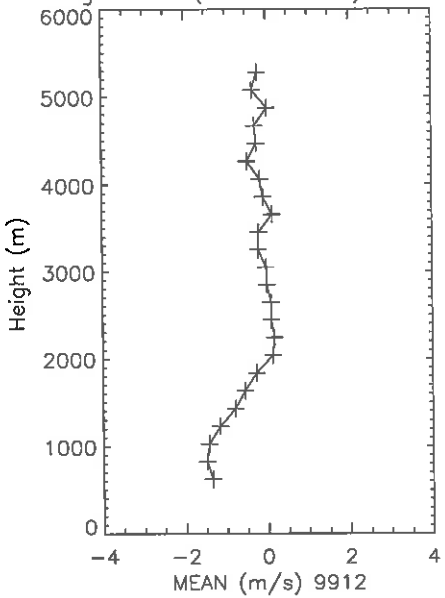

Fig. 26b (CABWP–UM) v–wind

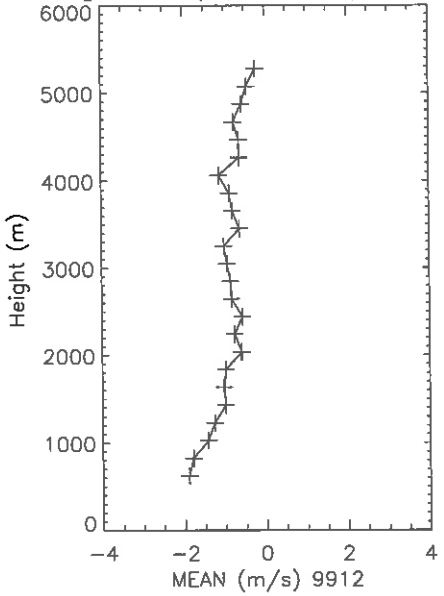

Fig. 26c (CABWP–UM) speed

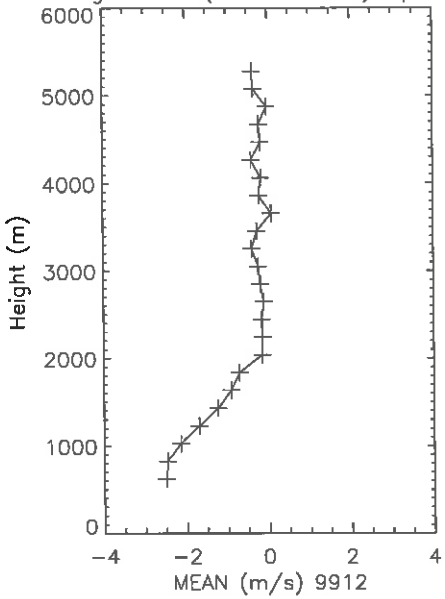

Fig. 26d (CABWP–UM) dirn.

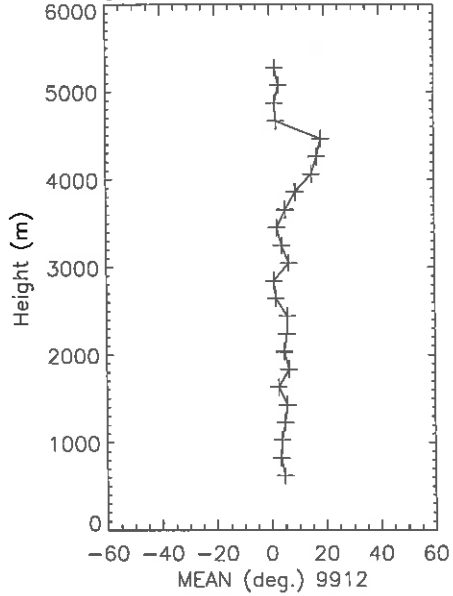

Fig. 26e (CABWP–UM) u–wind

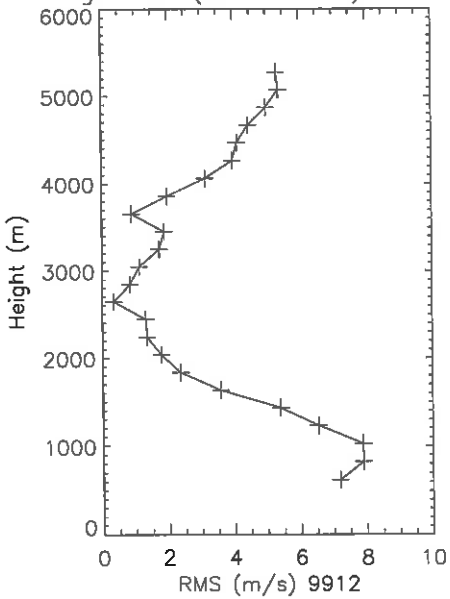

Fig. 26f (CABWP–UM) v–wind

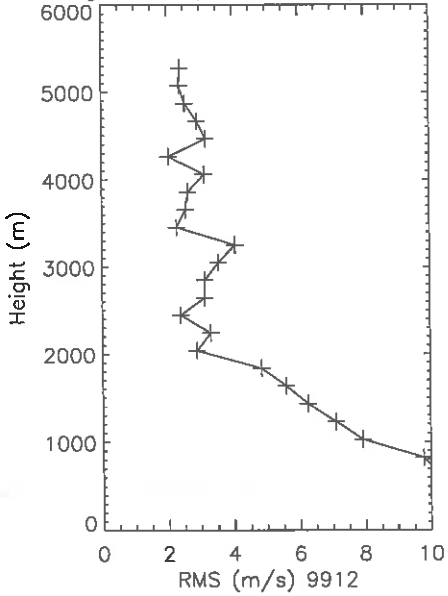

Fig. 26g (CABWP–UM) speed

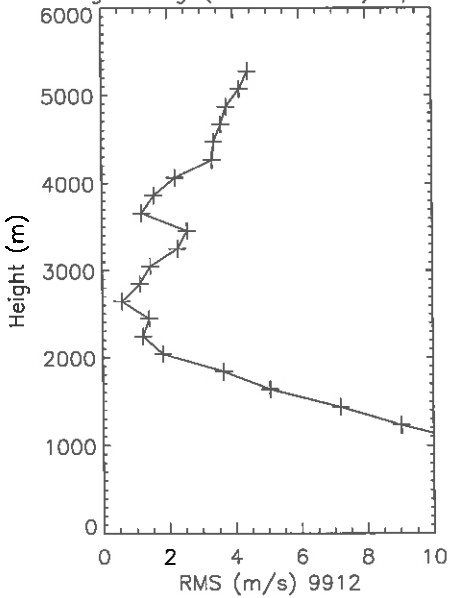

Fig. 26h (CABWP–UM) dirn.

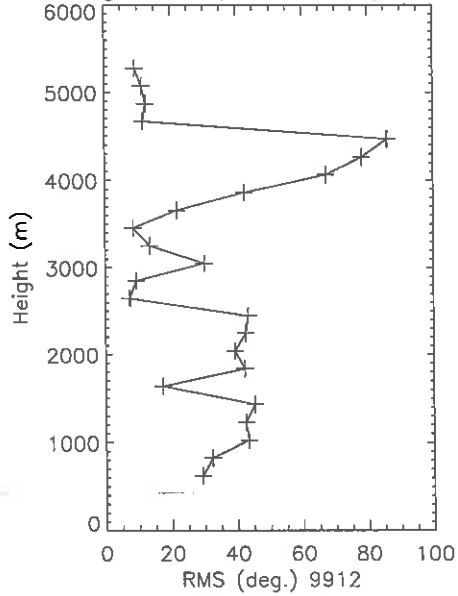

Fig. 27a (CABWP–UM) u–wind

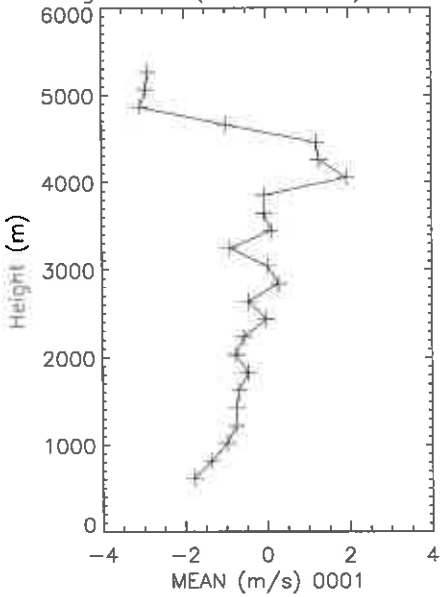

Fig. 27b (CABWP–UM) v–wind

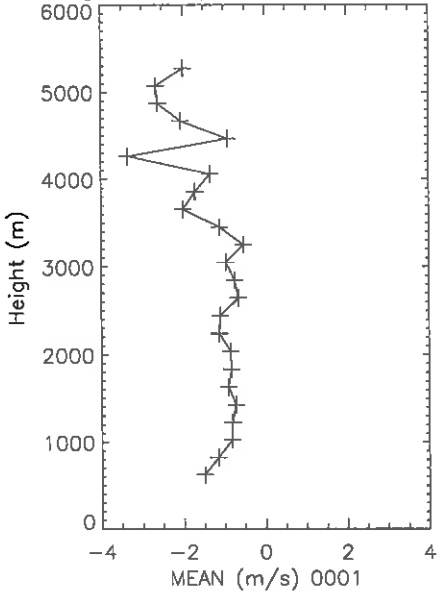

Fig. 27c (CABWP–UM) speed

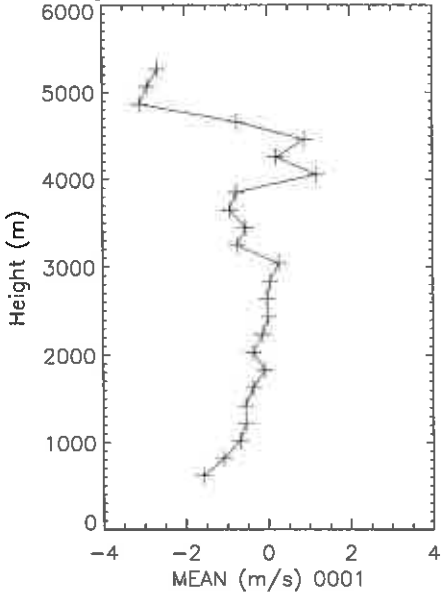

Fig. 27d (CABWP–UM) dirn.

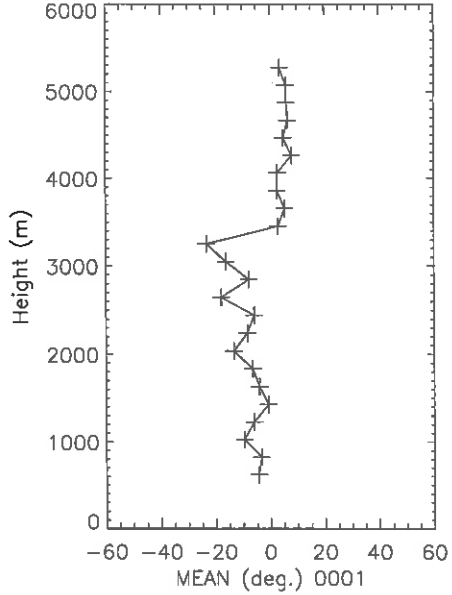

Fig. 27e (CABWP–UM) u–wind

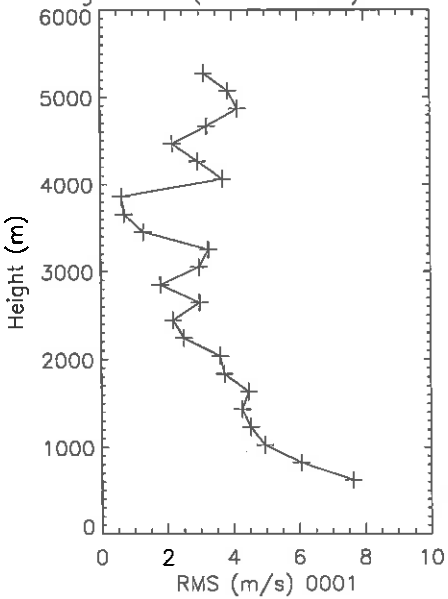

Fig. 27f (CABWP–UM) v–wind

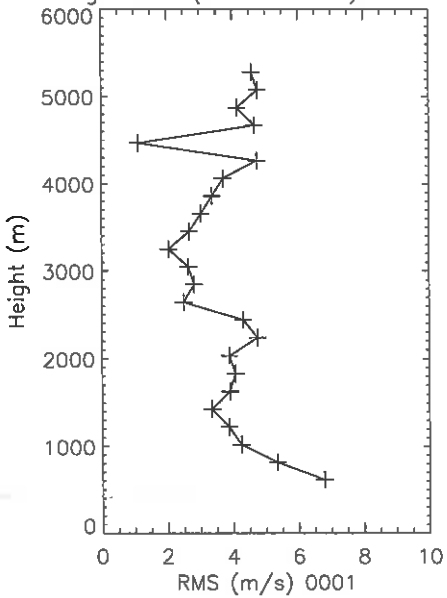

Fig. 27g (CABWP–UM) speed

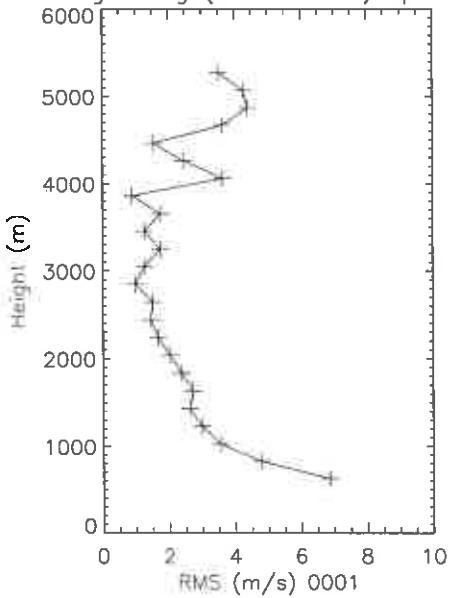

Fig. 27h (CABWP–UM) dirn.

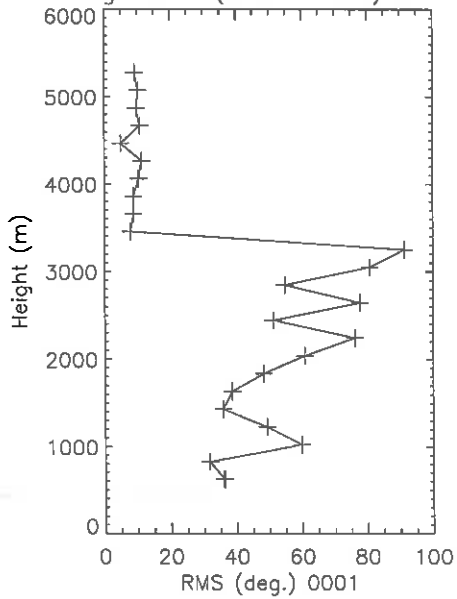

Fig. 28a (CABWP–UM) u–wind

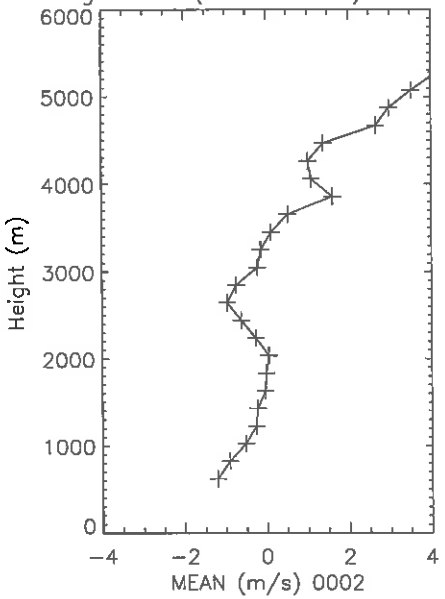

Fig. 28b (CABWP–UM) v–wind

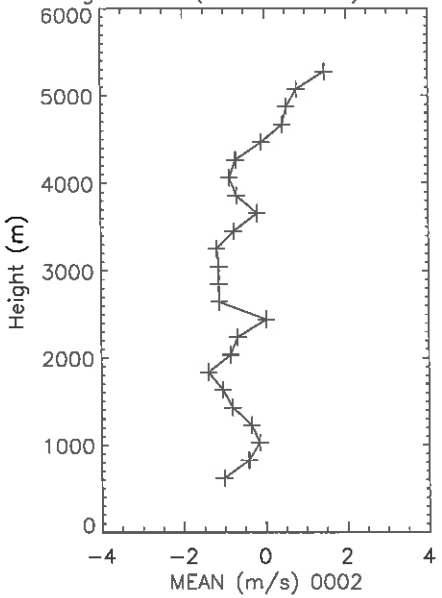

Fig. 28c (CABWP–UM) speed

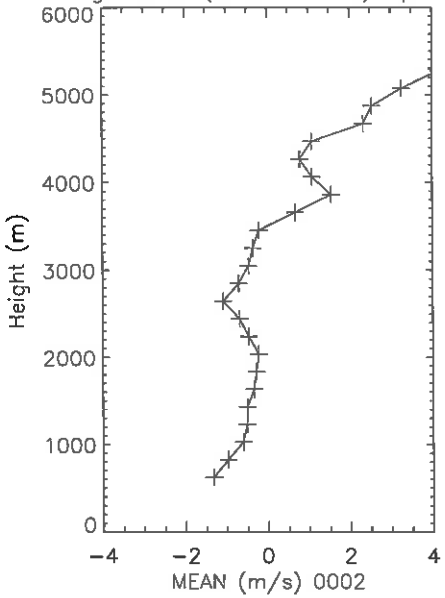

Fig. 28d (CABWP–UM) dirn.

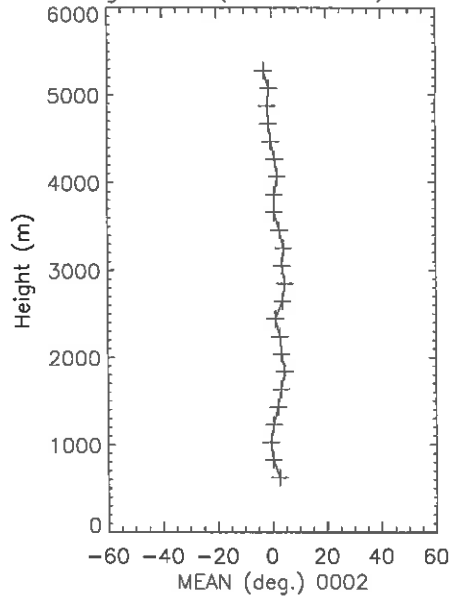

Fig. 28e (CABWP–UM) u–wind

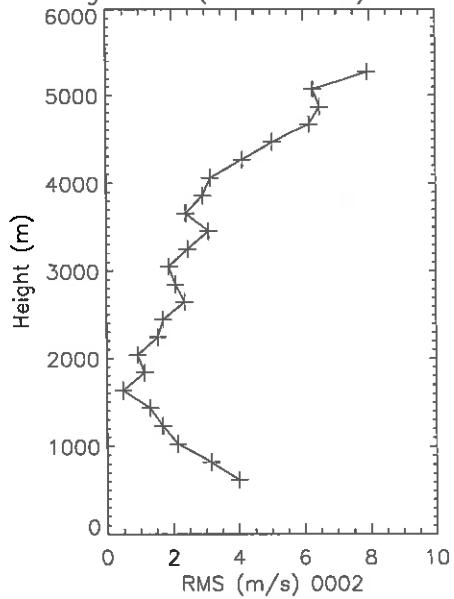

Fig. 28f (CABWP–UM) v–wind

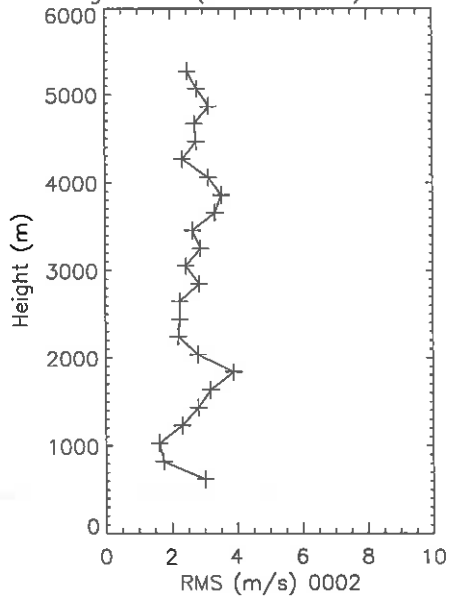

Fig. 28g (CABWP–UM) speed

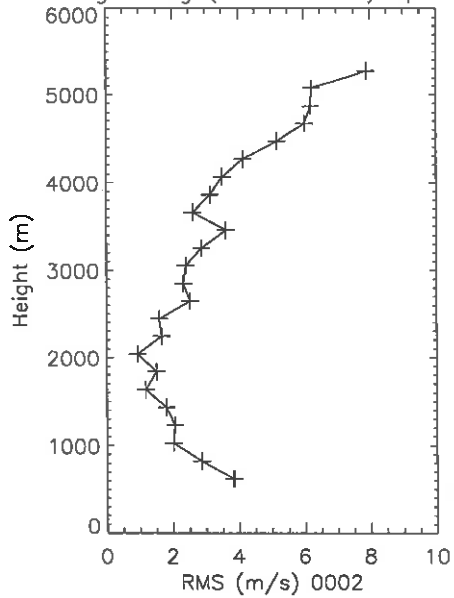

Fig. 28h (CABWP–UM) dirn.

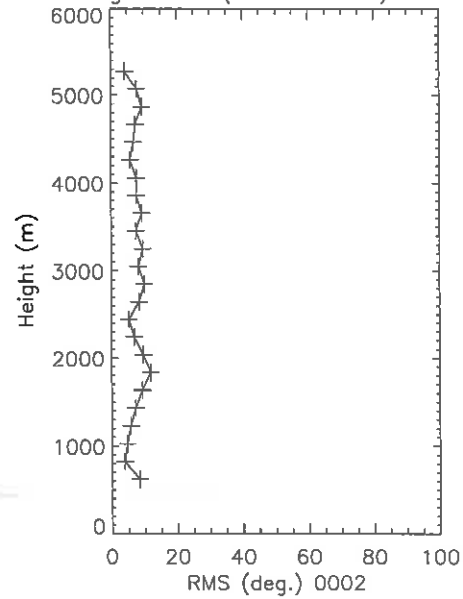

Fig. 29a (CAMWP−UM) u−wind

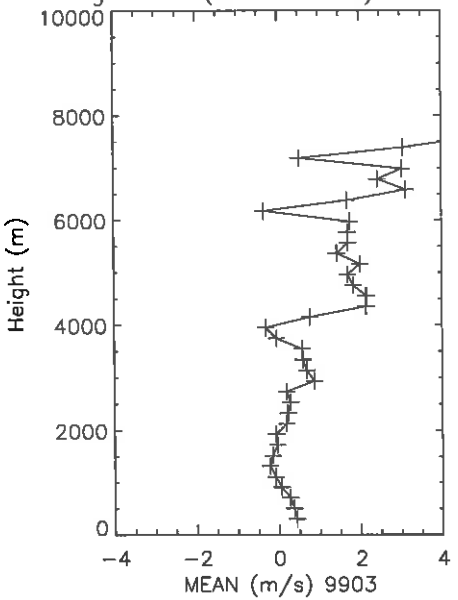

Fig. 29b (CAMWP−UM) v−wind

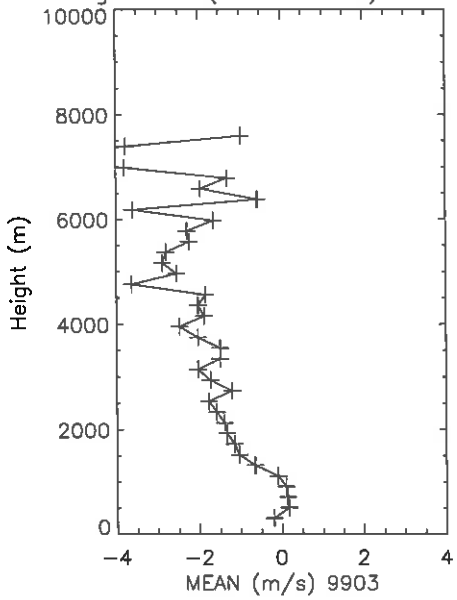

Fig. 29c (CAMWP−UM) speed

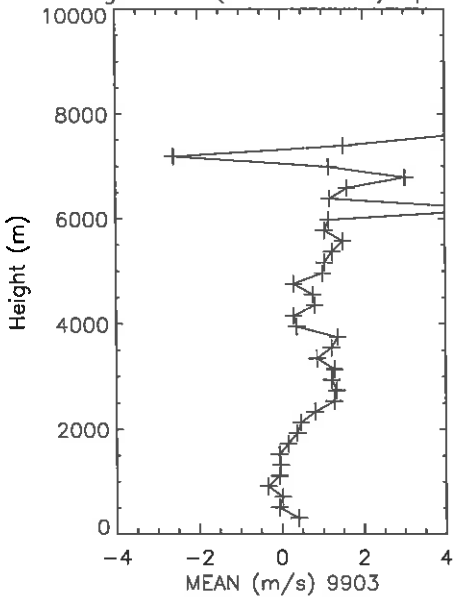

Fig. 29d (CAMWP−UM) dirn.

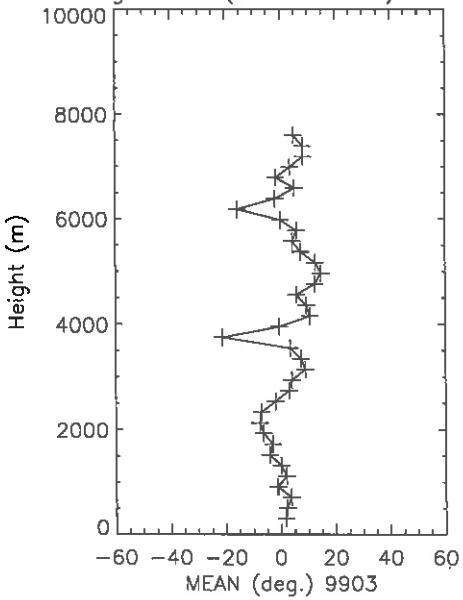

Fig. 29e (CAMWP−UM) u−wind

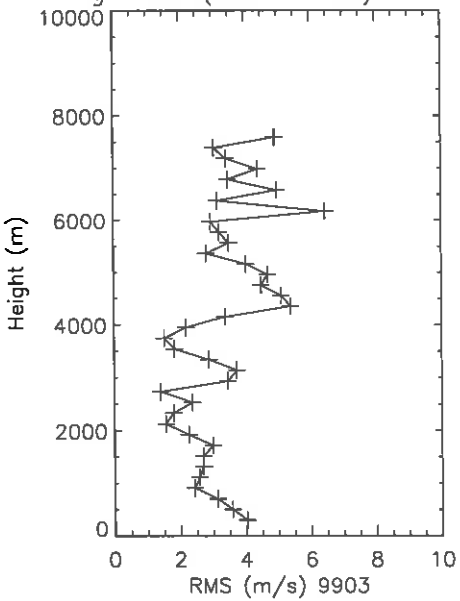

Fig. 29f (CAMWP−UM) v−wind

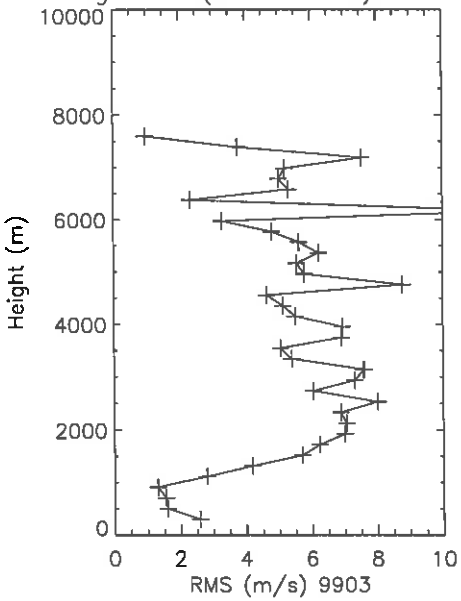

Fig. 29g (CAMWP−UM) speed

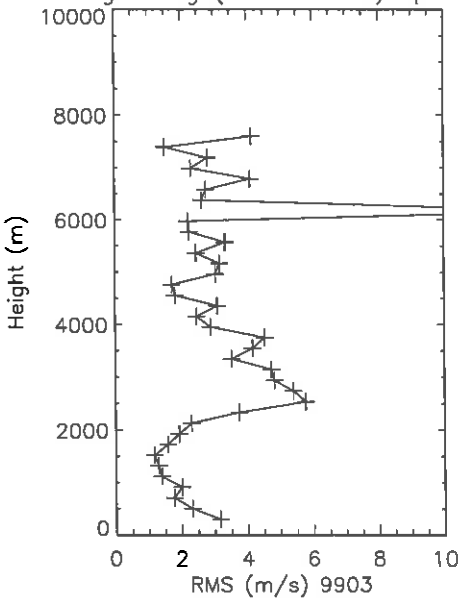

Fig. 29h (CAMWP−UM) dirn.

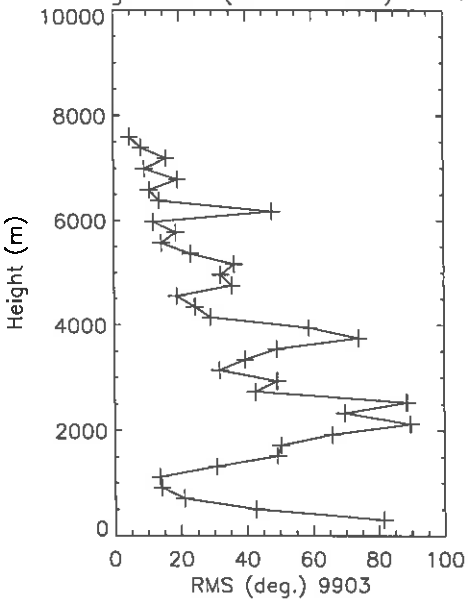

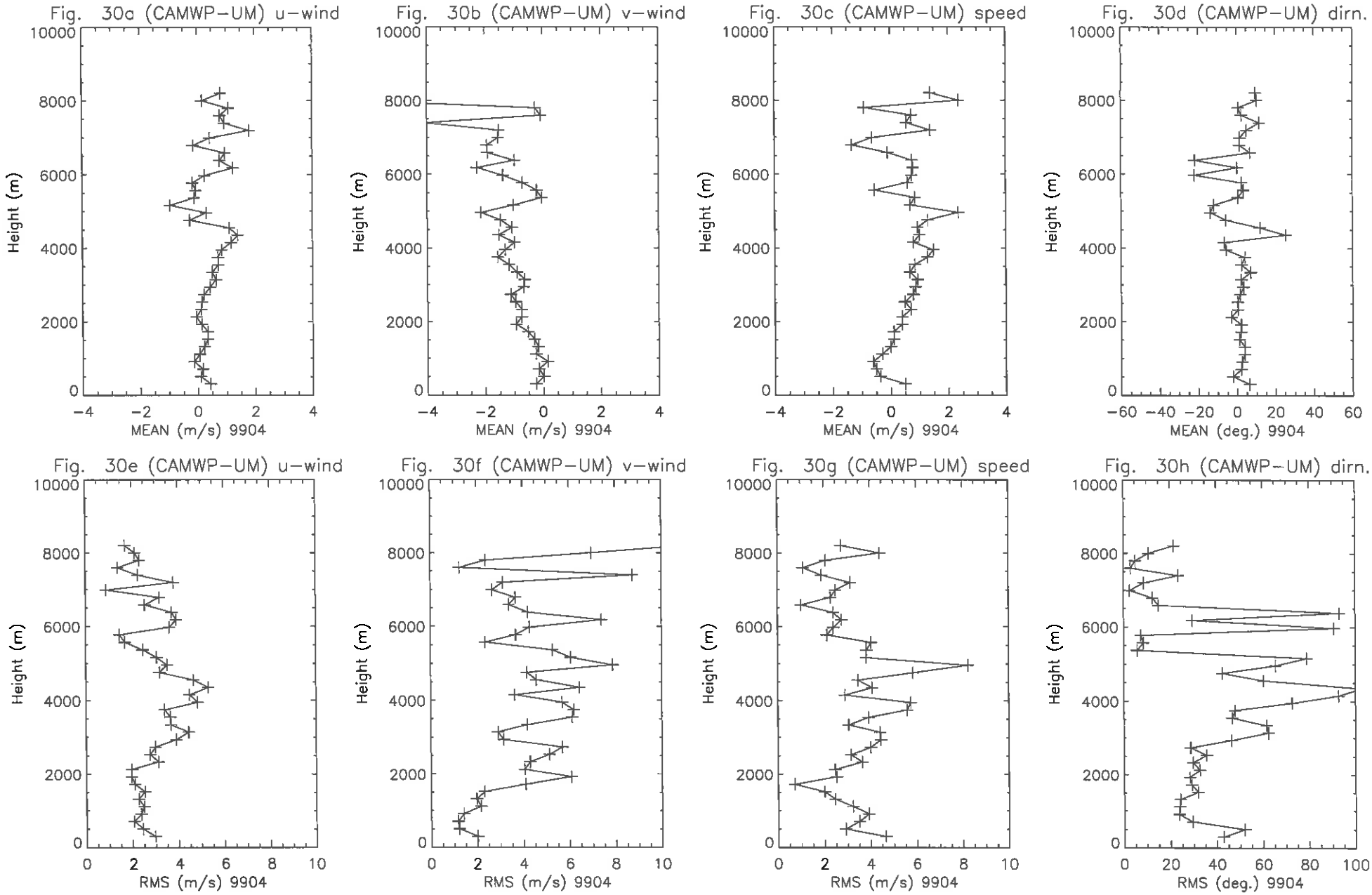
Fig. 30a (CAMWP-UM) u-wind
Fig. 30b (CAMWP-UM) v-wind
Fig. 30c (CAMWP-UM) speed
Fig. 30d (CAMWP-UM) dirn.
Fig. 30e (CAMWP-UM) u-wind
Fig. 30f (CAMWP-UM) v-wind
Fig. 30g (CAMWP-UM) speed
Fig. 30h (CAMWP-UM) dirn.
Height (m)
MEAN (m/s) 9904
MEAN (deg.) 9904
RMS (m/s) 9904
RMS (deg.) 9904

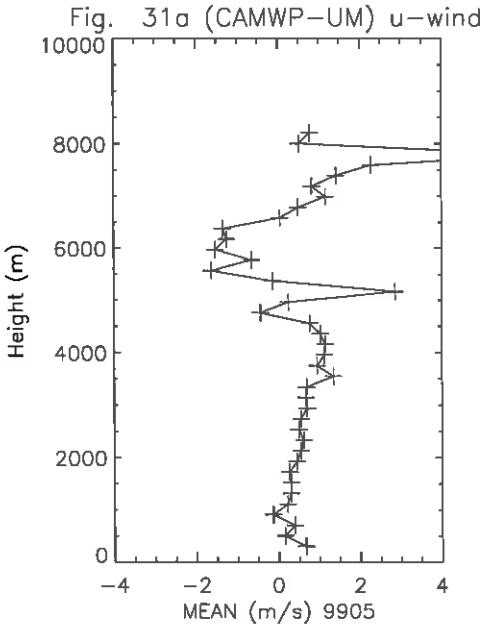
Fig. 31a (CAMWP-UM) u-wind
Height (m)
MEAN (m/s) 9905

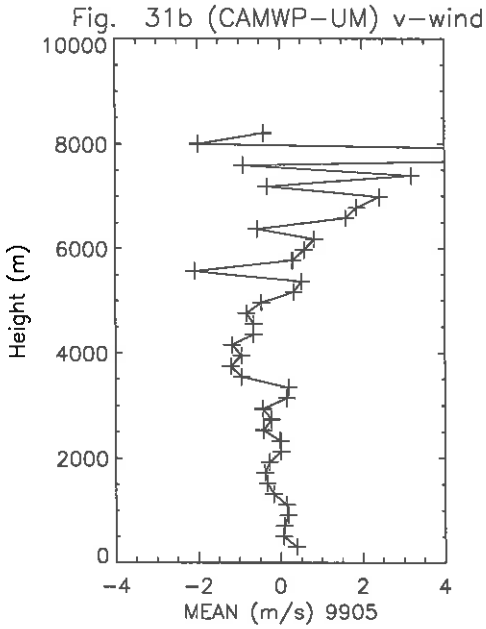
Fig. 31b (CAMWP-UM) v-wind
Height (m)
MEAN (m/s) 9905

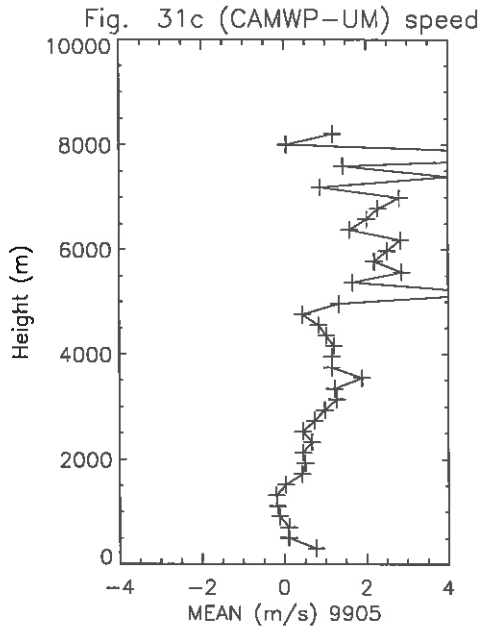
Fig. 31c (CAMWP-UM) speed
Height (m)
MEAN (m/s) 9905

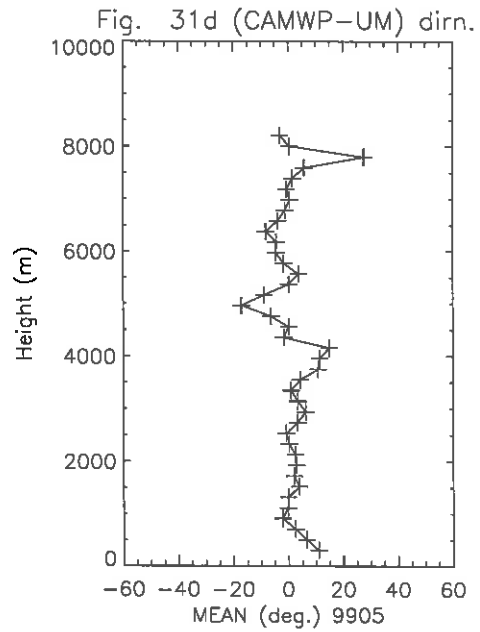
Fig. 31d (CAMWP-UM) dirn.
Height (m)
MEAN (deg.) 9905

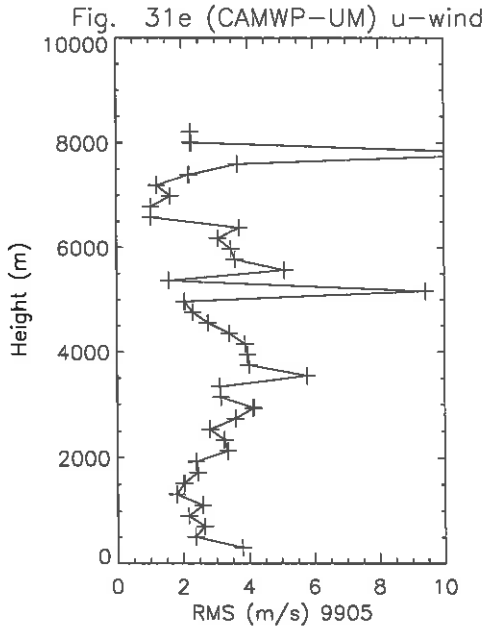
Fig. 31e (CAMWP-UM) u-wind
Height (m)
RMS (m/s) 9905

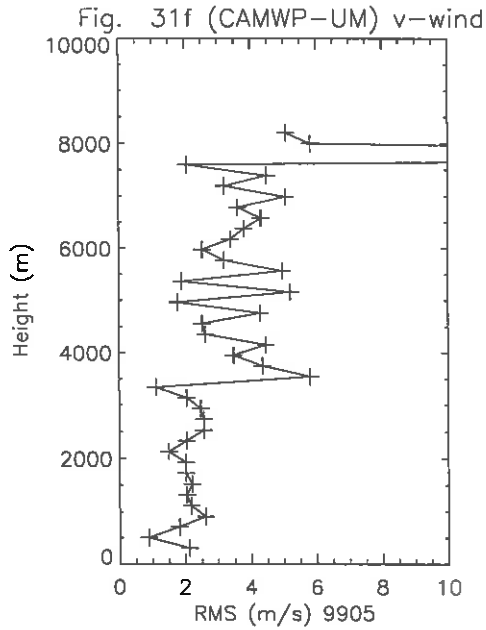
Fig. 31f (CAMWP-UM) v-wind
Height (m)
RMS (m/s) 9905

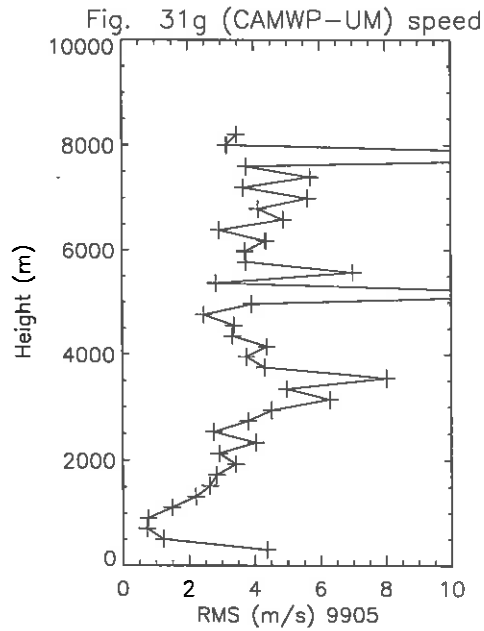
Fig. 31g (CAMWP-UM) speed
Height (m)
RMS (m/s) 9905

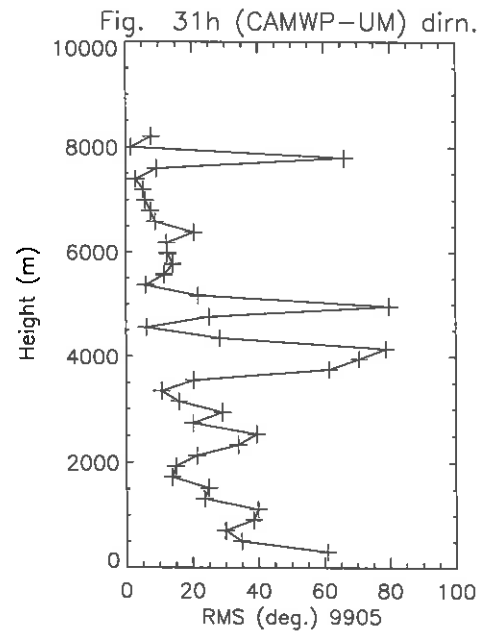
Fig. 31h (CAMWP-UM) dirn.
Height (m)
RMS (deg.) 9905

Fig. 32a (CAMWP−UM) u−wind

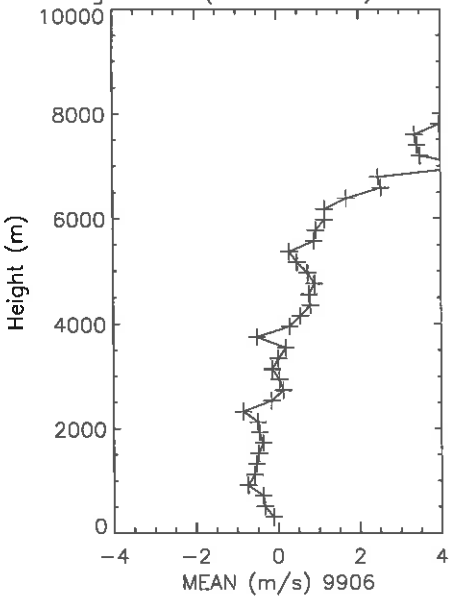

Fig. 32b (CAMWP−UM) v−wind

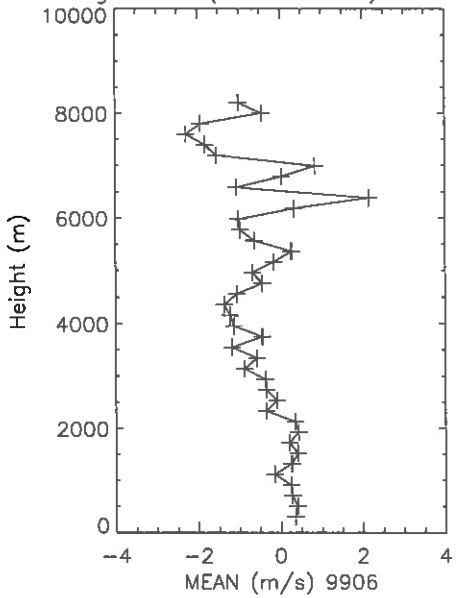

Fig. 32c (CAMWP−UM) speed

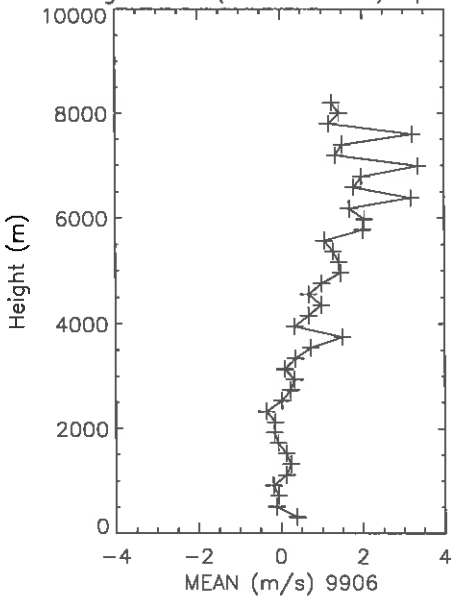

Fig. 32d (CAMWP−UM) dirn.

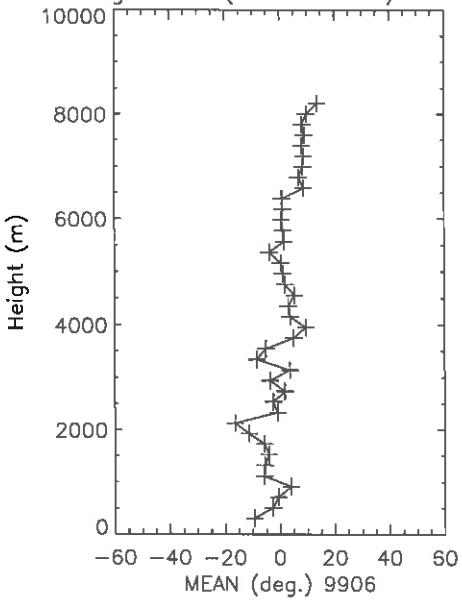

Fig. 32e (CAMWP−UM) u−wind

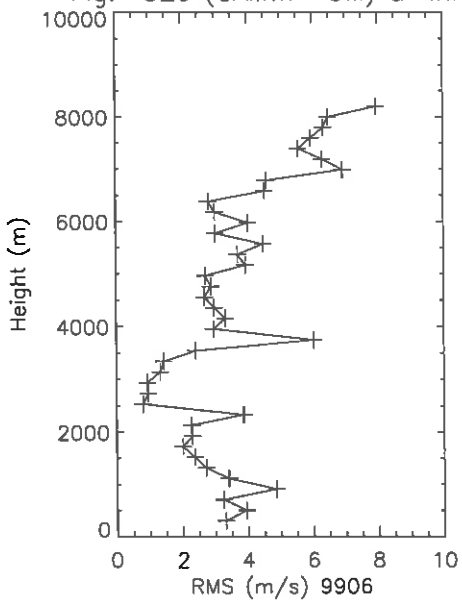

Fig. 32f (CAMWP−UM) v−wind

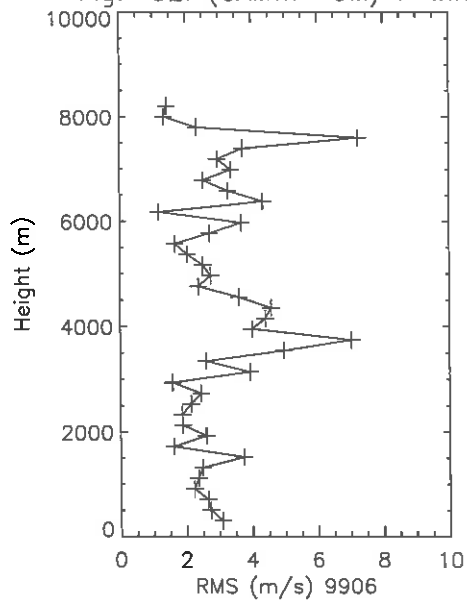

Fig. 32g (CAMWP−UM) speed

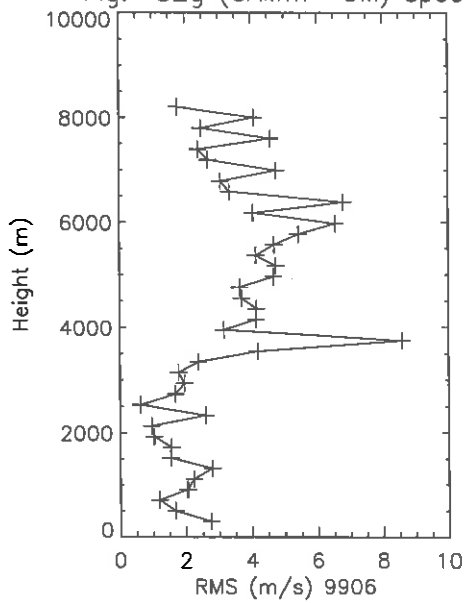

Fig. 32h (CAMWP−UM) dirn.

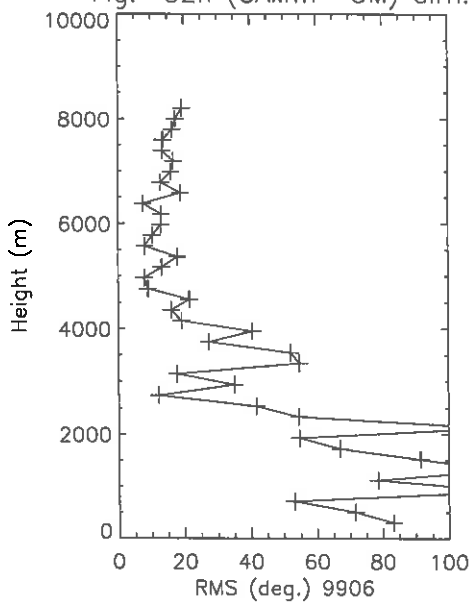

Fig. 33a (CAMWP−UM) u−wind

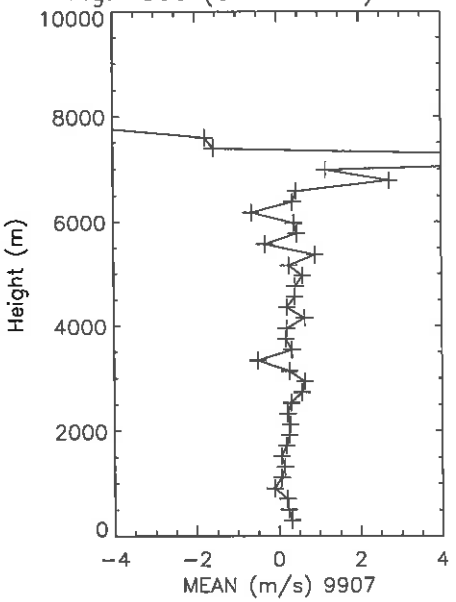

Fig. 33b (CAMWP−UM) v−wind

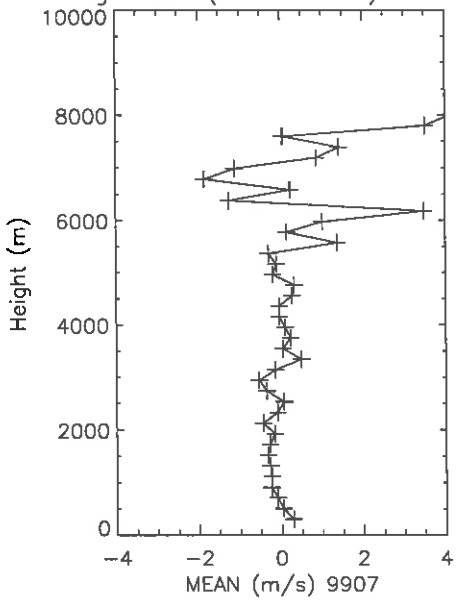

Fig. 33c (CAMWP−UM) speed

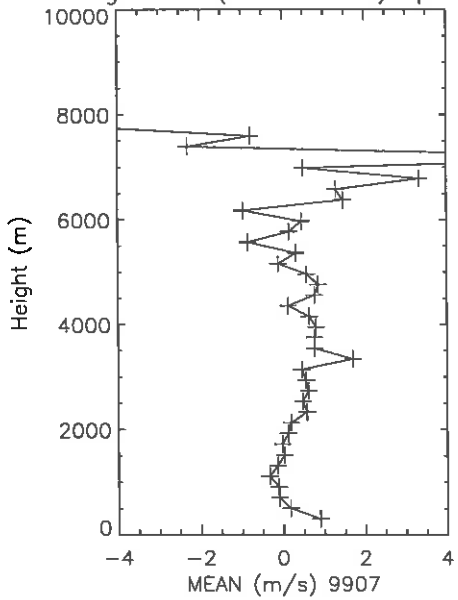

Fig. 33d (CAMWP−UM) dirn.

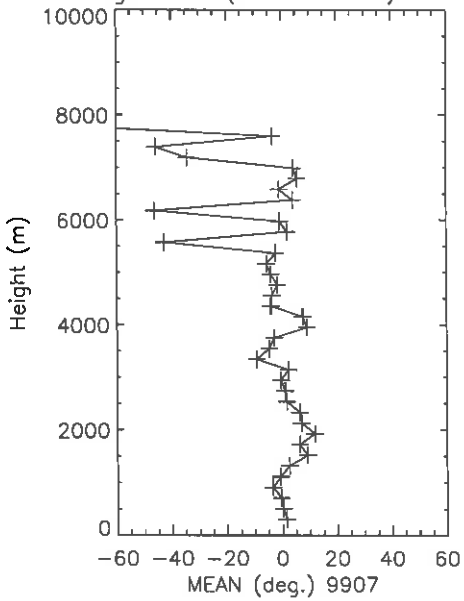

Fig. 33e (CAMWP−UM) u−wind

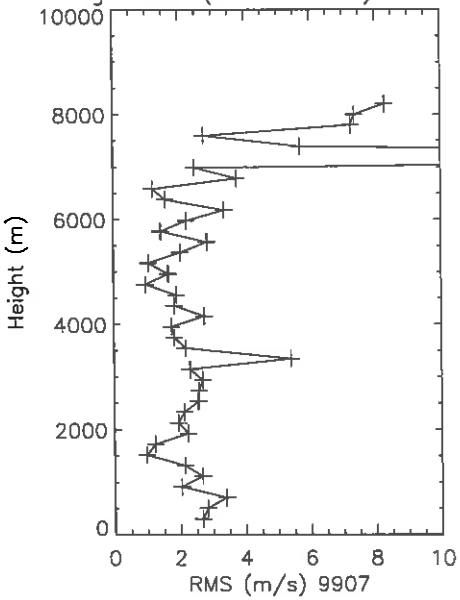

Fig. 33f (CAMWP−UM) v−wind

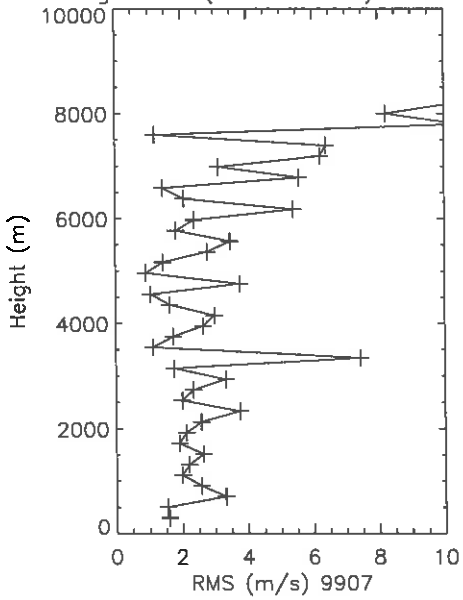

Fig. 33g (CAMWP−UM) speed

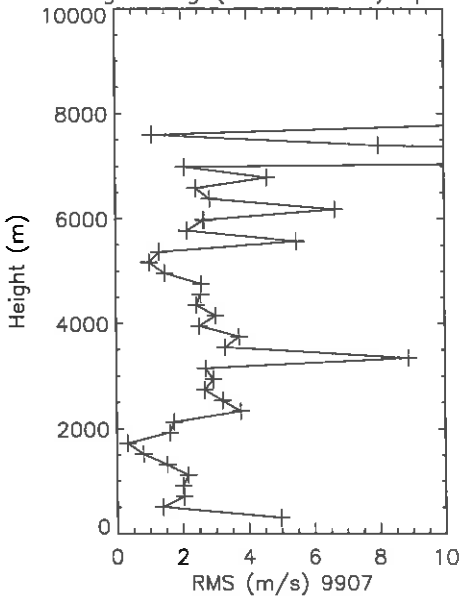

Fig. 33h (CAMWP−UM) dirn.

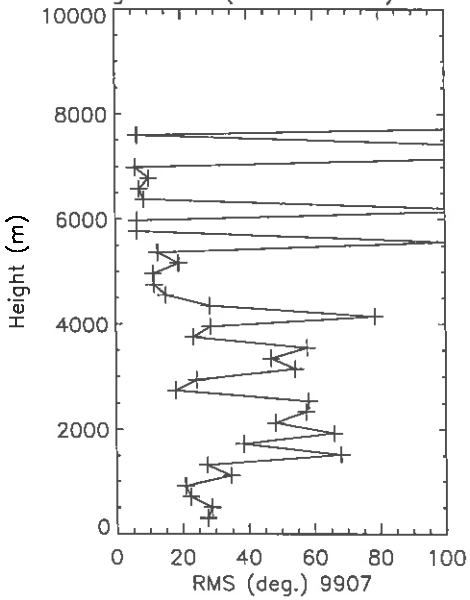

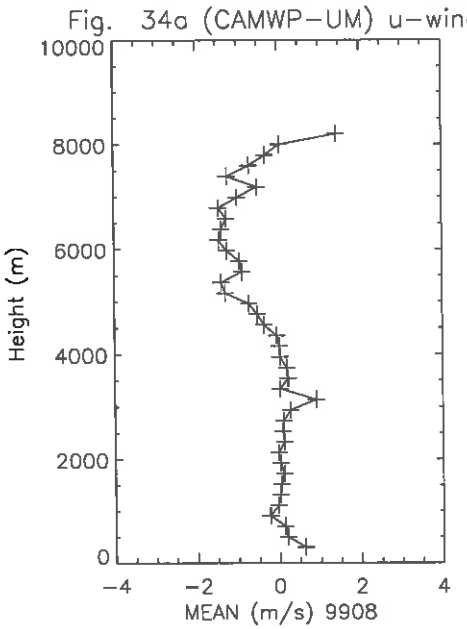
Fig. 34a (CAMWP-UM) u-wind
Height (m)
MEAN (m/s) 9908

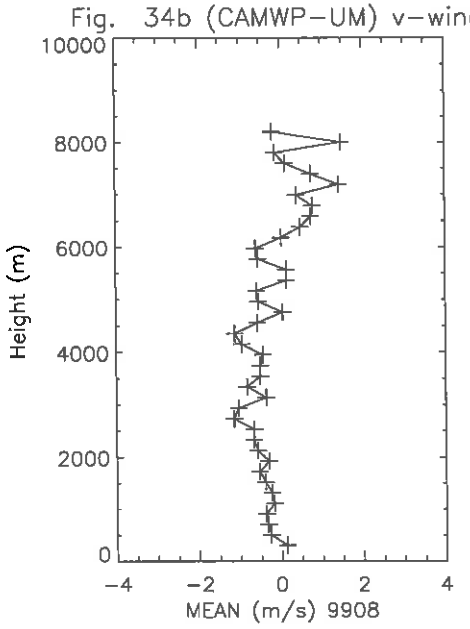
Fig. 34b (CAMWP-UM) v-wind
Height (m)
MEAN (m/s) 9908

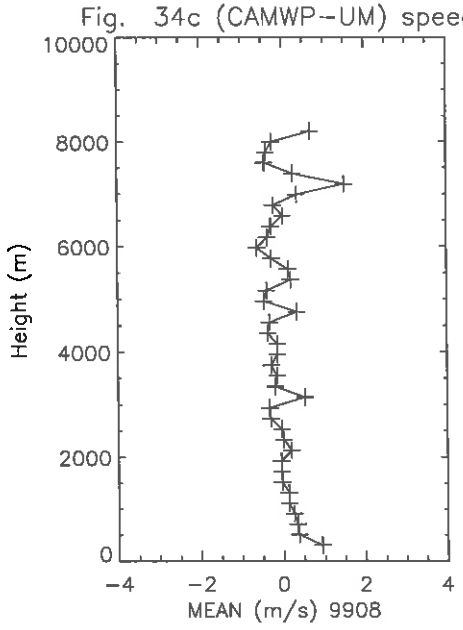
Fig. 34c (CAMWP-UM) speed
Height (m)
MEAN (m/s) 9908

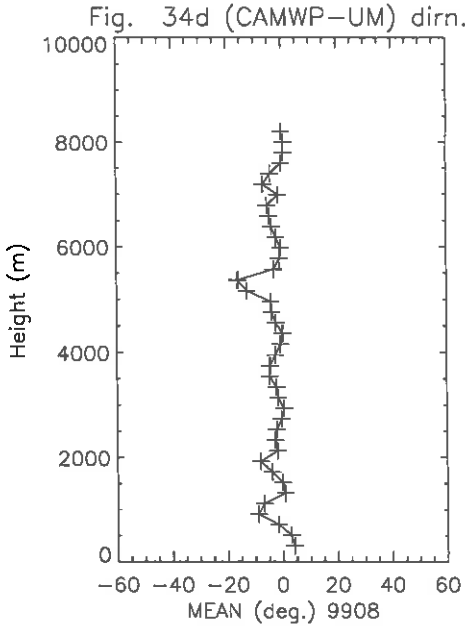
Fig. 34d (CAMWP-UM) dirn.
Height (m)
MEAN (deg.) 9908

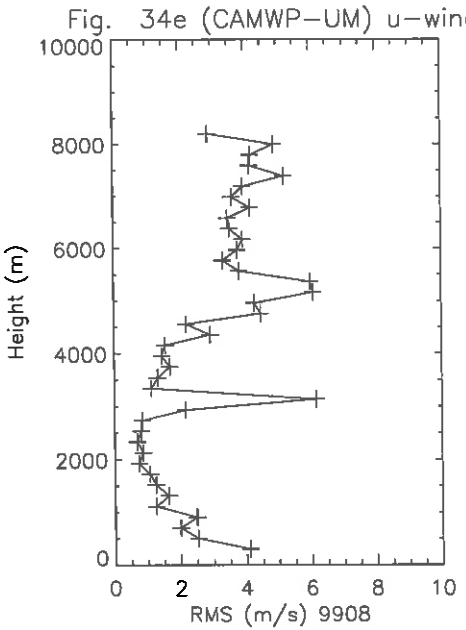
Fig. 34e (CAMWP-UM) u-wind
Height (m)
RMS (m/s) 9908

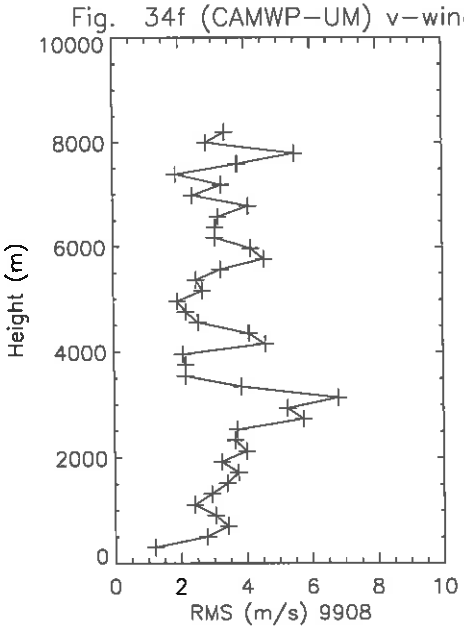
Fig. 34f (CAMWP-UM) v-wind
Height (m)
RMS (m/s) 9908

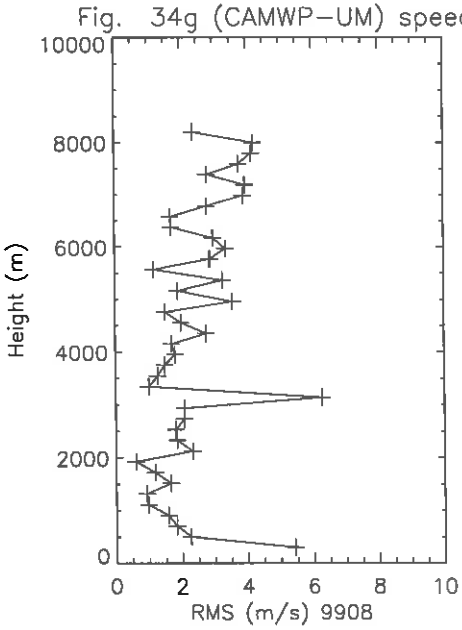
Fig. 34g (CAMWP-UM) speed
Height (m)
RMS (m/s) 9908

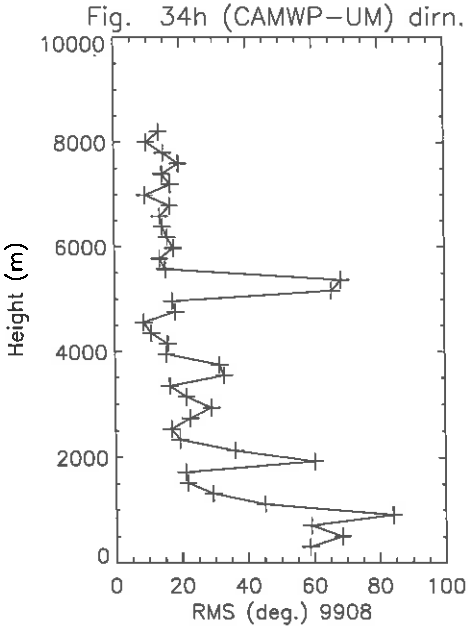
Fig. 34h (CAMWP-UM) dirn.
Height (m)
RMS (deg.) 9908

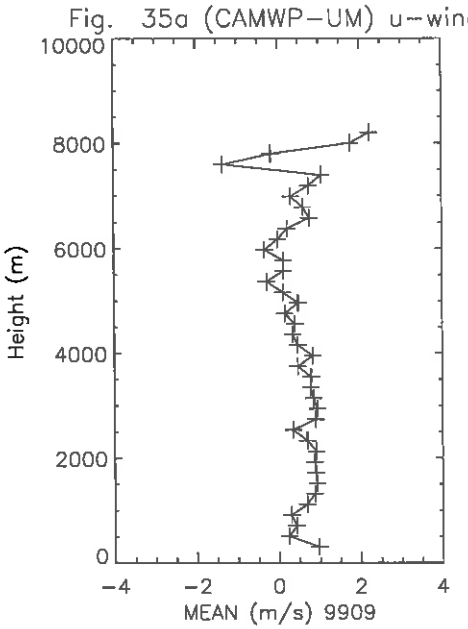
Fig. 35a (CAMWP-UM) u-wind
Height (m)
MEAN (m/s) 9909

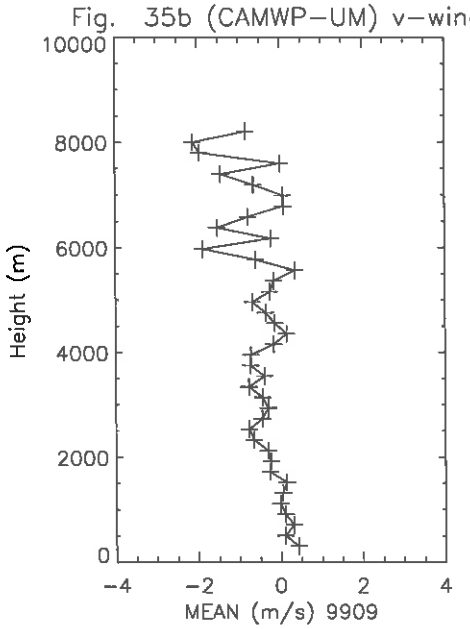
Fig. 35b (CAMWP-UM) v-wind
Height (m)
MEAN (m/s) 9909

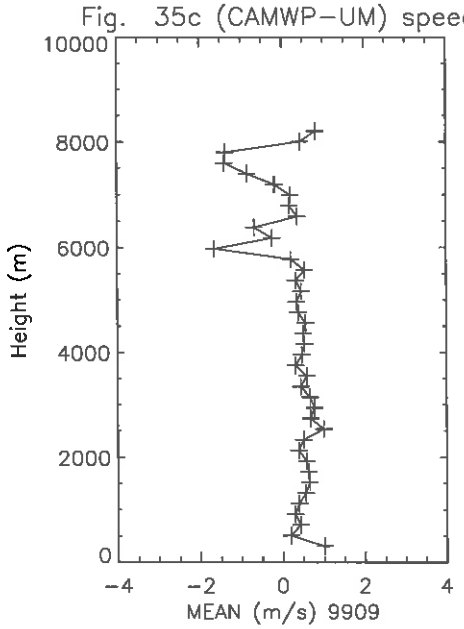
Fig. 35c (CAMWP-UM) speed
Height (m)
MEAN (m/s) 9909

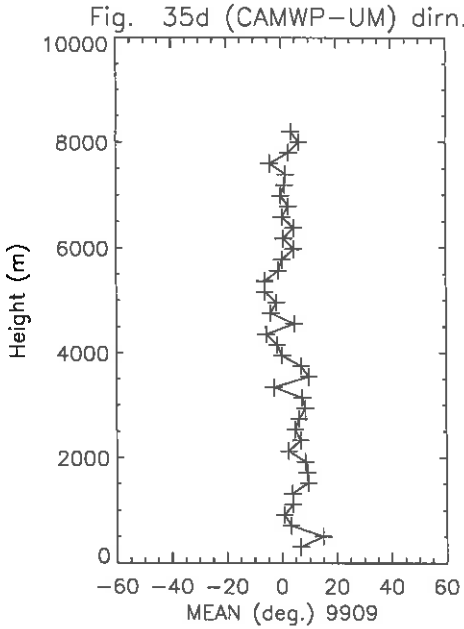
Fig. 35d (CAMWP-UM) dirn.
Height (m)
MEAN (deg.) 9909

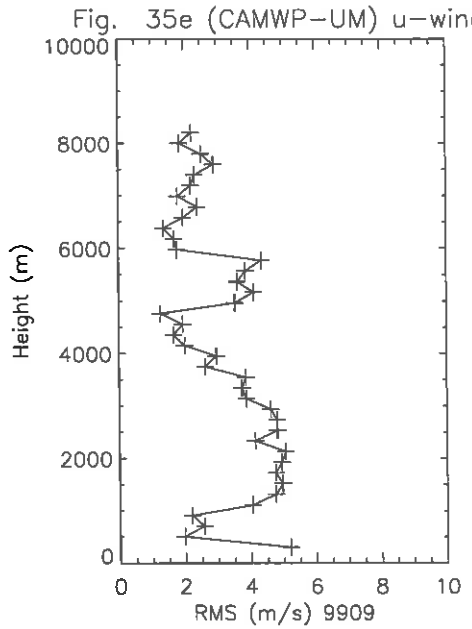
Fig. 35e (CAMWP-UM) u-wind
Height (m)
RMS (m/s) 9909

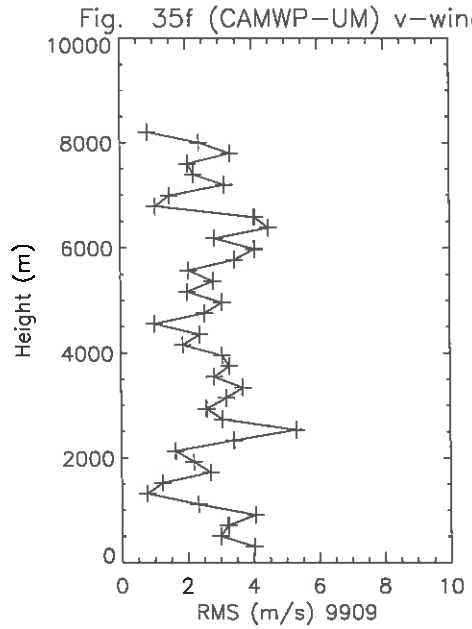
Fig. 35f (CAMWP-UM) v-wind
Height (m)
RMS (m/s) 9909

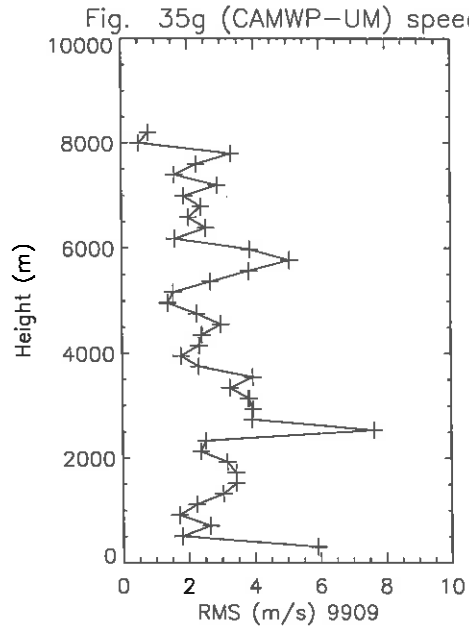
Fig. 35g (CAMWP-UM) speed
Height (m)
RMS (m/s) 9909

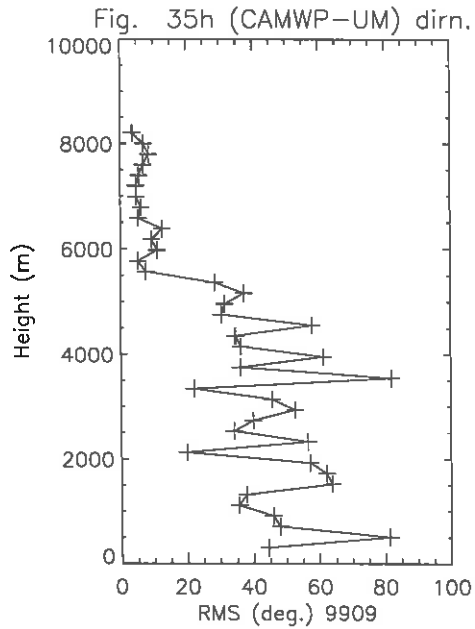
Fig. 35h (CAMWP-UM) dirn.
Height (m)
RMS (deg.) 9909

Fig. 36a (CAMWP–UM) u–wind

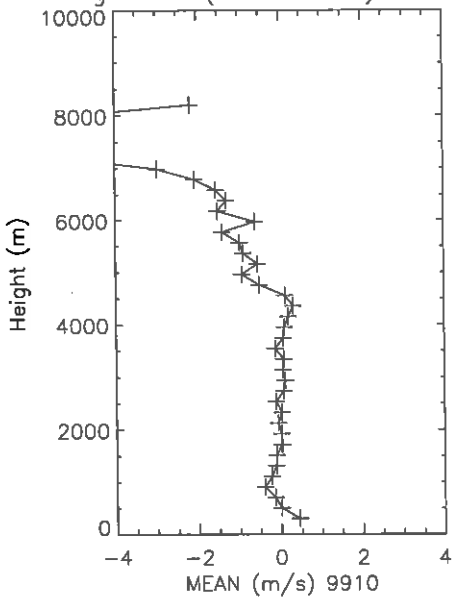

Fig. 36b (CAMWP–UM) v–wind

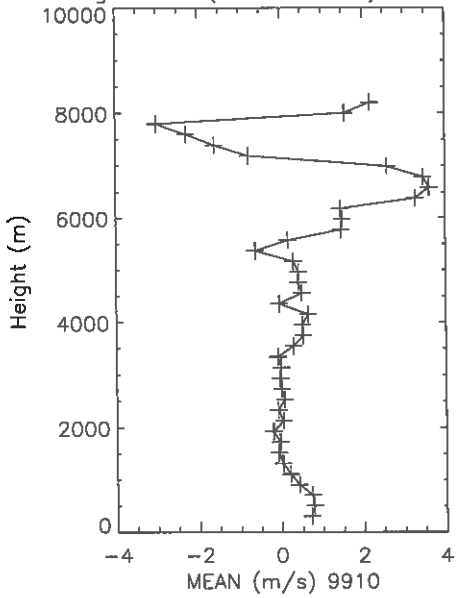

Fig. 36c (CAMWP–UM) speed

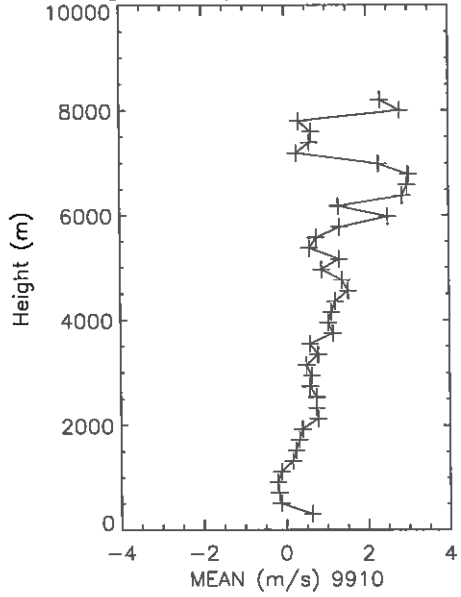

Fig. 36d (CAMWP–UM) dirn.

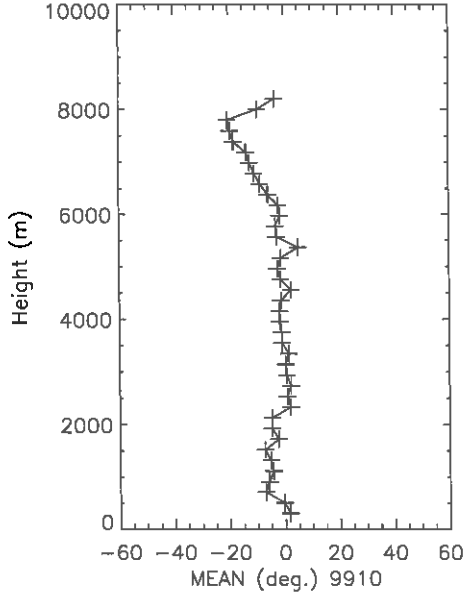

Fig. 36e (CAMWP–UM) u–wind

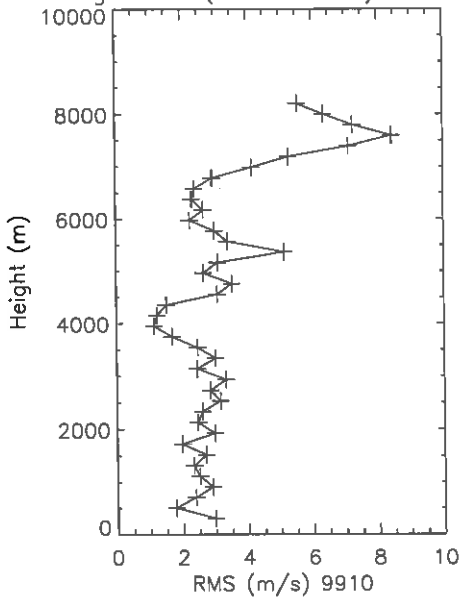

Fig. 36f (CAMWP–UM) v–wind

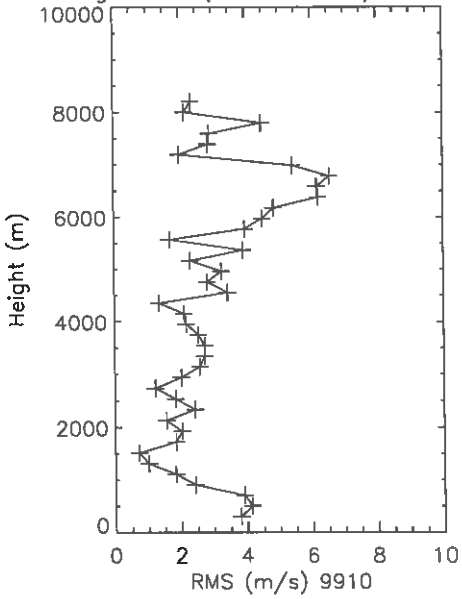

Fig. 36g (CAMWP–UM) speed

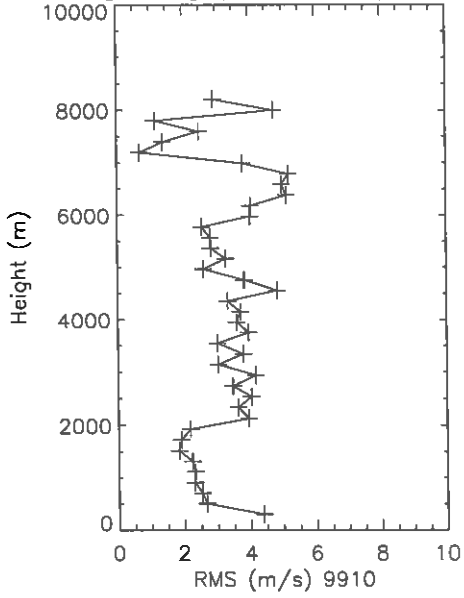

Fig. 36h (CAMWP–UM) dirn.

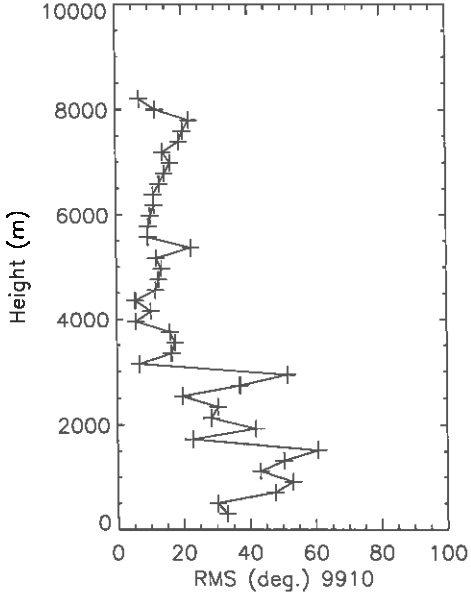

Fig. 37a (CAMWP–UM) u–wind

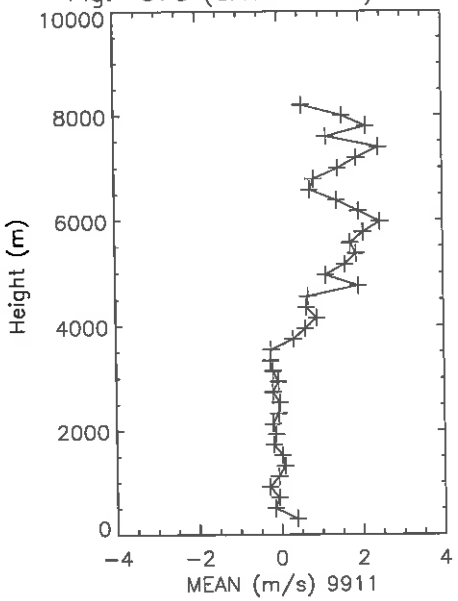

Fig. 37b (CAMWP–UM) v–wind

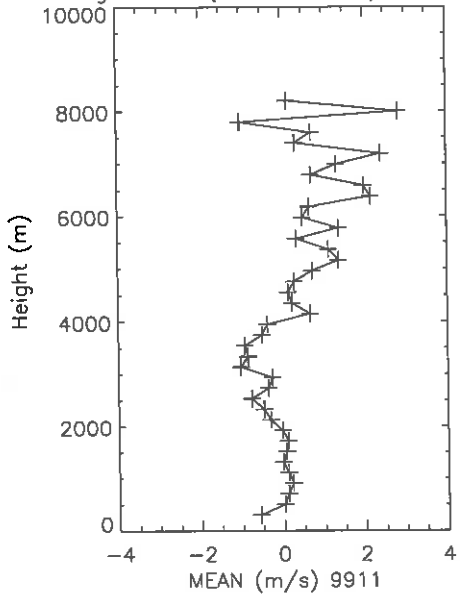

Fig. 37c (CAMWP–UM) speed

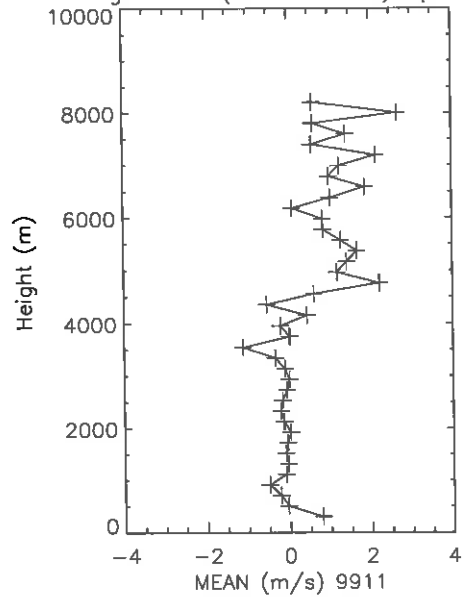

Fig. 37d (CAMWP–UM) dirn.

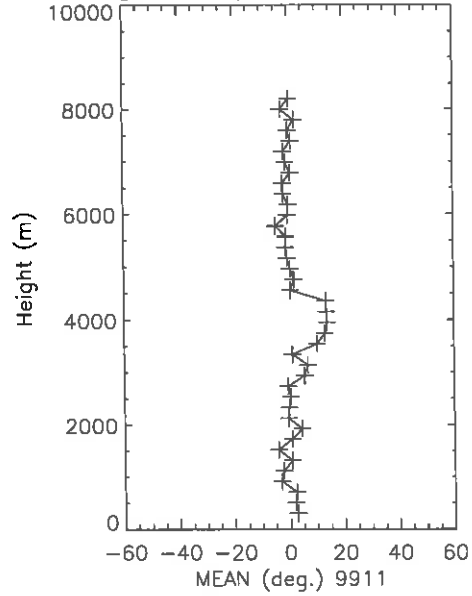

Fig. 37e (CAMWP–UM) u–wind

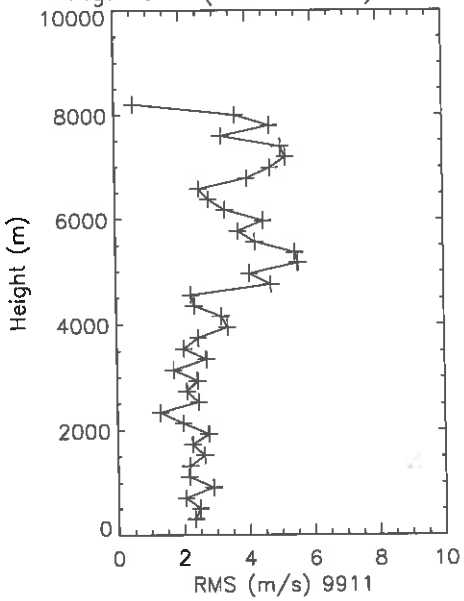

Fig. 37f (CAMWP–UM) v–wind

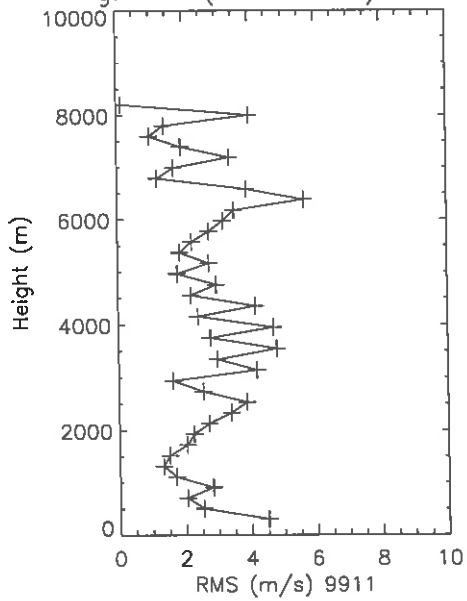

Fig. 37g (CAMWP–UM) speed

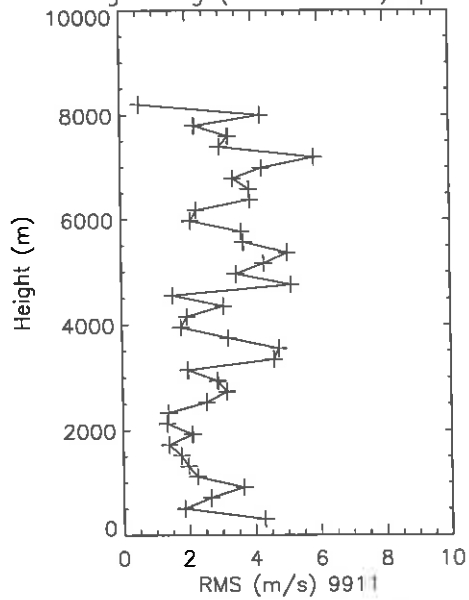

Fig. 37h (CAMWP–UM) dirn.

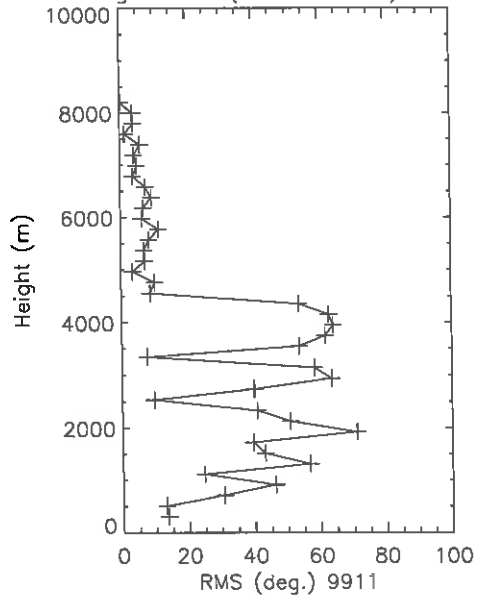

Fig. 38a (CAMWP–UM) u–wind

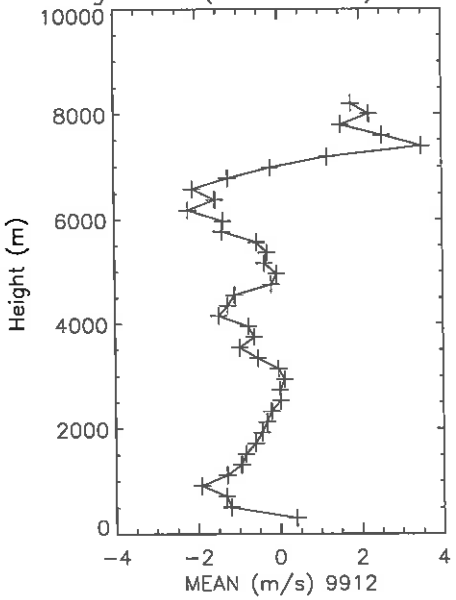

Fig. 38b (CAMWP–UM) v–wind

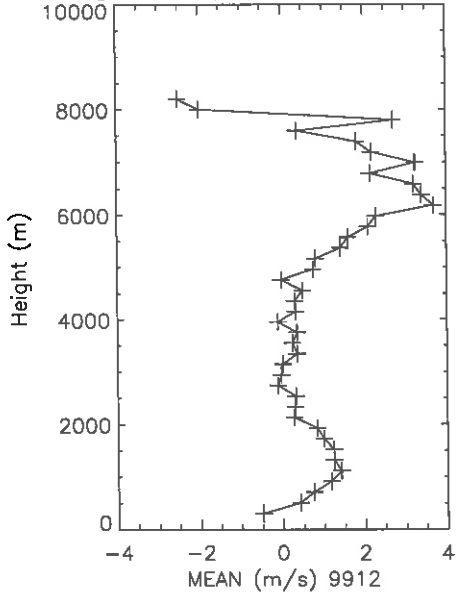

Fig. 38c (CAMWP–UM) speed

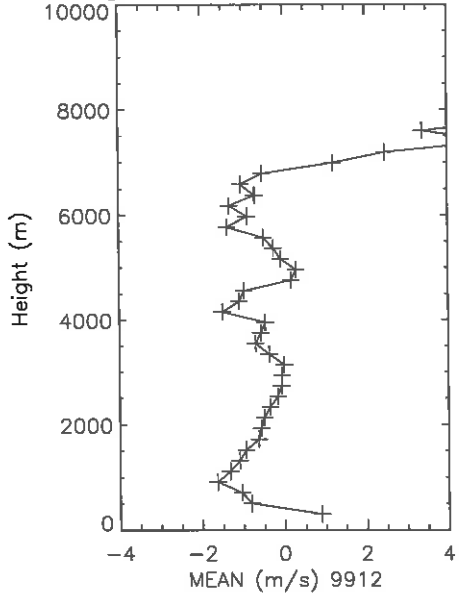

Fig. 38d (CAMWP–UM) dirn.

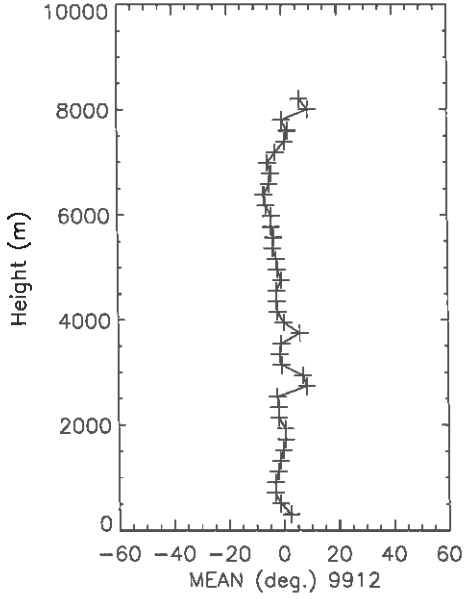

Fig. 38e (CAMWP–UM) u–wind

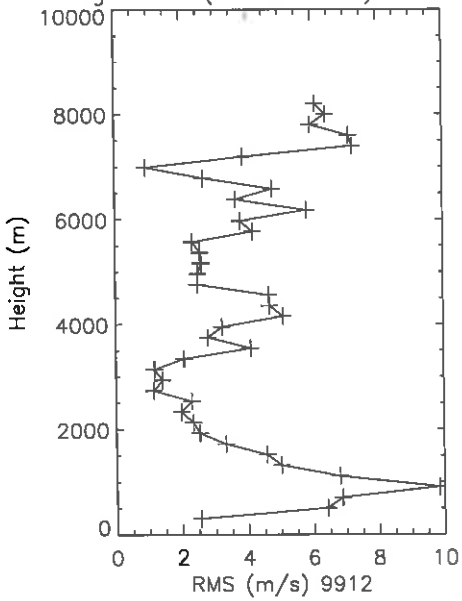

Fig. 38f (CAMWP–UM) v–wind

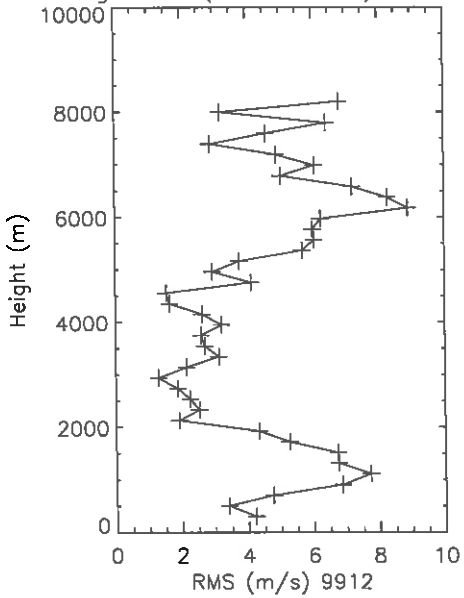

Fig. 38g (CAMWP–UM) speed

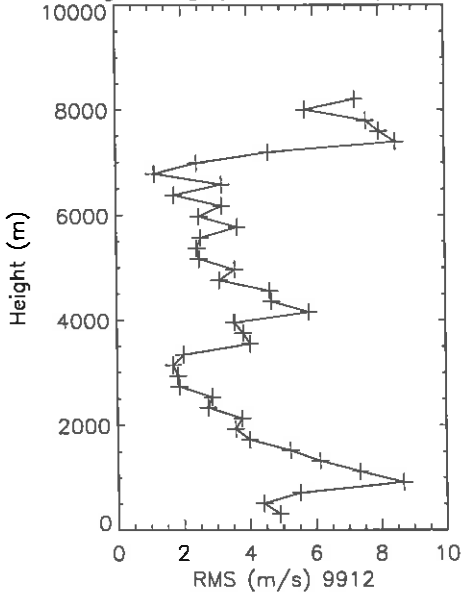

Fig. 38h (CAMWP–UM) dirn.

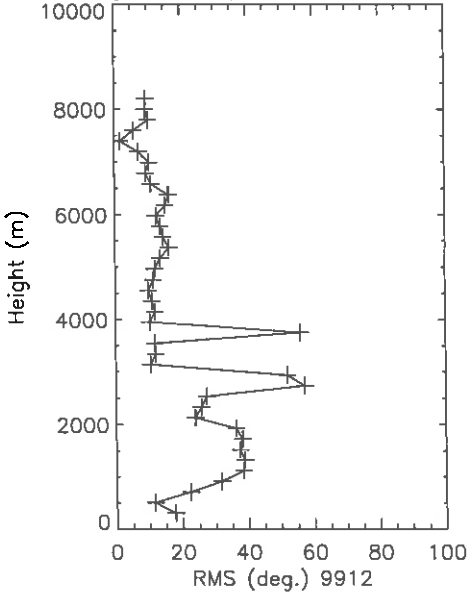

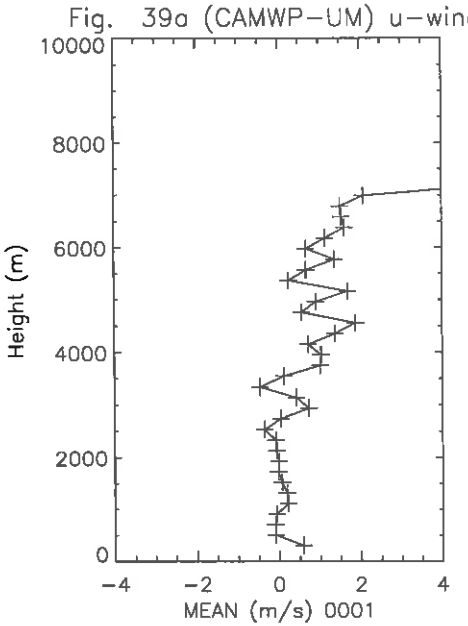
Fig. 39a (CAMWP-UM) u-wind
Height (m)
MEAN (m/s) 0001

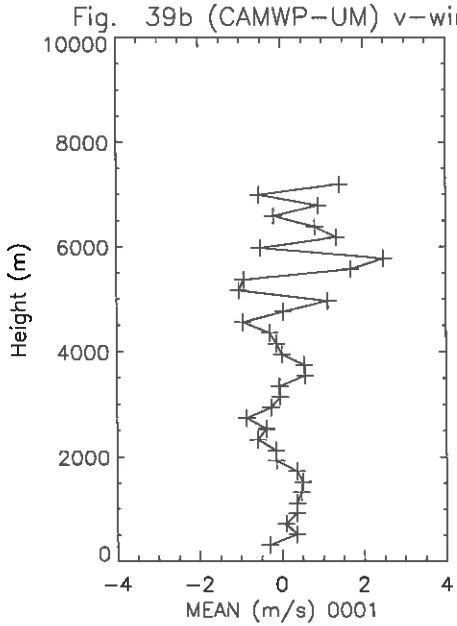
Fig. 39b (CAMWP-UM) v-wind
Height (m)
MEAN (m/s) 0001

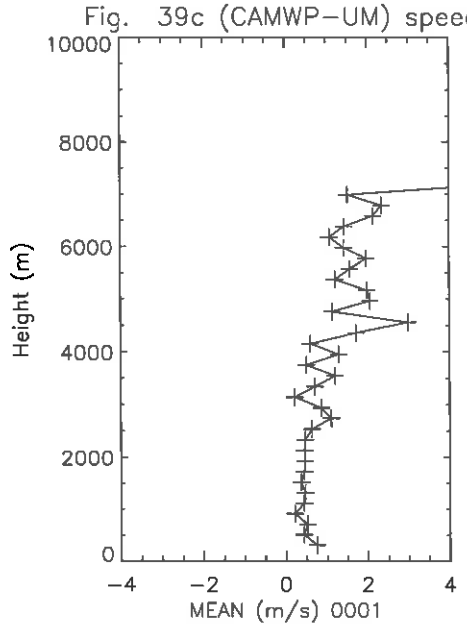
Fig. 39c (CAMWP-UM) speed
Height (m)
MEAN (m/s) 0001

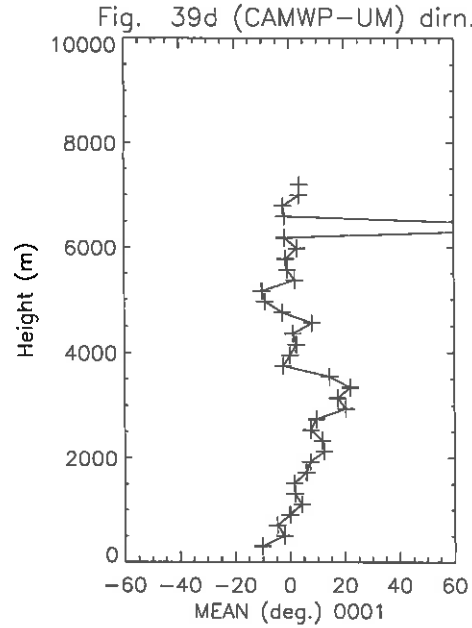
Fig. 39d (CAMWP-UM) dirn.
Height (m)
MEAN (deg.) 0001

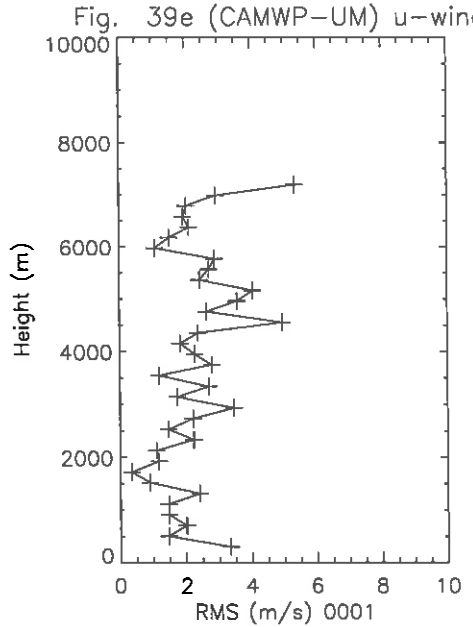
Fig. 39e (CAMWP-UM) u-wind
Height (m)
RMS (m/s) 0001

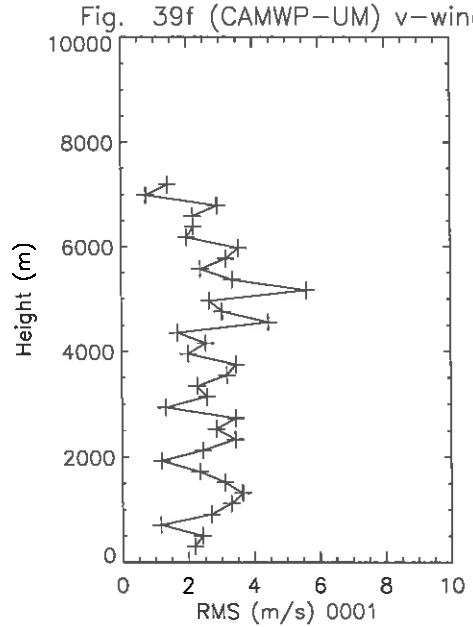
Fig. 39f (CAMWP-UM) v-wind
Height (m)
RMS (m/s) 0001

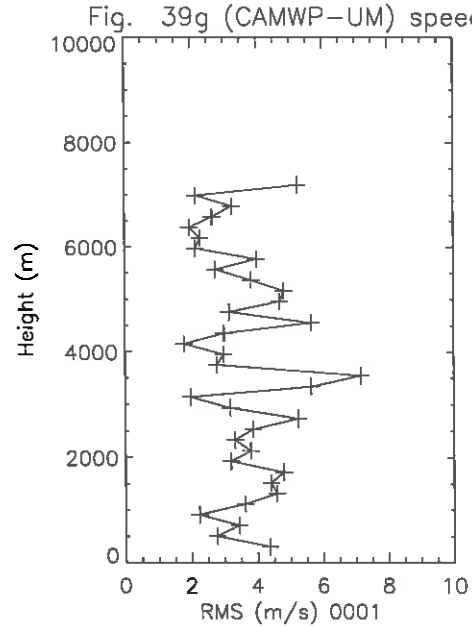
Fig. 39g (CAMWP-UM) speed
Height (m)
RMS (m/s) 0001

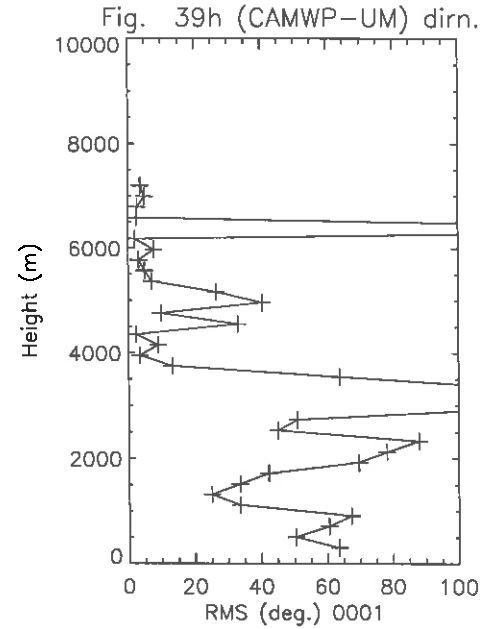
Fig. 39h (CAMWP-UM) dirn.
Height (m)
RMS (deg.) 0001

Fig. 40a (CAMWP–UM) u–wind

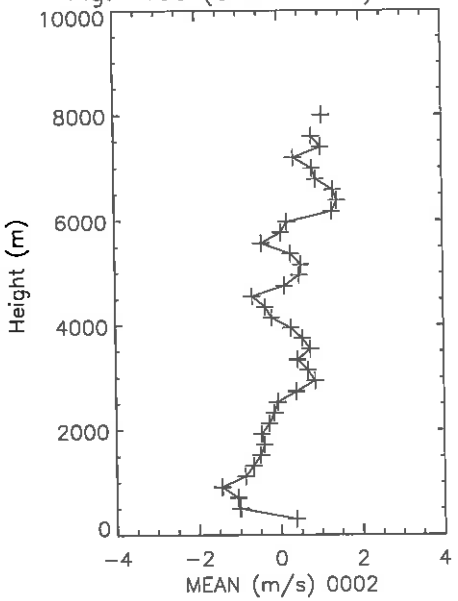

Fig. 40b (CAMWP–UM) v–wind

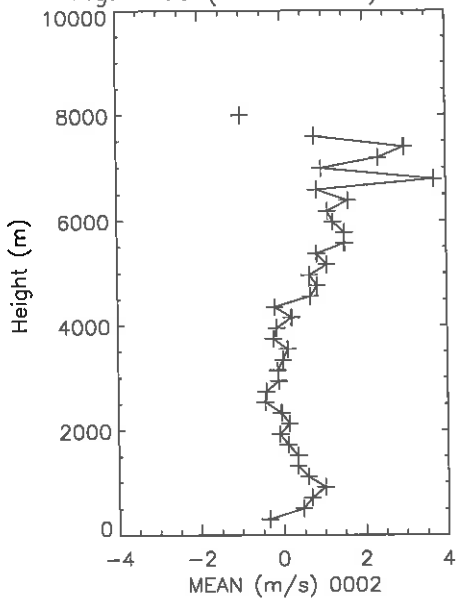

Fig. 40c (CAMWP–UM) speed

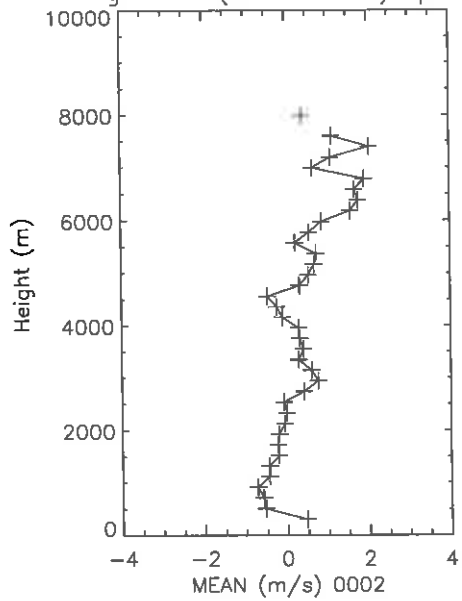

Fig. 40d (CAMWP–UM) dirn.

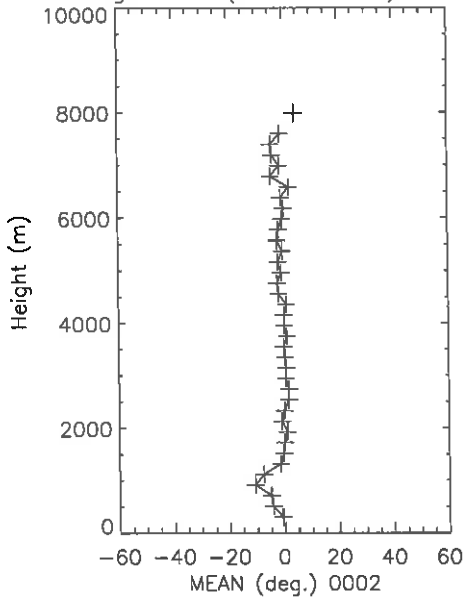

Fig. 40e (CAMWP–UM) u–wind

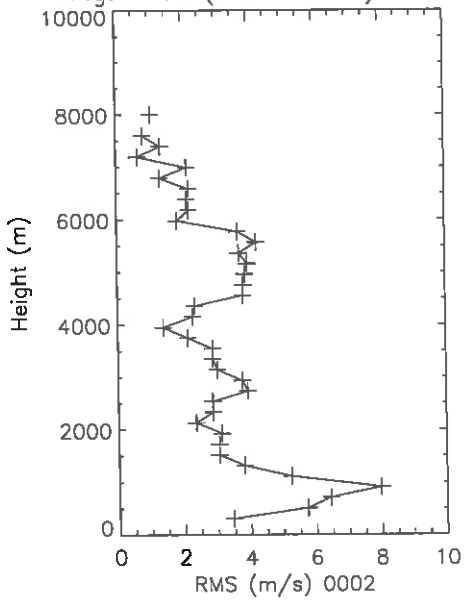

Fig. 40f (CAMWP–UM) v–wind

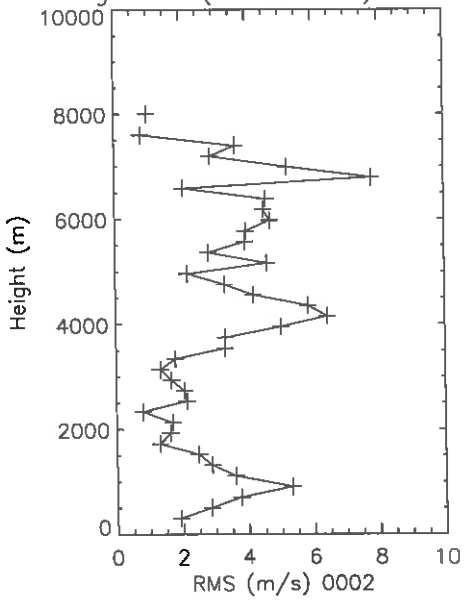

Fig. 40g (CAMWP–UM) speed

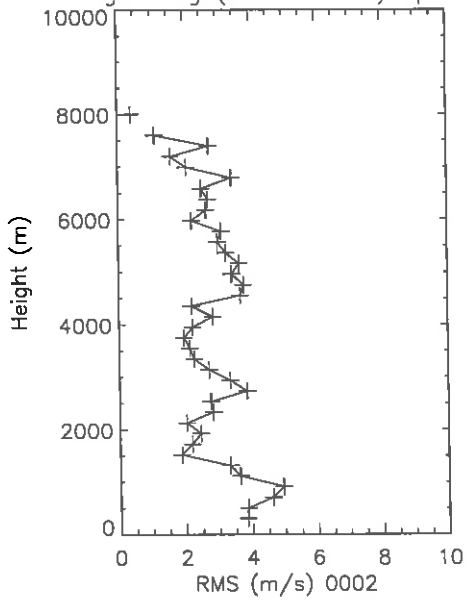

Fig. 40h (CAMWP–UM) dirn.

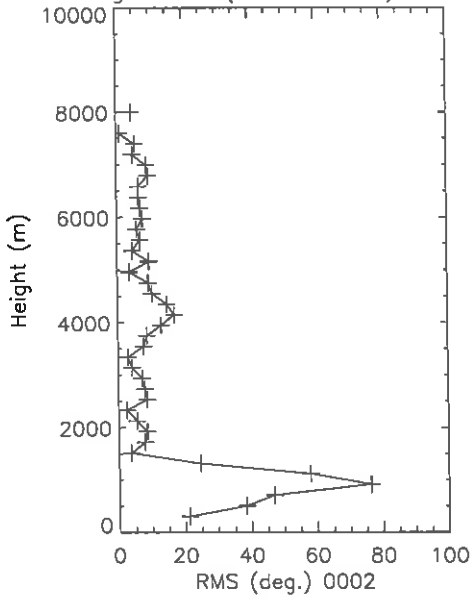

Fig. 41a (CAMWP–UM) u–wind

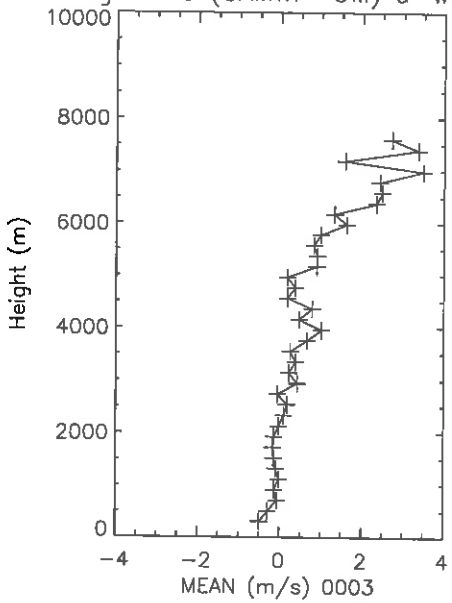

Fig. 41b (CAMWP–UM) v–wind

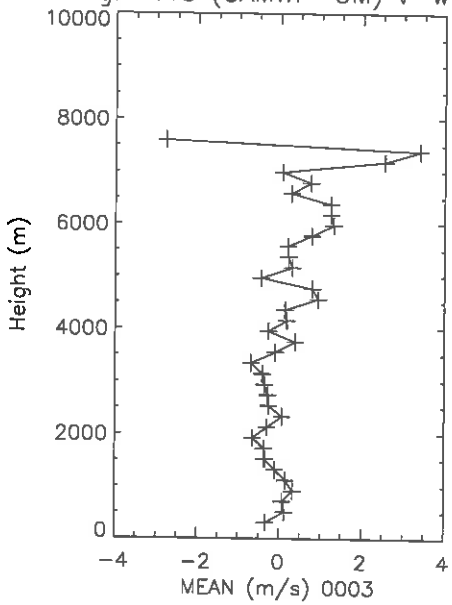

Fig. 41c (CAMWP–UM) speed

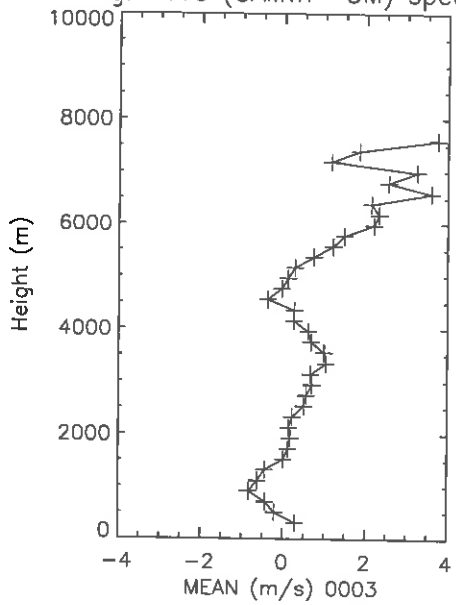

Fig. 41d (CAMWP–UM) dirn.

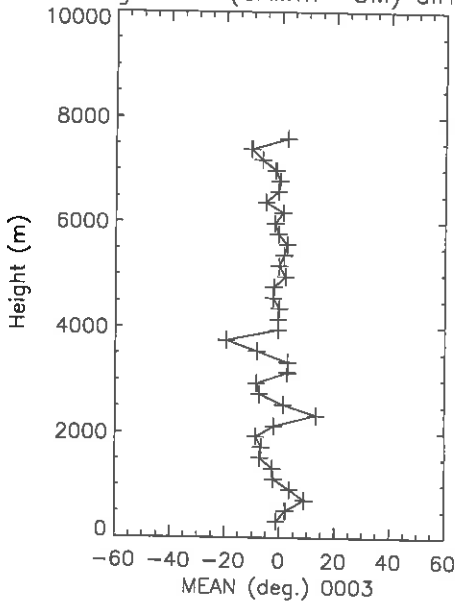

Fig. 41e (CAMWP–UM) u–wind

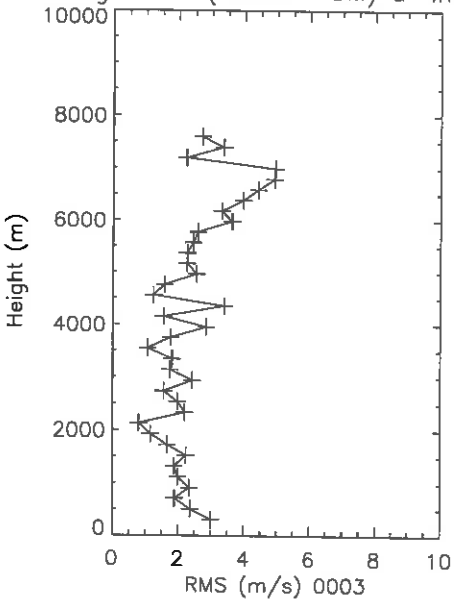

Fig. 41f (CAMWP–UM) v–wind

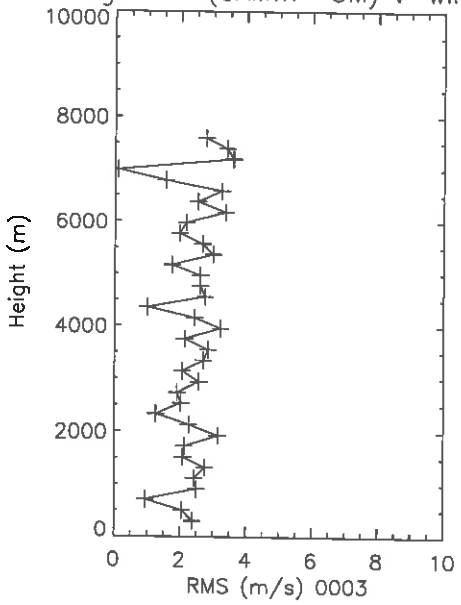

Fig. 41g (CAMWP–UM) speed

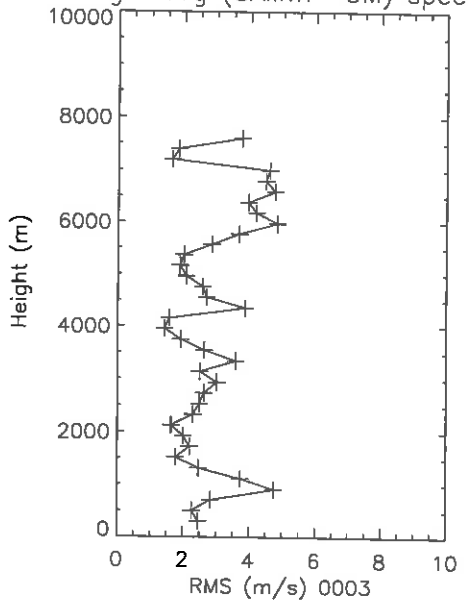

Fig. 41h (CAMWP–UM) dirn.

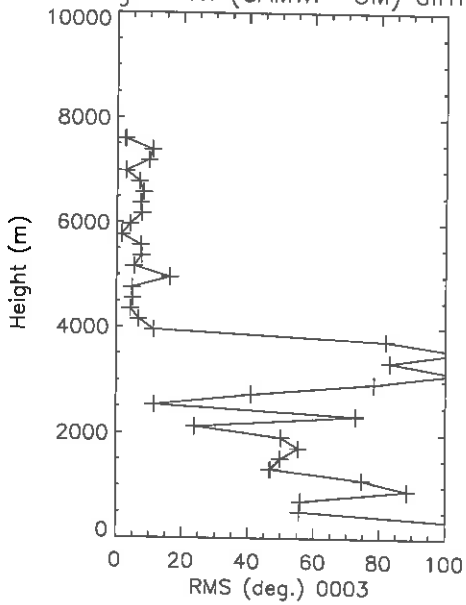

Fig. 42a (DUNWP–UM) u–wind

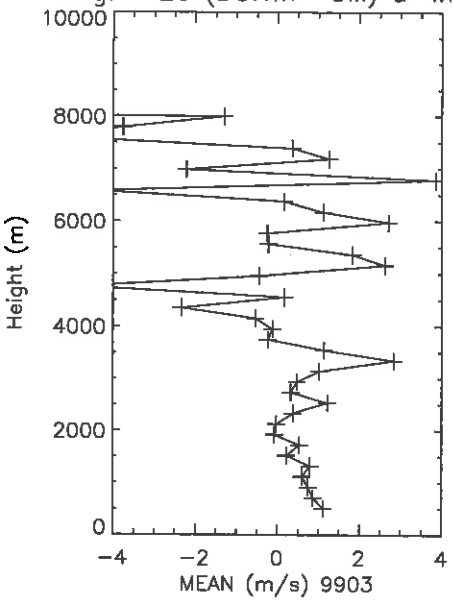

Fig. 42b (DUNWP–UM) v–wind

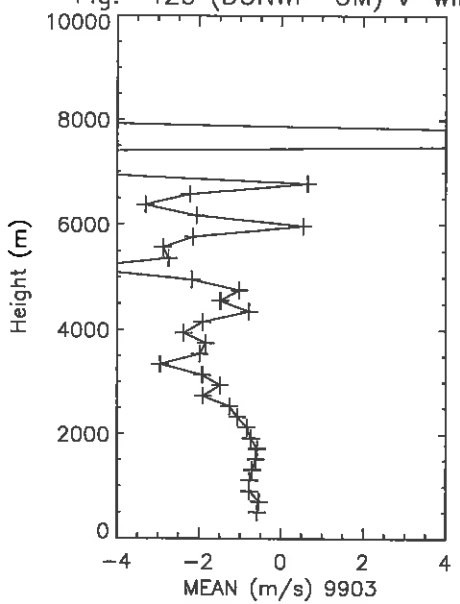

Fig. 42c (DUNWP–UM) speed

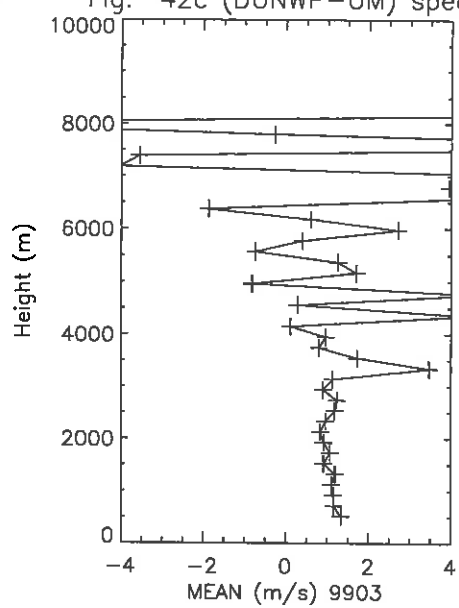

Fig. 42d (DUNWP–UM) dirn.

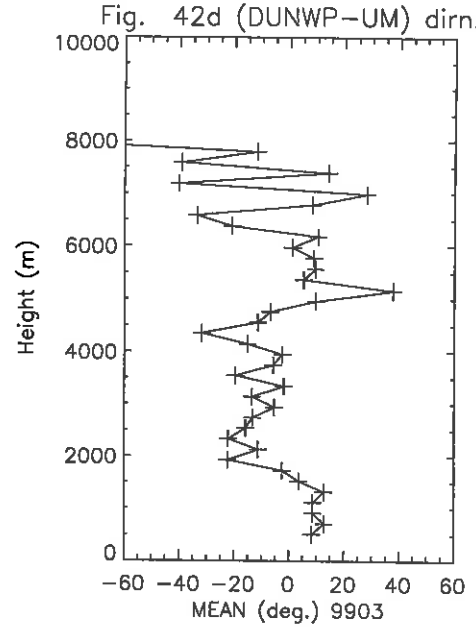

Fig. 42e (DUNWP–UM) u–wind

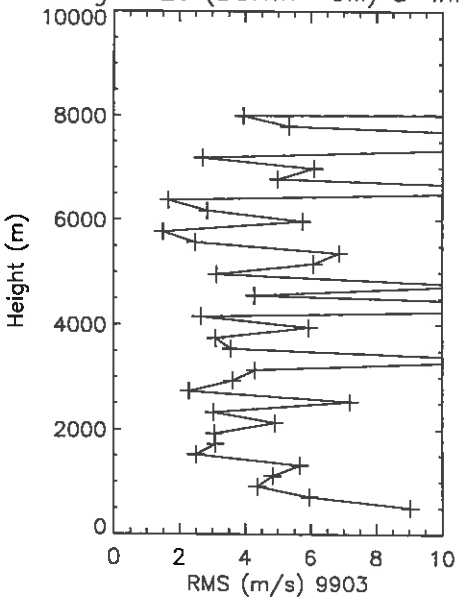

Fig. 42f (DUNWP–UM) v–wind

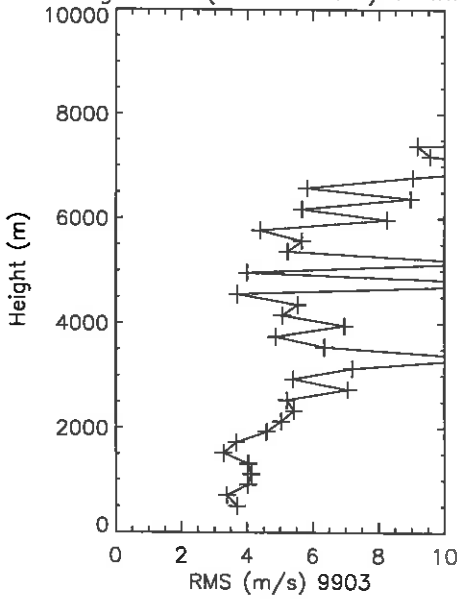

Fig. 42g (DUNWP–UM) speed

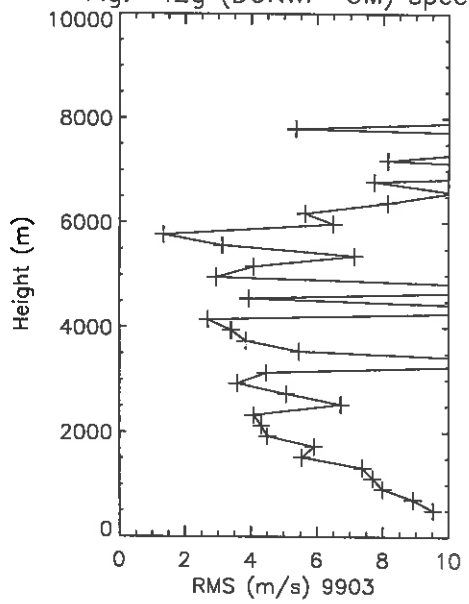

Fig. 42h (DUNWP–UM) dirn.

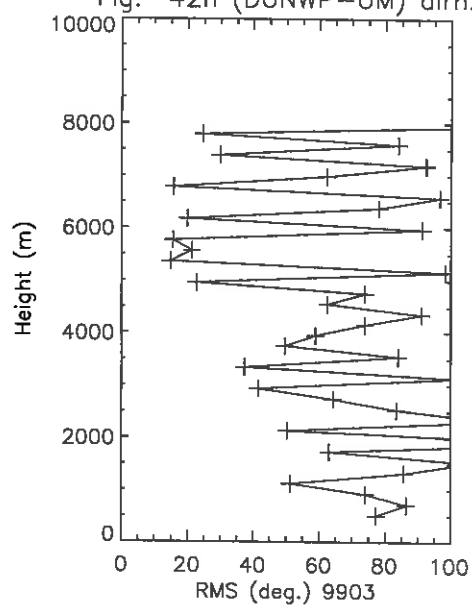

CURRENT JCMM INTERNAL REPORTS

This series of JCMM Internal Reports, initiated in 1993, contains unpublished reports and also versions of articles submitted for publication. The complete set of Internal Reports is available from the National Meteorological Library on loan, if required.

1. **Research strategy and programme**
   K A Browning et al
   January 1993

2. **The GEWEX Cloud System Study (GCSS)**
   GEWEX Cloud System Science Team
   January 1993

3. **Evolution of a mesoscale upper tropospheric vorticity maximum and comma cloud from a cloud-free two dimensional potential vorticity anomaly**
   K A Browning
   January 1993

4. **The global energy and water cycle**
   K A Browning
   July 1993

5. **Structure of a midlatitude cyclone before occlusion**
   K A Browning and N Roberts
   July 1993

6. **Developments in systems and tools for weather forecasting**
   K A Browning and G Szejwach
   July 1993

7. **Diagnostic study of a narrow cold frontal rainband and severe winds associated with a stratospheric intrusion**
   K A Browning and R Reynolds
   August 1993

8. **Survey of perceived priority issues in the parametrizations of cloud-related processes in GCMs**
   K A Browning
   September 1993

9. **The effect of rain on longwave radiation**
   I Dharssi
   September 1993

10. **Cloud microphysical processes - a description of the parametrization used in the large eddy model**
    H Swann
    October 1993

11. **An appreciation of the meteorological research of Ernst Kleinschmidt**
    A J Thorpe
    May 1992

12. **Potential vorticity of flow along the Alps**
    A J Thorpe, H Volkert and Dietrich Heimann
    August 1992

13. **The representation of fronts**
    A J Thorpe
    January 1993

14. **A parametrization scheme for symmetric instability: test for an idealised flow**
C S Chan and A J Thorpe
February 1993

15. **The Fronts 92 Experiment: a Quicklook Atlas**
Edited by T D Hewson
November 1993

16. **Frontal wave stability during moist deformation frontogenesis**
Part 1: Linear wave dynamics
C H Bishop and A J Thorpe
May 1993

17. **Frontal wave stability during moist deformation frontogenesis**
Part 2. The suppression of non-linear wave development
C H Bishop and A J Thorpe
May 1993

18. **Gravity waves in sheared ducts**
S Monserrat and A J Thorpe
October 1993

19. **Potential vorticity and the electrostatics analogy: quasi-geostrophic theory**
C Bishop and A J Thorpe
November 1993

20. **Recent advances in the measurement of precipitation by radar**
A J Illingworth
April 1993

21. **Micro-physique et givrage: cloud microphysics and aircraft icing**
A J Illingworth
May 1993

22. **Differential phase measurements of precipitation**
M Blackman and A J Illingworth
May 1993

23. **Estimation of effective radius of cloud particles from the radar reflectivity**
N I Fox and A J Illingworth
May 1993

24. **A simple method of Dopplerising a pulsed magnetron radar**
A Hua, A J Illingworth and J Eastment
November 1993

25. **Radiation and polar lows**
George C Craig
February 1994

26. **Collected preprints submitted to the International Symposium on the Life Cycles of Extratropical Cyclones; Bergen, Norway, 27 June - 1 July 1994**
April 1994

27. **Convective frontogenesis**
Douglas J Parker and Alan J Thorpe
April 1994

28. **Improved measurement of the ice water content in cirrus using a total water evaporator**
Philip R A Brown and Peter N Francis
April 1994

29. **Mesoscale effects of a dry intrusion within a vigorous cyclone**
K A Browning and B W Golding
April 1994

30. **GEWEX Cloud System Study, Science Plan**
May 1994

31. **Parametrization of momentum transport by convectively generated gravity waves**
R Kershaw
May 1994

32. **Mesoscale Modelling Newsletter No 5**
May 1994

33. **Observations of the mesoscale sub-structure in the cold air of a developing frontal cyclone**
K A Browning, S A Clough, C S A Davitt, N M Roberts and T D Hewson
May 1994

34. **Longwave radiative forcing of a simulated tropical squall line**
Imtiaz Dharssi
July 1994

35. **On the nature of the convective circulation at a kata-cold front**
K A Browning
September 1994

36. **Collective preprints of papers submitted to the COST-75 International Seminar on Advanced Weather Radar Systems, Brussels, 20-23 September 1994**
November 1994

37. **Use of satellite imagery to diagnose events leading to frontal thunderstorms: Parts I and II of a case study**
K A Browning and N M Roberts
November 1994

38. **The role of spaceborne millimetre-wave radar in the global monitoring of ice cloud**
P R A Brown, A J Illingworth, A J Heymsfield, G M McFarquhar, K A Browning and M Gosset
December 1994

39. **Potential vorticity inversion**
Michal Ziemianski
October 1994

40. **Theory of mature tropical cyclones; a comparison between Kleinschmidt (1951) and Emanuel (1986)**
Suzanne L Gray
December 1994

41. **Dispersion and removal of pollutants during the passage of an atmospheric frontal system**
N R Gimson
December 1994

42. **The role of snow sublimation in frontogenesis**
D J Parker and A J Thorpe
December 1994

43. **Potential vorticity and the electrostatics Analogy: Ertel-Rossby formulation**
A J Thorpe and C H Bishop
December 1994

44. **Mesoscale aspect of extratropical cyclones: an observational perspective**
K A Browning
January 1995

45. **A polar low outbreak: evolution and mesoscale structures**
T D Hewson, G C Craig and C Claud
February 1995

46. **Generation of near-surface gusts of deep convection**
K Nakamura and R Kershaw
April 1995

47. **Attribution concepts applied to the Omega Equation**
S A Clough, C S A Davitt and A J Thorpe
June 1995

48. **Parametrization of mixed-phase cloud and precipitation**
Susan P Ballard and M Gerard Hutchinson
June 1995

49. **Short-range forecasting of stratocumulus: initialization prediction**
Susan P Ballard, Simon D Jackson and B Macpherson
June 1995

50. **Contributions of the JCMM/Dept of Meteorology Radar Group to the 27th AMS Radar Meteorology Conference, Vail October 1995**
June 1995

51. **Cold pools in shear**
Douglas J Parker
September 1995

52. **High-resolution analysis of frontal fracture**
K A Browning, S P Ballard and C S A Davitt
September 1995

53. **The albedo of broken cloud fields: calculations using a modified two stream radiation code**
Imtiaz Dharssi and Roy Kershaw
October 1995

54. **Parametrization of momentum transport by convection. I: theory and cloud modelling results**
R Kershaw and D Gregory
November 1995

55. **Variation of frontal structure along a cold front**
K A Browning and N M Roberts
November 1995

56. **Secondary frontal waves**
Douglas Parker
December 1995

57. **Objective fronts**
T D Hewson
March 1996

58. **Mesoscale analysis of the activation of a cold front during cyclogenesis**
K A Browning, N M Roberts and A J Illingworth
June 1996

59. **Investigation of different representations of rain in a 1-d evaporation model**
H Swann
May 1996

60. **Parametrization of diabatic processes in the inversion of the omega-equation**
M Athanassiadou and A J Thorpe
June 1996

61. **The role of the environmental flow in the development of secondary frontal cyclones**
I A Renfrew, A J Thorpe and A Joly
June 1996

62. **Consequences of the geostrophic momentum approximation on barotropic instability**
S Malardel, A J Thorpe and A Joly
June 1996

63. **Contributions to the AMS/RMS Conference on Mesoscale Processes**
Reading, 9-13 September 1996

64. **Vorticity and potential vorticity in stratified flows interacting with an isolated obstacle**
Jorge A Gutiérrez and A J Thorpe
September 1996

65. **Triple point development: two case studies**
Douglas Parker
September 1996

66. **Radar observations of wind-shear splitting within evolving atmospheric Kelvin-Helmholtz billows**
D Chapman and K A Browning
April 1997

67. **Cold frontal structure derived from radar wind profilers**
K A Browning, D Jerrett, J Nash, T Oakley and N M Roberts
May 1997

68. **The dry intrusion and its effect on the frontal, cloud and precipitation structure of extratropical cyclones**
K A Browning - Text of invited special lecture at the Spring Conference
of the Meteorological Society of Japan, University of Tsukuba, 22 May 1997

69. **Met. Office Unified Model data, diagnostics, graphics programs, and other observational data available from the JCMM through the aegis of the Universities Weather Research Network (UWERN).** (Plus supplement)
Peter Panagi and Ed Dicks
June 1997

70. **Contributions of the JCMM/Dept of Meteorology Radar Group to the 28th AMS Radar Meteorology Conference.** Austin, Texas
September 1997

71. **Sensitivity of short-range weather forecasts to local potential vorticity modifications**
Meral Demirtas and Alan Thorpe
July 1997

72. **Objective identification of frontal wave cyclones**
T D Hewson
August 1997

73. **Attribution and its application to mesoscale structure associated with tropopause folds**
A J Thorpe
September 1997

74. **The role of the environmental flow in the development of secondary frontal cyclones**
Ian A Renfrew, Alan J Thorpe and Craig H Bishop
September 1997

75. **Potential vorticity: a short history of its definitions and uses**
Alan J Thorpe and Hans Volkert
September 1997

76. **Superposing semi-geostrophic potential vorticity anomalies**
H R Birkett and A J Thorpe
September 1997

77. **Short period forecasting of catchment-scale precipitation.**
Part 1: the role of Numerical Weather Prediction
M A Pedder, M Haile and A J Thorpe
September 1997

78. **Verification of the tracking technique used in an experimental cloud motion wind inferring system**
Z Wang, K A Browning and G A Kelly
October 1997

79. **A preliminary study of Fourier series analysis for cloud tracking with GOES high temporal resolution images**
Z Wang
October 1997

80. **Analysis of an ex-tropical cyclone after reintensifying as a warm-core extratropical cyclone**
K A Browning, G Vaughan and P Panagi
November 1997

81. **A JCMM overview of FASTEX IOPs**
S A Clough, H W Lean, N M Roberts, H Birkett, J-P Chaboureau, R Dixon, M Griffiths, T D Hewson and A Montani
January 1998

82. **Programs for PV inversion and modification**
Meral Demirtas
December 1997

83. **Release of potential shearing instability in warm frontal zones**
D Chapman and K A Browning
February 1998

84. **The European Cloud-Resolving Modelling Programme (EUCREM)**
Summary Report from the coordinator
P W White
April 1998

85. **A frontal wave database**
T D Hewson
April 1998

86. **Layering observed in dropsoundings from IOP 1 of Fronts 92**
S A Clough
May 1998

87. **Use of wind-shear displays for Doppler radar data**
D Chapman and K A Browning
May 1998

88. **Radar estimates of rainfall rates at the ground in bright band and non-bright band events**
T J Smyth and A J Illingworth
June 1998

89. **Correction for attenuation of radar reflectivity using polarisation data**
T J Smyth and A J Illingworth
June 1998

90. **The effects of convection on chemical reactions and precipitation scavenging**
Neil R Gimson
July 1998

91. **How to use the display program DISP**
Nigel Roberts
August 1998

92. **Conceptual models of cyclogenesis**
Adrian T Semple
August 1998

93. **Observations of oblate hail using dual polarisation radar and implications for hail detection schemes**
T J Smyth, T M Blackman and A J Illingworth
September 1998

94. **The semigeostrophic diagnosis of vertical motion. Part I: Formulation and co-ordinate transformations**
Mike A Pedder and Alan J Thorpe
September 1998

95. **The semigeostrophic diagnosis of vertical motion. Part II: Results for an idealised baroclinic wave life cycle**
Alan J Thorpe and Mike A Pedder
September 1998

96. **Convective destabilisation by a tropopause fold diagnosed using potential vorticity inversion**
Morwenna Griffiths, Alan Thorpe and Keith Browning
October 1998

97. **Forecast skill of the ECMWF model using targeted observations during FASTEX**
A Montani, A J Thorpe, R Buizza and P Unden
October 1998

98. **Observations and model simulations of the FASTEX IOP 16 frontal wave - effects of sublimation**
Sid A Clough, Humphrey W Lean, Nigel M Roberts and Richard M Forbes
December 1998

99. **The application of conceptual models in NWP**
Adrian T Semple
January 1999

100. **Mesoscale analysis of arc rainbands in a dry slot**
K A Browning and N M Roberts
January 1999

101. **Interaction of mesoscale tropopause depressions with a warm-core cyclone: observational and model analyses, and sensitivity to analysis errors**
K A Browning, A J Thorpe, A Montani, D Parsons, M Griffiths, P Panagi and E M Dicks
February 1999

102. **The use of water vapour imagery and PV inversion to adjust initial conditions in NWP**
Sean J Swarbrick
February 1999
This report is no longer available; see Internal Report No.108

103. **Summary notes for a lecture course on Waves in the Atmosphere and Ocean**
A A White
March 1999

104. **Results of a questionnaire on the operational value of conceptual models (CMs) of fronts and cyclones**
N M Roberts & M V Young
July 1999

105. **Contributions to the Poster Session at the 1998 UWERN Annual Science Meeting**
assembled by A A White
August 1999

106. **The objective analysis of dropsonde data from FASTEX**
Richard Forbes, Sid Clough, Mark Dixon, Andy Macallan & Nigel Roberts
January 2000

107. *NWP Technical Report No.302*
Implications for Mesoscale Modelling from a Study of the FASTEX IOP 16 Mid-latitude Cyclone
Richard M Forbes, Humphrey W Lean, Nigel M Roberts and Peter A Clark
March 2000

108. *NWP Technical Report No.291*
The use of water vapour imagery and PV inversion to adjust initial conditions in NWP
Final Project Report
Sean J Swarbrick
September 1999

109. *NWP Technical Report No.294*
A guide to aspects of water vapour imagery interpretation: the significance of dry regions
Nigel M Roberts
January 2000

110. *NWP Technical Report No.300*
The relationship between water vapour imagery and thunderstorms
Nigel M Roberts
February 2000

111. *NWP Technical Report No.293*
Holomorphic structures in hydrodynamical models of nearly geostrophic flow
V N Roubtsov and I Roulstone
January 2000

112. *NWP Technical Report No.301*
Multi-sensor synthesis of the mesoscale structure of a cold-air comma cloud system
K A Browning, P Panagi and E M Dicks
March 2000

113. *NWP Technical Report No.307*
Observations of stratospheric air entering the circulation of a polar low
K A Browning and E M Dicks
May 2000

114. *NWP Technical Report No.309*
Wind profiler – Unified Model comparison statistics
Peter Panagi & Ed Dicks
March 2000

Met Office Joint Centre for Mesoscale Meteorology Department of Meteorology
University of Reading PO Box 243 Reading RG6 6BB United Kingdom
Tel: +44 (0)118 931 8425 Fax: +44 (0)118 931 8791
www.metoffice.com